

UNIVERSITE DE SAAD DAHLED DE BLIDA

Faculté des Sciences de l'Ingénieur
Département d'Electronique

THESE DE DOCTORAT D'ETAT

Spécialité : Electronique

**RECONNAISSANCE DE CARACTERES
IMPRIMES ET MANUSCRITS.
APPLICATION AU CHEQUE POSTAL ALGERIEN**

Présentée par :

NAMANE Abderrahmane

Devant le jury composé de :

M. BENSEBTI	Professeur, U.S.D. de Blida	Président
D. BERKANI	Professeur, E.N.P.A, Alger	Examineur
Y. SMARA	Professeur, U.S.T.H.B, Alger	Examineur
A. GUESSOUM	Professeur, U.S.D. de Blida	Rapporteur
M. BRUYNOOGHE	Professeur, U.L.Pasteur, France	Co-rapporteur

Blida, Juin 2007

ABSTRACT

The character recognition is a significant stage in all document recognition systems. Character recognition is considered as assignment problem and decision of a given character, and is active research subject in many disciplines. This thesis is related mainly to the recognition of the degraded printed and handwritten characters. New solutions were brought to the field of the document image analysis (DIA). One finds initially, the development of two recognition methods for the handwritten numeral character, namely, the method based on the use of Fourier-Mellin transform (FMT) and the self-organization map (SOM), and the parallel combination of HMM-based classifiers using as parameter extraction a new projection technique. In second place, one finds a new holistic recognition method of handwritten words applied to the French legal amount. In third place, two recognition methods based on neural networks have been developed for the degraded printed character applied to the Algerian postal check. The first work is based on the sequential combination and the second used a serial combination based mainly on the introduction of a relative distance for the quality measurement of the degraded character. During the development of this thesis, methods of preprocessing were also developed, in particular, the handwritten numeral slant correction, the handwritten word central zone detection and its slope.

RESUME

La reconnaissance de caractères est une étape importante dans tout système de reconnaissance de document. Cette reconnaissance de caractère est considérée comme un problème d'affectation et de décision de caractères, et a fait l'objet de recherches dans de nombreuses disciplines. Cette thèse porte principalement sur la reconnaissance du caractère imprimé dégradé et manuscrit. De nouvelles solutions ont été apportées au domaine de l'analyse du document image (ADI). On trouve en premier lieu, le développement de deux méthodes de reconnaissance du chiffre manuscrit, notamment, la méthode basée sur l'utilisation de la transformée de Fourier-Mellin (TFM) et la carte auto-organisatrice (CAO), et l'utilisation de la combinaison parallèle basée sur les HMMs comme classificateurs de bases, avec comme extracteur de paramètres une nouvelle technique de projection. En deuxième lieu, on trouve une nouvelle méthode de reconnaissance holistique de mots manuscrits appliquée au montant légal Français. En troisième lieu, deux travaux basés sur les réseaux de neurones ont été réalisés sur la reconnaissance du caractère imprimé dégradé et appliqués au chèque postal Algérien. Le premier travail est basé sur la combinaison séquentielle et le deuxième a fait l'objet d'une combinaison série basé sur l'introduction d'une distance relative pour la mesure de qualité du caractère dégradé. Lors de l'élaboration de ce travail, des méthodes de prétraitement ont été aussi développées, notamment, la correction de l'inclinaison du chiffre manuscrit, la détection de la zone centrale du mot manuscrit ainsi que sa pente.

المخلص

التعرف على الاحرف مرحلة مهمة في كل نظام التعرف على الوثائق، هذا التعرف على الاحرف يعتبر كمشكل توجيه وقرار الاحرف، وكان محل بحث في كل الميادين. هذه الاطروحة تتعلق اساسا على التعرف على الاحرف الالية التالفة والمكتوبة باليد. حلول جديدة اضيفت في ميدان التحليل لصورة الوثيقة. نجد في المرتبة الأولى انجاز طريقتان جديدتان للتعرف على الارقام المكتوبة باليد، خصوصا الطريقة التي تستند إلى استعمال طريقة تحويل "فوريي - ميلان" وخريطة ذات تنظيم ذاتي، واستعمال التركيب المتوازي الذي يستند على سلسلة "ماركوف" المخفية كمصنفات اساسية تعتمد على مستخرجات للمعالم كتقنية جديدة. في المرتبة الثانية نجد طريقة جديدة للتعرف الاجمالي على الكلمات المكتوبة باليد والمطبقة على المبلغ المكتوب بالفرنسية. و في المرتبة الثالثة انجازان يتأسسان على شبكة الخلايا العصبية تم انجازهما للتعرف على الاحرف الالية المتلفة والمطبقة على الصك البريدي الجزائري. الانجاز الأول يرتكز على التركيب المتعاقب والثاني على التركيب المتسلسل مع ادخال مسافة نسبية لقياس نوعية الحرف المتلف. خلال اعداد هذا العمل، تم انجاز طرق ما قبل المعالجة، خصوصا، تصحيح ميلان الرقم المكتوب باليد، تحديد المنطقة الوسطى للكلمة المكتوبة وكذلك انحدارها.

ACKNOWLEDGEMENT

I would like to express my sincere appreciation to my supervisor, Professor Abderrezak GUESSOUM for his valuable suggestions, guidance, support and helpful remarks throughout the course of this work. I would like also to thank my co-supervisor Professor Michel BRUYNOOGHE from the University of Louis Pasteur.

I am also grateful to; Prof. Messaoud BENSEBTI, Prof. Daoud BERKANI and Prof. Youcef SMARA for their acceptance to be part of my committee members.

I wish to thank all my colleagues from the department of Electronic of the University of Saad Dahleb of Blida, and particularly those from signal and image processing laboratory (SIPL).

Last but not least, i extend my sincerest thanks to all my beloved parents, my wife and my two children.

TABLE OF CONTENTS

ABSTRACT.....	II
ACKNOWLEDGEMENTS	V
TABLE OF CONTENTS.....	VI
ABBREVIATIONS LIST	VIII
SYMBOLS LIST	IX
FIGURES AND TABLES LIST.....	X
INTRODUCTION	17
1. DOCUMENT RECOGNITION	21
1.1 Introduction.....	21
1.2 On-line and off-line systems.....	21
1.3 Analytical and global approaches	22
1.4 The OCR and the imagery.....	24
1.5 Process of document recognition.....	24
1.5.1 Physical world.....	24
1.5.2 Acquisition.....	25
1.5.3 Preprocessing.....	25
1.5.4 Feature extraction.....	27
1.5.5 Training.....	28
1.5.6 Classification.....	28
1.6 Methods of document recognition.....	29
1.6.1 Statistical methods.....	29
1.6.2 Connexionnist methods.....	30
1.6.3 Linguistic methods.....	31
1.7 Multiple classifiers.....	31
1.7.1 Serialcombination.....	32
1.7.2 Parallel combination.....	32
1.8 Conclusion.....	33
2. FEATURE EXTRACTION AND CLASSIFICATION.....	34
2.1 Introduction.....	34
2.2 State of the art.....	34
2.2.1 Degraded printed character recognition	36
2.2.2 Handwritten numeral recognition	37
2.2.3 Handwritten word recognition	40
2.3 Mathematical morphology	40
2.4 Fourier Mellin transform (FMT).....	42
2.5 Complementary similarity measure (CSM)	44
2.6 Multi-layer perceptron (MLP) neural network	46
2.7 Hopfield neural network	47

2.7.1 Autossociative memories	47
2.7.2 Synchronous and asynchronous modes	49
2.8 Self organization map (SOM)	50
2.9 Hidden Markov model (HMM)	51
1.8 Conclusion.....	54
3. EXPERIMENTAL RESULTS.....	55
3.1 Introduction	55
3.2 Handwritten writing processing	55
3.2.1 Handwritten numeral slant correction	52
3.2.2 New skew correction and central zone localization (SC-CZL)	57
3.3 Handwritten numeral recognition	62
3.3.1 FMT-SOM for handwritten numeral recognition	62
3.3.2 Multiple HMM for handwritten numeral recognition.....	66
3.4 New holistic handwritten word recognition	73
3.4.1 Proposed method	74
3.4.2 Handwritten word preprocessing	75
3.4.3 Experimental results	78
3.5 Degraded printed character recognition	82
3.5.1 Sequential combination for degraded character recognition	83
3.5.2 Serial combination for degraded character recognition	93
3.6 Conclusion	113
CONCLUSION.....	114
REFERENCES.....	116

ABBREVIATIONS LIST

OCR	: Optical character recognition
SC-CZL	: Skew correction and central zone localization
MICR	: Magnetic Ink Character Recognition
DCR	: Degraded character recognition
HMM	: Hidden Markov model
MRF	: Markov random field
SOM	: Self organization map
MLP	: Multi layer perceptron
EM	: Expectation-maximization
ACN	: Account check number
FMT	: Fourier-Mellin transform
CSM	: Complementary similarity measure
IC	: Individual classifier
EWC	: Equal weight combination
UWC	: Unequal weight combination
CBT	: Contour background transition
SC-LUC	: Slant correction with lower and upper centroids
AGN	: Additive Gaussian noise
ANDL	: Account number detection and localization
LAN	: Left account number
RAN	: Right account number
1-NN	: First nearest neighbor
HDM	: Highly degraded method
SC	: Sequential combination
ANS	: Account number segmentation
LANL	: Left account number localization
RANL	: Right account number localization
LANR	: Left account number recognition
RANR	: Right account number recognition
SNR	: Signal to noise ration

SYMBOLS LIST

$I_f(p, q)$: Discrete Fourier-Mellin transform
$H_{p, q}(k, l)$: Fourier-Mellin transform filter bank
S_c	: Complementary similarity measure
R_M	: MLP threshold reject
R_H	: Hopfield threshold reject
$\xi_{\alpha, \beta}$: Relative distance
w_{ij}, v_{ij}	: Neural network synaptic weights
α	: Training speed
ξ	: Viscosity
$S^{(m)}$: Memorized pattern
O_t	: Observation symbol
A	: Transition probability distribution
B	: Observation probability distribution
π	: Initial probability distribution
$P(O_t/\lambda)$: Probability that a particular model λ caused a certain observation O .
N_H	: French legal amount number
β_k	: Handwritten word number per class
T	: Iteration Hopfield model number
Thresh	: Threshold
μ	: Mean
σ	: Standard deviation

FIGURES AND TABLES LIST

Fig. 1.1	OCR block diagram	22
Fig. 1.2	The different areas of character recognition.	22
Fig. 1.3	Influence of the character “u” by its preceding character.	23
Fig. 1.4	Poor quality handwritten legal amounts.	23
Fig. 1.5	Influence of the character “u” by its preceding character.	25
Fig. 1.6	(a) Original image (b) Filtered image (c) Image binarization and skew detection (d) Skew correction (e) Slant detection (f) Contour detection (g) Thining application.	27
Fig. 1.7	Pattern recognition methods.	30
Fig. 1.8	(a) Parallel combination (b) Serial combination.	32
Fig. 2.1	MICR and CMC-7 code numerals and control characters.	35
Fig. 2.2	Poor quality account checks numbers.	36
Fig. 2.3	Morphological closing operation	41
Fig. 2.4	(a) Different rotation of the handwritten character. (b) Feature vector plots	43
Fig. 2.5	(a) Different scale of the handwritten character. (b) Feature vector plots with scaling invariance for $p=4$ and $q=4$.	43
Fig. 2.6	Complementary similarity measure illustration (a) Two character images y and x representing the image model and another image respectively. (b) Results of the application of the CSM to these images.	45
Fig. 2.7	MLP neural network architecture.	46
Fig. 2.8	Hopfield model neural network architecture.	48

Fig. 2.9	Pattern recovering example (a) Corrupted input pattern. (b) Centered pattern. (c)-(g) Memorized pattern restitution ((c)-(f) for the character "B").	48
Fig. 2.10	Synchronous and asynchronous illustration of step by step recognition.	50
Fig. 2.11	HMM with serial constraints of double transition.	52
Fig. 3.1	Slant correction method. (a) Slant angle calculation. (b) Character slant correction.	57
Fig. 3.2	Slant correction example. (a) and (e) Original handwritten numerals. (b) and (f) Results based on contour slant correction. (c) and (g) Results based on rows centroid slant correction. (b) and (f) Results of the proposed method.	57
Fig. 3.3	Poor quality handwritten legal amounts.	58
Fig. 3.4	Handwritten zones and skew correction.	59
Fig. 3.5	Lower case determination (a) Original word image (b) The opened version of (a). (c) Lower case determination. (d) Horizontal histogram and its thresholded version (represented in shaded lines).	60
Fig. 3.6	Skew correction and lower case zone detection. (a) Original image. (b) Lower case zone detection before skew correction. (c) and (d) Lower case zone detection after skew correction. (e) The corresponding $\rho(\theta_k)$ with the estimated skew detected at the maximum of ρ ($\max(\rho) = 1.545442$) giving an angle $\theta = -4.0$ degrees.	61
Fig. 3.7	Skew correction and lower case localization; the first column represents the original words, the second column represents lower case localization before skew correction and the last columns represents results of lower case zone localization after skew correction carried out simultaneously.	61
Fig. 3.8	Recognition synoptic block diagram.	62
Fig. 3.9	Preprocessing. (a) Original image character of size 64x64 pixels. (b) filtered character. (c) Binarized character. (d) application of the proposed slant correction method. (e) Normalised version of the character in (d).	63

Fig. 3.10	Recognition results comparison (a) for various FMT order and SOM dimension (b) for FMT-SOM and FMT-SOM-MLP ($p=4$ and $q=4$).	63
Fig. 3.11	SOM card of 20x20 dimension.	65
Fig. 3.12	Handwritten numerals correctly recognized.	66
Fig 3.13.	Feature extraction. (a) The four CBTs used for feature extraction. (b) CBT-4 showing the transition for 6α (c) Result of feature extraction procedure for 6α .	67
Fig. 3.14	Recognition system block diagram.	68
Fig. 3.15	Example of digitized data.	70
Fig. 3.16	Results of recognition with training set number (P).	71
Fig. 3.17	Results of recognition with iteration number $L=10$.	71
Fig. 3.18	Results of recognition with number of iteration $L=30$	72
Fig. 3.19	Results of recognition with iteration number $L=50$.	72
Fig. 3.20	Recognition rate versus state number (N) for fixed iteration number (L).	73
Fig. 3.21	Poor quality handwritten French legal amounts	77
Fig. 3.22	Proposed method illustration example (a) Handwritten word preprocessing (b) sequential combination method for prototype recognition	75
Fig. 3.23	Slant correction (a) Original image (b-d) result of application of SC-CZL (e) Result of application of SC-LUC on (d). (f) Slant correction based on contour slant estimation	76
Fig. 3.24.	Preprocessing (a) binarized image (b) Application of SC-CZL method (c) Horizontal slant correction (d) Normalized version of (c) in the frame 32-by-50 pixels	77
Fig. 3.25	Prototype creation (a) Four different normalized words from handwritten word class "douze" (b) Superposition operation (c) Dilation and prototype processing (d) Prototype result.(e) Samples of handwritten words used for prototype creation.	77

Fig. 3.26	Prototypes used for holistic recognition and their corresponding handwritten classes and β_k (below each prototype image)	78
Fig. 3.27	Starting “d” and dot detection (a) Original image word (b) Application of SC-CZL method (c) Starting “d” and dot detection (d) Original images (e) Dilated version of the normalized image (32-by-50). (f) Hopfield model output (g) Result of prototype recognition by Hopf-MLP classifier. (h) Results of holistic word recognition by combining result of (g) and word characteristics (“d” and dot).	79
Fig. 3.28	Recognition results. (a) Error-reject plots (b) Recognition-reject plots	81
Fig. 3.29	Handwritten word samples correctly recognized	82
Fig. 3.30	Recognition synoptic block diagram of sequential combination method.	84
Fig. 3.31	Poor quality documents a) Algerian post check b) Account check number c) Customer first and last name.	85
Fig. 3.32	Proposed method illustration example for printed character recognition.	85
Fig. 3.33	Character image divided into 10×10 segments.	86
Fig. 3.34	40-by-40 pixels character class a) Customer first and last name character classes b) Account check number character classes.	86
Fig. 3.35	Error versus reject plots a) Error versus reject plot for three classifiers using various threshold values for R_H and R_M b) Error versus reject plot for the combined method showing the effect of using different Hopfield iteration number; $R_H=0.12$ and $T=\{1, 2, 3\}$.	89
Fig. 3.36	Grey level real printed characters recognized correctly	90
Fig. 3.37	Misclassified gray level real printed characters	90
Fig. 3.38	Degraded character processing a) Original images b) Binarization of (a) c) Corresponding Hopfield model outputs of images in (b) for $T=1$.	90

Fig. 3.39	Recognition versus reject thresholds (R_M) plots; the MLP based classifier plot and the combined method plot for $R_H=0.12$ and $T=1$.	91
Fig. 3.40	Reached SNR for 100% recognition rate for account number and customer first and last name	92
Fig. 3.41	Recognized degraded account number characters by various Added Gaussian Noise (AGN) a) Original image characters b) Noisy grey level images with $\sigma=0.2$ c) Noisy grey level images with $\sigma=0.4$ d) Noisy grey level images with $\sigma=0.6$.	92
Fig. 3.42	Broken and incomplete real characters correctly recognized.	92
Fig. 3.43	Recognition synoptic block diagram (a) Sequential combination method (b) Serial combination method	93
Fig. 3.44	ANDL procedure (a) Post checks. (b) Opened image horizontal projection. (c) Post check thresholding.	95
Fig. 3.45	ANS procedure (a) Account number zone showing ten regions of interest. (b) Morphological closing operation of image in (a). (c) Binarisation operation of the closed image in (b). (d) Contour detection. (e) The LAN of (a) zoomed for illustration, showing the detected blocks delimited by five contours of (d).	97
Fig. 3.46	Clean account number character set of 40x40 pixels.	98
Fig. 3.47	Effect of the iteration number on the pattern recovering (a) Image recovering of degraded patterns at different T and their corresponding ξ (below each image). (b) Relative distance variation (ξ) for the images shown in (a) at different T .	100
Fig. 3.48	Relative distance (ξ) for quality measurement of the printed character for $T=1$.	101
Fig. 3.49	Error vs reject plot for the Hopfield-based classifier showing the effect of using different iteration numbers; $T=\{1, 2, 3\}$.	101
Fig. 3.50	Error vs reject plot for three classifiers using various thresholds values for R_H and R_M .	102

Fig. 3.51	Error vs reject plot for the combined method showing the effect of R_M using various thresholds values; $R_M=\{0.5, 0.6, 0.7, 0.8, 0.9\}$.	102
Fig. 3.52	Recognition vs error plot for three classifiers using various thresholds values for R_H and R_M .	103
Fig. 3.53	Gray level real printed characters recognition results (a) Recognized characters (b) Rejected characters (c) Misclassified characters.	104
Fig. 3.54	Error vs reject showing comparison results of six classifiers.	105
Fig. 3.55	Recognition vs error showing comparison results of six classifiers.	106
Fig. 3.56	Post checks processing for account number recognition.	108
Fig. 3.57	Recognition results illustration (a-b) Recognized account number images and their corresponding output results (below each image). (c) Rejected account number images and their corresponding output results (below each image).	109
Fig. 3.58	Reached SNR for 100% recognition rate.	110
Fig. 3.59	Recognition results for characters corrupted with Added Gaussian Noise (AGN). (a) Noisy grey level images with $\sigma=0.6$ and their corresponding class between “ ”. (b) Successfully recovered and recognized pattern of (a) and their corresponding output results (below each image).	110
Fig. 3.60	Rejection and misclassification of characters corrupted with Added Gaussian Noise (AGN). (a) Noisy grey level images with $\sigma=0.8$ and their corresponding class between “ ”. (b) Proposed method output results; misclassified (“M”) and rejected (“R”) patterns of (a).	111
Fig. 3.61	Successfully recognized patterns and their corresponding SNR (below each set) at different noise level (a) Training set (b) 1-NN (c) HDM (d) MLP-Assoc. (e) CSM (f) SC (g) Hopfield-MLP.	111
Fig. 3.62	Broken and incomplete real post check characters correctly recognized and their corresponding output results (below each column images of the same class).	112

Table 3.1	Recognition rate (%) performance as a function of the SOM dimension and filter bank order (p, q).	64
Table 3.2	Recognition rate performance as a function of the SOM dimension for FMT-SOM and FMT-SOM-MLP for $p=4$ and $q=4$.	64
Table 3.3	Confusion matrix result of TFM-SOM	65
Table 3.4	Confusion matrix result of TFM-SOM-MLP	65
Table 3.5	Recognition rate (%) comparison for $L=50$.	71
Table 3.6	Recognition rate (%) with UWC for L and N	72
Table 3.7	Best performance comparison of the three classifiers using the test set of 16800 characters. For the combined method we chose $R_H=0.12$, $R_M=0.3$ and $T=1$.	90
Table 3.8	Best performance comparison of the three classifiers; the Hopfield network is trained with 13 printed characters and the MLP network with 2445 printed characters. The three classifiers were tested using the 15052 printed characters test set. For the proposed work we chose $R_H=0.58$, $R_M=0.5$ and $T=1$.	103
Table 3.9	Best performance comparisons of the six classifiers; the Hopfield network that constitutes the proposed work was trained with 13 characters, whereas the MLP and the five other classifiers were trained with 2445 printed characters. The six classifiers were tested using the 15052 printed characters test set. For the proposed work we chose $R_H=0.58$, $R_M=0.5$ and $T=1$. The parameters of the SC were set to $R_H=0.12$, $R_M=0.8$ and $T=1$, and those of the MLP-Assoc. to $R_M=0.8$ and $R_A=0.4$.	107
Table 3.10	Application results of the proposed method ($R_H=0.58$, $R_M=0.5$ and $T=1$) and the 1-NN-based classifier on 600 post checks.	107

INTRODUCTION

Today, the majority of information are stored, employed and distributed by electronic means. The sweeping modules can convert documents stored on papers into appropriate format to the computers. The daily increasing application of analysis systems for digital documents has supported the development of text processing digital units in order to obtain the information that appears on the digital documents. The digital or electronic document, resulting from the dematerialization of the paper documents, is thus on the way to preoccupy the companies and the organizations in the broad sense. Today however, it is considered that still 80% of the data processed by the companies are in pure paper forms. The considered cost of these treatments being about 10% of the sales turnover of the company, one measures the impact which could have a numerical solution since this one must be able to better carry out these treatments and more quickly.

The automatic identification of the writing is significant in a lot of applications, for instance, reading of postal address and bank check data acquisition at the banks. These two applications concern, for each one, several billion objects per annum. These operations gained a considerable interest for the industry as well as the scientific and research community.

The automatic reading machines of bank checks require an intensive study owing to the fact that it has a significant commercial application. That is due to the number of significant checks to treat each day in a bank. An automatic reading system must save much work in a way to make it possible to recognize half of the checks to be treated with a high score. Two types of writing are used in bank checks, namely, the *printed text* (account number, customer name and address) that constitutes a part of the check and the *handwritten word, numeral character*, and signature which represent the part to be filled in by the customer.

The optical character recognition (OCR) is one of the most successful applications in the field of the automatic pattern recognition. At the beginning of the Fifties, the OCR recognized only the **printed** documents of high qualities. The actually developed OCR can only identify the printed documents of high and medium quality. Current research in the OCR is addressed to the document that is not easy to handle by the available systems, by including

the documents that are severely *degraded*. Therefore much of the effort has been made to achieve an error rate of substitution and a rejection rate the lowest possible, even with printed text of bad quality as in the case of the present work. This kind of recognition system deals with the first type of writing mentioned above.

The goal of the recognition of the **handwritten** is to transform a written text into a representation understandable by a machine and easily reproducible by a text processing. This task is not trivial because the words have an *infinity of representations* due to the fact that each person has his own writing style. Thus, the recognition of the writing appears somewhat similar to the voice recognition, in the sense that there is a multitude of ways in writing a word, which makes this later task quite as difficult. According to the type of writing that a system must recognize (handwritten word and numeral), the operations to be carried out and the results can vary notably. This kind of recognition system deals with the second type of writing mentioned above.

The principal goal of these systems is the transformation of the text images into the identified ASCII code characters, which is mainly carried out with optical character recognition (OCR) systems. After intensive research during several decades, many algorithms have been proposed and impressive progress was accomplished in the area of automatic character recognition. Most of the share of these achievements is in automatic reading of bank checks. In spite of the significant successes reached in the field of the character recognition, recognition of the cursive writing, the handwritten numeral and the degraded printed character remain a challenge problem.

In this thesis, we propose new solutions to the problems raised previously, in particular, the recognition of the degraded printed character, the numeral and the handwritten word. Solutions are also proposed in the preprocessing step of the handwritten writing, namely, the horizontal slant correction of the numeral character and the word skew detection.

The three techniques developed within the framework of this thesis present originality. The originality of this work is always summarized in the performances reached. This originality can be in all the parts which integrate an automatic reading system, in some part or only in one part. The goal is that this intervention is likely to increase the performances of the system. Our contributions are summarised in the following paragraphs:

- Preprocessing and feature extraction:
 - New simple and efficient character slant correction based on lower and higher character centroids applied to handwritten numeral is developed.

-New feature extraction set is developed for off-line unconstrained handwritten numeral character recognition. The feature extraction used collects well the relevant information of the handwritten character according to different angles

-New method is introduced for accurate skew correction and central zone localization (SC-CZL) in order to detect the three zones, namely, lower, upper and central zones.

- Degraded printed character recognition:
 - A sequential combination method for degraded character recognition is developed. It is based on the combination on the Hopfield model and the MLP-based classifier using different reject threshold.
 - A method for degraded character recognition is presented. The main idea is based on the introduction of a quality measurement parameter of the degraded printed character using the Hopfield model at a fixed number of iterations.
- Handwritten numeral recognition:
 - Handwritten numeral recognition with multiple Markov models is introduced. The proposed method combines four recognition systems based on HMM with equally and unequally weight.
 - Handwritten numeral recognition using Fourier-Mellin transform and a self organisation map is also developed within the frame of this work.
- Handwritten word recognition:
 - A new global (holistic) handwritten word recognition applied to French legal amount is developed. The purpose of this method is to recognize the word in a global way from a dilated full form. Its originality is related to the choice of the class model or prototype. The objective of the recognition is to arrive at a reduced number of candidates and to determine the class to be recognized among these candidates. The choice is based on several tests and calibrations.

The work of this thesis consists in developing several recognition systems; it is divided into three essential and significant chapters as follows:

- The first chapter will be devoted to pattern recognition by introducing the basic tools relating to document recognition.

- The second chapter will present the state of the art, feature extraction and classification of a document recognition system. This chapter introduces briefly classical and neural network methods related to the methods developed in this work.
- The third chapter will be devoted to experimental results. This chapter will present two parts: the first one deals with preprocessing and feature extraction results and the second part presents results of degraded character recognition, handwritten numeral and global handwritten word recognition.

CHAPTER 1

DOCUMENT RECOGNITION

1.1 Introduction

The document recognition is defined as being the data-processing techniques of representation and decision, making it possible for the machines to simulate the automatic reading as a significant behaviour. The goal thus is to obtain programs making it possible to reproduce the phenomena of effective human being perception. The task of a recognition system consists in equipping the machine with sensorial organs (physical sensors such as: scanner, camera,...etc) collecting external information on various forms. It has for objective in one part to describe this captured information and in another part to make, on the representation thus obtained, a decision of identification by reference to a training set. The principal goal of these systems is the transformation of the text images into identified characters of ASCII code, which is mainly carried out with the optical character recognition (OCR) systems. An OCR system is often composed of a stage of preprocessing [1][2], a stage of comprehension and segmentation of document [3][4], a stage of feature extraction [5][6], and a stage of classification, [7][8] as shown in Fig. 1.1. The different areas covered under the general term "character recognition" fall into either the online or off-line categories (see Fig. 1.2), each having its own hardware and recognition algorithms.

1.2 On-line and off-line systems

The on-line systems are real-time operations [9][10]. On-line recognition is dynamic whose data acquisition proceeds during the writing using a styler and a digitizing tablet. The continuous response of the system makes it possible to the user to correct and modify its writing in a direct and instantaneous way. Off-line recognition, which is the field investigated in this thesis, is performed after the writing or printing is completed. It is a static recognition, which starts after the acquisition of the whole document [11]-[13]. It is appropriate for printed documents and the already written manuscripts.

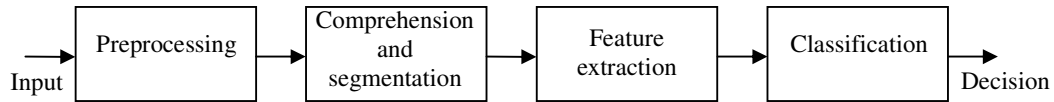


Fig. 1.1 OCR block diagram.

This mode allows the instantaneous acquisition of a significant number of words, but forces to carry out expensive preprocessing to find the reading order. In the first case, the space coordinates are regularly sampled and ordered according to the layout while in the second case, the data available are the image bitmap documents. It is the latter type of recognition which will be considered in our work.

1.3 Analytical and global approaches

The handwritten techniques of off-line recognition of the writing can be classified in two principal categories: analytical and global (holistic) [14]. In the analytical approach, the word is segmented in characters (or pseudo characters), and then identified in various characters (or pseudo characters) with the character models [15]. Since many combinations of characters are not readable, contextual post processing is carried out to detect errors and to correct them using a dictionary [16]. The advantage of this approach is that only few models or references are necessary for all the words, and the principal disadvantage is that the approach leads to likely segmental errors. In order to solve this problem, some methods employ implicit segmentation techniques. They carry out the segmentation and recognition at the same time [17]. However, they cannot completely avoid segmental errors. The individual character models ignore the relationship among neighboring characters in a cursive word. Figure 1.3 (a)-(c) shows the influence of the characters “u” by their preceding characters.

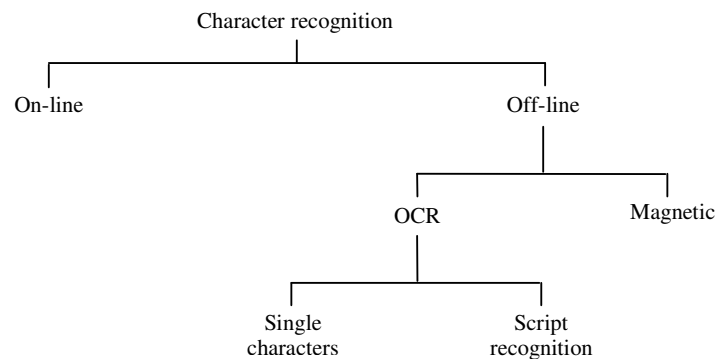


Fig. 1.2 The different areas of character recognition.

Another type of method is the global or holistic solution [18]-[20], which identifies a word like simple entity. The global approach recognizes a word like only one entity by the use of its characteristics in entirety without consideration of the characters. The word is represented by a vector or a list of primitives independent of the identity of the present characters. The global solution can avoid the segmental errors, but it needs at least a prototype or model for each word. Because this approach does not treat characters and does not employ the relationship among neighboring characters, they are usually regarded as tolerant with the dramatic deformations which affect the cursive unconstrained writings [21]. A principal disadvantage of the global methods is that the lexicon can be only updated by word samples. Therefore it is considered to be tolerant with the deformations which relate to cursive scripts.

The analytical approaches are sensitive to the style and the quality of writing (see Fig. 1.4), as they are strongly dependent on the effectiveness of the procedure of segmentation. Whereas the global solutions are generally employed in the fields with a lexicon of reduced size. Although many algorithms were developed by using the two approaches [11][22], the recognition of a word still represents a challenge for the scientific community.

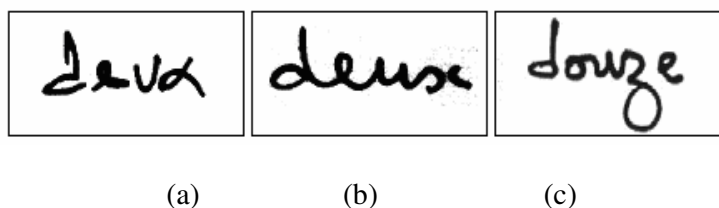


Fig. 1.3 Influence of the character “u” by its preceding character.

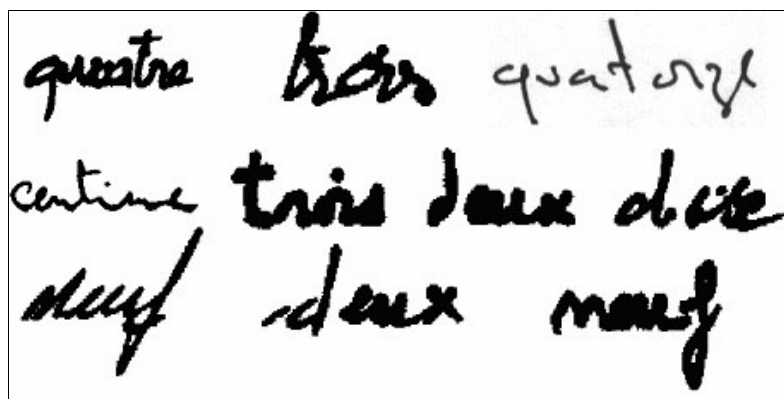


Fig. 1.4 Poor quality handwritten legal amounts.

1.4 OCR and imagery

Within the framework of the digital libraries, digitalization refers usually to the process of conversion, in electronic form, of a document on paper or film. Electronic conversion is carried out by imagery, a process which consists in sweeping a document, which produces an electronic representation of the original in the form of an image in dot mode. The optical character recognition is a later and optional process, which transforms the image into dot mode text printed in textual code, thus making it readable with the machine.

1.5 Process of document recognition

The objective of a pattern recognition is the identification of the forms at least as complex as those of the training set. The general structure of such a system is illustrated in Fig. 1.5. The recognition and the interpretation of the printed writing lie within the general scope of the man machine communication. The automatic reading of the printed writing is of undeniable interest in the achievement of the tiresome tasks as those which one meets in certain fields: reading of the postal cheques, bank checks, reading of purchase orders... etc. It offers today an increase of interest with the development of the new methods making it possible to communicate directly with the machine in a more natural way. It is in this context that our project is registered which aims at studying a handwritten recognition system and for printed characters in particular. It is certain that hundreds of thousands of bank checks are exchanged daily, which makes the processing operation of the checks expensive [23]. A pattern recognition system is composed of the following blocks:

1.5.1 Physical world

The chain starts from the physical world which is an analogical space of infinite dimension, external to the machine, also called *form space*. The objects in this space are described in various ways, with a multitude of properties, of which it would be difficult to take account of each one within the pattern recognition.

1.5.2 Acquisition

It is an operation of conversion of the continuous physical world towards a discrete numerical world. This last called also *representation space*, in a one or two dimension still too significant even if it is finite. The dimension of this space is selected voluntarily large so as to be able to have a maximum of information of the pattern.

1.5.3 Preprocessing

The number of functions that includes preprocessing step in a recognition system, depends strongly on the type of characters to be recognized. Its main objective is to produce a well represented version of the original image so that it can be used directly and effectively by the feature extraction component of the recognition system [1][24][25]. The objective of the preprocessing is to facilitate the characterization of the pattern (character, figure, word) to be recognized by: *denoising* the image representing the pattern, *correcting* the external pattern form, or *reducing the quantity of information* to be processed to keep only the most significant information.

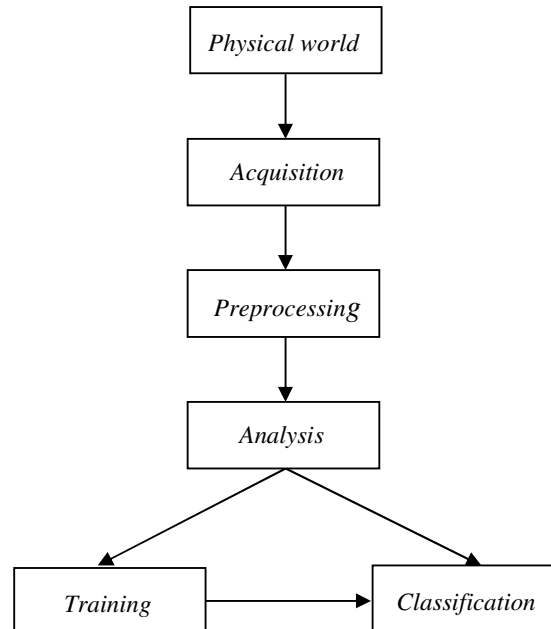


Fig. 1.5 Pattern recognition block diagram.

The image denoising primarily consists in reducing the residual noises due the acquisition systems, the quality of the impression and paper. The correction of the form relates to certain

slanted or skewed patterns (characters, figures, and words). Thus it is necessary to correct the slant and skew of the letters in a word in order to facilitate the segmentation and zones detection. The reduction of the quantity of information to be treated can be obtained starting from the operations aiming at bringing back the thickness of the feature to a pixel, that is to say by squelettisation or starting from extractors of higher, lower or interior contours. These operations are illustrated in Fig. 1.6. Thus, the preprocessing includes the follows stages:

-Filtering or noise reduction: The noise is a random error in the value of pixel; it is a value usually rising from the reproduction, the digitalization and the transmission of the original image [26]. The noise can be divided into three categories: noise dependent on the signal, noise nondependent on the signal and black and white noise. The noise cannot always be entirely removed; one often uses smoothing to replace the origin pixel value by the average of the values of the surrounding pixels.

-Binarisation: The digitized symbolic image presents a great quantity of important information. Part of this one is useless; it is convenient to process only the informative and useful data [27]. Then the thresholding (binarisation) makes it possible to distinguish an object in contrast with a background. The levels of gray are partitioned in two classes black and white, where the black represents the object, and the white represents the background. The binarization of an image has several advantages, one of the most significant is certainly the low memory capacity needed, as well as the simplicity of the operators that are associated to it. The operation of thresholding consists in comparing the intensity of all the pixels with a value of reference "threshold" [28]. Thresholding techniques can be categorized into two classes: *global* and *local*. Global thresholding [29] algorithms us single thresholds, while local thresholding [30] compute a separate threshold for each pixel based on a neighborhood of the pixel.

-Form correction and normalization: In handwritten numeral characters, one of the major variation in writing style is caused by slant, skew and size, which are defined as the slopes of the general writing trend with respect to the vertical and horizontal lines, and the image size respectively. The slant correction operation consists in correcting the tilted character in order to return it right. Whereas, the skew correction or deskewing is correction of the character horizontal slope in order to return it to horizontal. Size normalization is used to reduce the

variation in size. Directly scaling [31] of characters or words to an identical size will result in a standard size.

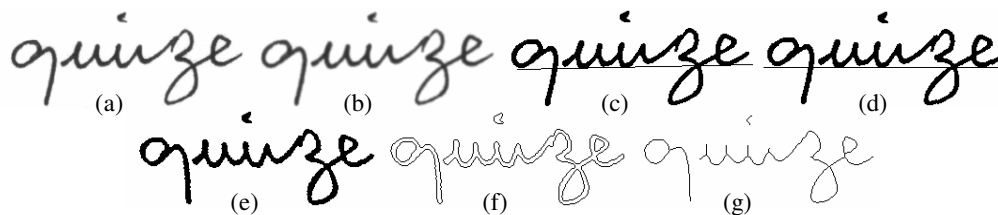


Fig. 1.6 (a) Original image (b) Filtered image (c) Image binarization and skew detection (d) Skew correction (e) Slant detection (f) Contour detection (g) Thining application.

-Contour detection and thinning: Contours in symbolic images represent the border between the objects, or the limit between two pixels of which the gray levels represents a significant difference. The contour extraction consists in identifying in the image the points which separate two different textures. Thining operation consists in extracting the median axis from a character [32]. The skeleton must preserve the form, connexity, topology and extremities of the layout, and should not introduce parasitic elements. The resulted output is a form of one pixel thick. Figure 1.6 illustrates contour detection and thinning operations.

-Segmentation: The characters can be produced in attached letters. They can also overlap. When it is a question of a character recognition system which must manage to identify characters (instead of identifying complete words simply), it is necessary to determine (roughly) where a character begins and where it ends [5][2]. It is primarily the goal of the segmentation. There are systems [3] which make it possible to classify without segmenting explicitly the handwritten word.

1.5.4 Feature extraction

The feature (parameter) extraction is in fact one of the essential functions of a recognition system. It includes the measurement of the characteristics of the shape of the cleaned pattern which are relevant to classification. When the extraction of the characteristics is complete, the pattern is represented by a set of features vector that represents extracted characteristics. There is an infinite number of possible features that one can extract from a finite pattern. It is necessary however to keep only the features that have

a possible relevance for classification. This supposes that during the training phase, the features vector should be chosen, according to certain classifiers, that will produce the best results. The features are classified in two categories [36]: structural features and statistical features. These two types can be combined forming a vector of features. Several techniques have suggested some feature extractors in the character recognition field [14][33]-[35].

1.5.5 Training

The recognition techniques calculate a certain number of characteristics, which must have the maximum of useful information serving as the only data representing the form. The training is a key stage in the recognition chain. Its role is to inform the decision using a priori knowledge on the patterns. From specific criteria to the patterns, the training tries to define references or models to characterize classes of decision. This makes it possible to dictate to the system the most adequate algorithm of decision with respect to the selected rules of the chosen modelling.

The training phase consists in characterizing the pattern classes so as to well distinguish the pattern of homogeneous families. It is a key phase in the recognition system. One distinguishes two types of training: *supervised* training and *unsupervised* training. In the case of the supervised training, a representative sample of the the patterns set to be recognized, is provided to the training module. Each pattern is labelled by an operator called professor; this label makes it possible to indicate to the training module the class in which the professor wishes that the form be arranged. In the case of the unsupervised training, one provides to the recognition system a great number of patterns that are not labelled. The classification phase will then be charged to identify automatically the patterns that belong to the same class.

1.5.6 Classification

Classification is the stage of recognition itself. Its role is to identify the test pattern starting from the realized training. The method of decision is often exhibited by the training, which means that the criteria used for the recognition are the same as those used for the training. Among the techniques used, some are founded on the concept of proximity

and require calculating a distance or a probability from resemblance to the defined models. Others are founded on the analysis of the structure of the form and rather try to check certain coherence in the different substructures. The response of the decision can be, according to the case, the name of the pattern in case of good knowledge, several names in the case of ambiguity, or the rejection of the pattern in the event of incompatibility of description with the forms of reference.

1.6 Methods of document recognition

There are several techniques of document recognition (see Fig. 1.7), the most classic are the statistical methods [37]-[41], and structural models [40]-[42], which have been applied for a long time. Since the beginning of the Eighties, one observed the introduction of a new revolutionary method known as connexionnist or neural. The linguistic methods are interested in the structure of the forms and have their description in terms of assembly of primitive sub forms. The connexionnist methods are based on the networks of formal neurons, which are regarded as complex non linear discriminators. The geometrical or statistical methods, merge on a statistical characterization of the parameters of the studied forms, they make it possible to make a decision of classification of an unknown form according to a criterion of *maximum probability of membership* to a class. The description of these methods is detailed hereafter.

1.6.1 Statistical methods

This approach consists in determining the extracted features of a given pattern in order to characterize them in a statistical way. In this approach, all the methods try to extract from the pattern, a set of measurements (such as perimeter, surface...etc) which define and distinguish it from the class to which it belongs. These methods make it possible to make a decision of classification on the unknown form according to a criterion of "maximum probability of membership of a class". Statistical pattern recognition can be classified into a *parametric* method and a *non-parametric* method. In the case of a parametric method, the probability distribution type of target patterns is defined in advance. With a non-parametric method, on the other hand, recognition equipment can be designed only from sample patterns, without any prior knowledge. In other words, a non-parametric method can process various

recognition patterns that have different probabilistic statistical natures simultaneously and easily.

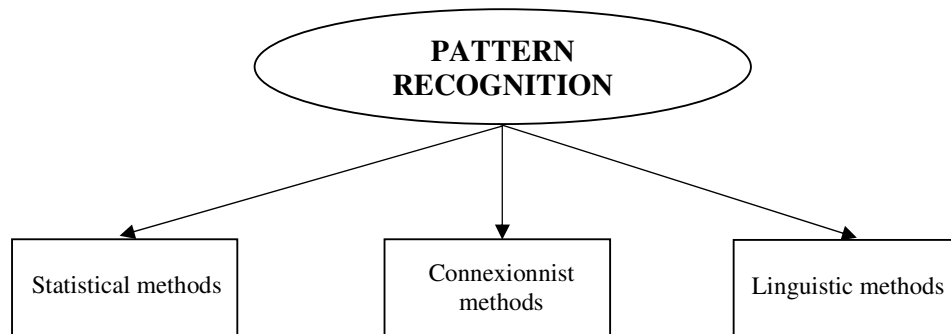


Fig. 1.7 Pattern recognition methods.

1.6.2 Connexionnist methods

The connexionnist methods take an increasingly significant share among the methods of pattern recognition [43]-[47]. This is due primarily to the neuronal basis of their methods. They constitute an alternative to the traditional methods and offer operational solutions to solve complex problems on real data (speech, image...etc). A connexionnist model can approximate any function, such a model can easily associate the input shape to its class. Thus, a problem of classification can be solved by finding a function that associates a set of input patterns to a set of output classes. The connexionnist network will then play the role of a transfer function which for a value in input will provide the value of corresponding output. For automatic classification, the output value corresponds to a membership class of the input value. One can summarize the advantages of the connexionnist techniques by the following points:

- Power of approximation: the multi-layer connexionnist networks in theory are able to approximate any transfer function if the number of neurons is sufficiently large.
- Robustness: as shown by the majority of the experiments in various research [45][47], the connexionnist models are very effective for very difficult tasks of pattern recognition.
- Ability to parallel implementation.

1.6.3 Linguistic methods

The preceding techniques indicate many calculations of distance between vectors, conditional probabilities and present the major disadvantage to be unaware of the topological side and structural form. To solve this defect, the linguistic methods do not regard merely the form as a unit of points represented in a geometrical space, but like a set of elementary forms or symbols arranged between them and describing the form as well as possible. Linguistic pattern recognition can be classified into a *syntactic* method and a *structural* method [48]-[51]. Automatic feature derivation was required to automate the inference of a classifier from the raw data. Several statistical inference techniques were developed to overcome this problem, but soon the complexity of numerical feature derivation became evident. More complex feature representations were required to represent the components of the objects in an image, which led to introduction of symbolic features and their spatial relationships. This area became known as syntactic pattern recognition when formal language theory was used as a way to integrate symbols and their interrelationships, the analysis of samples and the inference of grammars and languages from a set of symbolic samples.

Formal languages appear to be a natural way to deal with the problems involved with symbolic features. However, it was soon realized that when the main issue is to emphasize feature analysis and a description of their relationships, then symbolic analysis could be treated by means of other mathematical tools, such as string, tree or graph matching. This area of research became known as structural pattern recognition.

1.7 Multiple classifiers

The idea of combining different classifiers for improving their performance received a lot of attention in the last few years [52]-[54]. A single feature extraction method and a single classification algorithm do not yield a high recognition rate when compared to systems using several feature extractors and classifiers [55]. In pattern recognition applications, the classification power of a system can be improved by combining several classifiers [56]-[58]. Obviously performance of the system cannot be improved if the individual classifiers make the same mistakes, thus it is important to use different features and different structures in the individual classifiers [59]. In the literature we can distinguish *parallel* and *serial* combinations [55][58].

1.7.1 Parallel combination

In the parallel combination, all the classifiers run on the same data in order to produce a decision on the class corresponding to the unknown pattern [55]. All these decisions are fed into a combiner (see figure 1.8). The combination rules employed by the combiner include functions such as product, sum, mean and median. In this type of combination the individual classifiers are working independently of each other.

1.7.2 Serial combination

In serial combination, the classifiers are arranged in a list, for each pattern to be recognized, the first classifier is used to decide if a possible refinement of the decision is required by one or more subsequent classifiers. Among different combination architectures, the most common are the conditional and the hierarchical ones. In the conditional combination architecture, the second classifier is applied only when the first one rejects the incoming pattern [58]. The decision of the first classifier in a serial combination is rejected if its confidence level falls below a pre-defined threshold. Usually, the initial classifier represents coarser decisions than the final classifier [60].

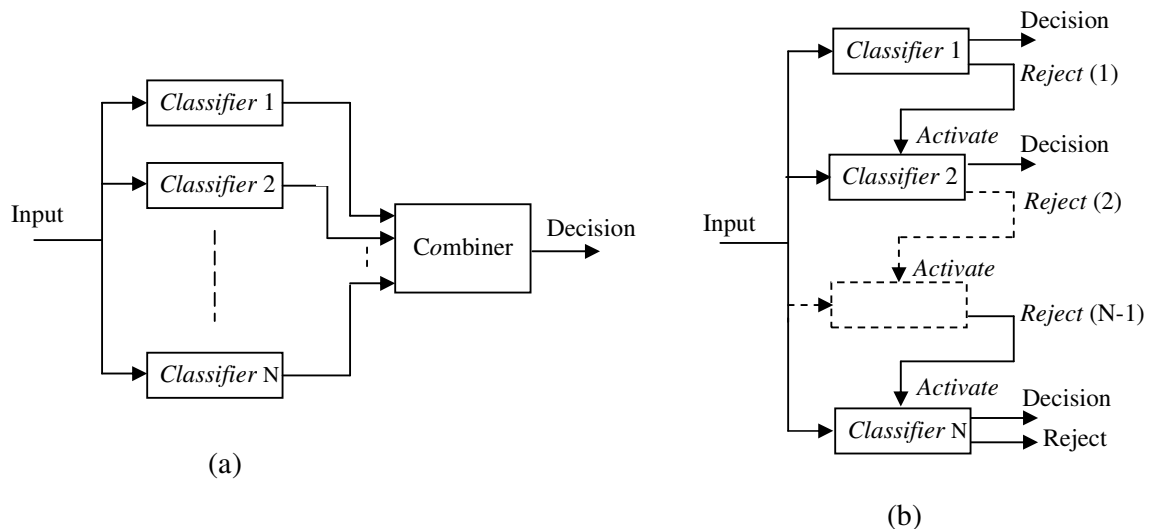


Fig. 1.8 (a) Parallel combination (b) Serial combination.

1.8 Conclusion

This chapter enabled us to have a global outline of a pattern recognition system, namely, the preprocessing, the feature extraction and the classification. We have also presented the basics of a pattern recognition system by introducing the tools related to this field. Among these basics, in first place, one finds the on-line and off-line recognition which constitute the starting point of each recognition system. In second place, one finds also different systems based on the analytical and global or holistic approaches. These approaches, rest in three types of methods of pattern recognition systems, namely, the statistical methods which are the most classic, the structural methods and the connexionist methods which are based on networks with formal neurones. And finally, we end with the introduction of combined methods based on the use of several classifiers in serial or parallel manner. They have for prime objective to obtain performances largely exceeding those of the single classifiers that compose them.

CHAPTER 2

FEATURE EXTRACTION AND CLASSIFICATION

2.1 Introduction

In this chapter we will present the state of the art in recognition methods, namely, the recognition of the degraded printed character recognition, the handwritten numeral character and the handwritten word recognition. This will be followed by brief explanations of some feature extraction methods that are parts of our developed work. This chapter will present also a brief explanation of classical and neural network classifiers related to the developed methods in this work.

The automatic reading of printed text and the handwritten writing is of considerable interest in the achievement of the fastidious tasks as those which one meets in certain fields: reading of the postal checks, bank checks, reading of command... etc. The reading of the bank checks is one of the most significant applications of the recognition of the writing. Everyday, a standard bank sorts thousands of checks and the operation is expensive. The recognition of the bank checks presents a big challenge of research in the field of recognition and document analysis. A reasonably high rejection rate could be allowed for the processing system of a bank check, but the error rate in the recognition must be as small as possible. Thus, the processing system must be able to effectively treat the written data of various styles.

2.2 State of the art

A significant number of applications of the handwritten character recognition was carried out during the previous decade. Most of these achievements are in the reading of postal address and amount of a bank check [14][22]. In spite of the successes reached in the field of character recognition [61]-[63], recognition of the cursive writing, the numeral character and the degraded character remains a challenging problem. The performance of a character recognition system depends

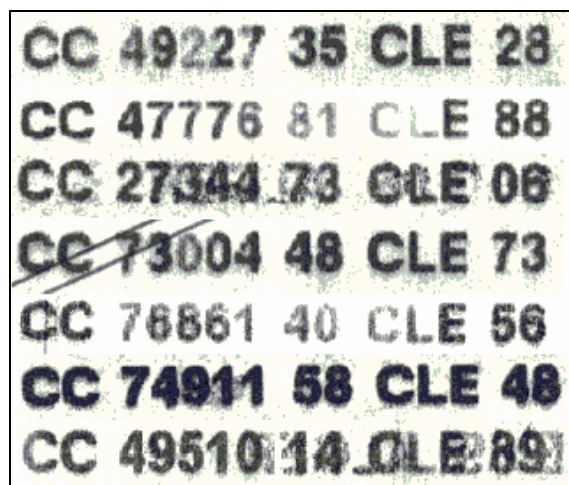


Fig. 2.2 Poor quality account checks numbers.

Thus the methods that really correspond to this type of checks (for example Algerian post checks) are those applied in degraded character recognition (DCR) [1][22][23].

The recognition of degraded documents remains an ongoing challenge in the field of optical character recognition. This is due to the degradation which could be originated from: low quality originals, quantization errors in the digitization process and non optimal light and contrast settings. This could come from the copying or scanning process, non-sharp or low-contrast printing on the document, transmission errors, or paper defects and/or dirty optical or sensor systems.

In spite of significant improvements in the area of optical character recognition [73]-[75], the recognition of degraded printed characters, in particular, is still lacking satisfactory solutions. Studies on designing recognition systems with high performance for degraded documents are in progress along three different aspects. One is to use a robust classifier, a second is to enhance the degraded documents images for better display quality and accurate recognition, and the third is to use several different classifiers [76]-[78]. Many attempts have been made in order to solve the problem of the degraded character recognition [79]-[82]. A. J. Elms and J. Illingworth [83] suggest Hidden Markov models (HMM) to capture the shape profile of the character. This method was applied with some success in recognizing degraded printed text. J. D. Hobby and T. K. Ho [77] proposed a method to enhance such degraded document images for better display quality and recognition accuracy applied to fax images. Outline descriptions of the symbols are then obtained that can be rendered at arbitrary resolution. T. K. Ho and al. [78] proposed three methods for

class set reranking based on the highest rank, the Borda count, and logistic regression. These methods have been tested in applications of degraded machine-printed characters and work for large lexicons, resulting in substantial improvement in overall correctness. M. Sawaki and N. Hagita [79] proposed a robust recognition method based on a complementary similarity measure for characters with graphical designs and degraded characters. Their experimental results for newspaper headlines with graphical designs show a recognition rate of 97.7 percent. H. Liu et al. [80] used a simple post processing algorithm, based on the similarity measure techniques for the optical recognition of degraded characters. Tests were carried out on input images that may be blurred, rotated, or corrupted by additive Gaussian noise using computer simulation. A. Tonazzini et al. [81] proposed a recognition system for highly degraded printed documents for the purpose of recognizing text characters applied to ancient printed texts. They used blind deconvolution and Markov random field (MRF) based segmentation techniques, and feedforward multilayer neural for printed character recognition. Their experimental results show that the proposed system performs a very precise segmentation of the characters and then a highly effective recognition of even strongly degraded texts.

2.2.2 Handwritten numeral recognition

Cariou and al. [82] proposed an original methodology which allows the detection and the recognition of multi-oriented and multi-scaled patterns. The proposed method was applied firstly to isolated pattern and secondly to connected shapes from technical documents representing the network of the French telephone operator, France Telecom. They show that the results of the application of this technique are very encouraging since the classification rate reaches excellent scores in comparison with classical techniques. Sadykhov and Selinger [83] developed a fast algorithm for calculation of the Fourier-Mellin moments of binary images for recognition of handwritten characters (Arabic numerals). A significant multiple reductions in the number of required operations was achieved. Around 90% recognition rate was obtained. Adam et al. [84] focused on the computation of a new set of features allowing the classification of multi oriented and multi scaled patterns.

This set of invariants is based on the Fourier-Mellin transform. The interests of this computation rely on the excellent classification rate obtained with this method and also on using this Fourier-Mellin transform within a filtering mode with which we can solve the well known difficult problem of connected character recognition. Chi et al. [85] proposed a handwritten numeral recognition using combined self-organizing maps and fuzzy rules. The SOM algorithm was used to produce prototypes which together with corresponding variances are used to determine fuzzy regions and membership functions. They show that the combination technique achieves satisfactory results in terms of classification accuracy and time, and computer memory required. Cho [86] presented three neural network classifiers including the self organizing maps (SOM) to solve complex pattern recognition problems. Experiments were performed with the unconstrained numeral database of Concordia University. The SOM classifiers achieved a 96.05 % in the recognition rate. Lim et al. [87] proposed a method to classify handwritten numerals using modular neural networks with image dithering. The initial clusters produced by SOM learning are extended to further include the clusters which overlap each other. Each MLP is assigned to each extended cluster. The gating network to combine the decisions of the expert MLP networks is designed and trained on such clusters. The experimental results demonstrated that the proposed method produces very good recognition performance.

A single feature extraction method and a single classification algorithm do not yield a high recognition rate when comparing to systems using several features extractor and classifiers. In pattern recognition applications, the classification power of a system can be improved by combining several classifiers [88]. Obviously performance of the system cannot be improved if the individual classifiers make the same mistakes, thus it is important to use different features and different structures in the individual classifiers [89]. Recent works concerned multiple expert systems for handwritten numeral recognition [90]-[92] and many approaches and techniques have been developed and evaluated [89][93]. The recent studies on designing recognition systems with high performance are in progress along two different aspects. One is to construct a recognizer using several features at the same time, and the other is to use several recognizers [94][95]. J. Grim et al. [96] designed a statistically and biologically compatible neural network model based on the expectation-maximization (EM) algorithm. It was applied to recognize unconstrained handwritten numerals.

They achieved a recognition accuracy of about 95% on the Concordia University database. A. Jr. Britto et al. [92] proposed a handwritten numeral string recognition method composed of two HMM-based stages. They used two stages; the first stage is an implicit segmentation strategy based on string contextual information to provide multiple segmentation-recognition paths. Whereas the second stage is a verification stage based on a digit classifier. The two system stages are shown to be complementary in the sense that the verification stage is shown to be a promising idea to deal with the loss in terms of recognition performance brought about by the necessary tradeoff between segmentation and recognition carried out in the first system stage. T. D. Pham and Y. Hong [97] proposed a methodology for dealing with the fusion of multiple classifiers. It uses the concepts of fuzzy measure and fuzzy integral. A fuzzy-integral model for the fusion of multiple classifiers was introduced. Their experimental results on recognition of handwritten characters using their proposed fusion model technique were also improved with genetic algorithms. Ye Xiangyun et al. [94] proposed generic frameworks for hierarchical and parallel combination of multiple string recognizers and a parallel combination system, StrCombo, is implemented based on three independent alphanumeric handwritten string recognizers that act as black boxes. They achieved a substantial improvement over any one of the individual recognizers, as demonstrated by experimental results on standard numeral string databases and a non-standard alphanumeric string database from real-life applications. J. K. Hee and W.L. Seong [98] used the upper bound of a Bayes error rate bounded by the conditional entropy of a class variable. Hence the multiple classifiers recognizing unconstrained handwritten numerals were combined by the approximation scheme based on the minimization of the Bayes error rate, and high recognition rates were obtained. L. Kwanyong et al. [95] proposed a multistage combination method for unconstrained handwritten numerals recognition. The method is a two-stage combination method which uses multiple combination methods at the same time. The recognizers are first combined by several combination methods of different classes simultaneously, and then the results are combined by another combination method to generate a final result. Five recognizers and eight combination methods were used in the proposed system. The experimental results showed that the recognition rates on CENPARMI and CEDAR data were 97.75% and 98.6%, respectively and the recognition performance could be improved as the process passed through stages.

2.2.3 Handwritten word recognition

Since in our work we propose the global solution to the handwritten word, then the state of the art will concern only this type of solution. D. Guillevic and C.Y. Suen [99], used a combination of a global feature scheme with a hidden Markov model (HMM) module. The global features consist of the encoding of the relative positions of the ascenders, descenders and loops within a word. The HMM uses one feature set based on the uncertain contour points as well as their distance to the baselines. The developed system was also applied to a balanced French database of approximately 2000 checks with specified amounts. Paquet et al. [100], investigate three different approaches for the global modeling and recognition of words used to write the legal amount on French bank checks. A lexicon of 27 amounts was used, written in mixed cursive and discrete styles. The first model is a global one since it does not require any explicit letter level and the two others are based on an analytical approach. The three approaches have been tested on real images of bank checks scanned for the French Postal Technical Research Service (SRTP). De-Almendra-Freitas-CO and al. [101], presented a system for the recognition of the handwritten legal amount in Brazilian bank checks. Their recognizer, based on hidden Markov models, does a global word analysis. The word image is transformed into a sequence of observations using pre-processing and feature extraction stages. Their experimental results, when tested on database simulating Brazilian bank checks, show the viability of the developed approach.

2.3 Mathematical morphology

We give in this section a brief illustration on mathematical morphology and its main role in the area of image processing related to our method. The mathematical morphology techniques are based on place-theoretic concepts and the nonlinear superposition of the signals and images. Morphological operations were applied successfully to a range of problems including the image processing, the analysis tasks, the noise suppression, the extraction and the identification of models [102]-[105].

Let us consider a gray level image containing an object A, and B a structuring element comparable to a particular geometrical form. B_x indicates a structuring element B

whose origin is placed into x . The erosion and dilation of A by B can be written in the following way [106][107]:

$$A \ominus B = \{x \mid B_x \subseteq A\} \quad (2.1)$$

and

$$A \oplus B = \{x \mid B_x \cap A \neq \emptyset\} \quad (2.2)$$

From the operation of erosion and dilation, one can define morphological opening and closing. These operations are also usually used in image processing. The opening and closing of A by structuring element B are given by:

$$A \circ B = (A \oplus B) \ominus B \quad (2.3)$$

and

$$A \bullet B = (A \ominus B) \oplus B \quad (2.4)$$

The opening generally causes to smooth the contour of the objects, to cut the narrow isthmuses and to remove the small islands or the narrow courses. They play the role of morphological filtering. The application of morphology in our case was to localize and detect the account check number (ACN) on the post check. Once the ACN is localized it is automatically closed to detect and localize the 10 blocks that include the account character (see Fig. 2.3). The structuring element was chosen to be horizontal of 1 row by 13 columns using the following equation:

$$g = f \bullet h \quad (2.5)$$

Where f is the input image and h is the structuring element.

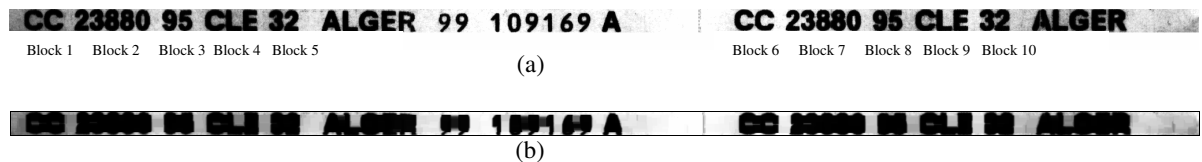


Fig. 2.3 Morphological closing operation (a) Postal account number image (b) Closing operation with horizontal structuring element.

2.4 Fourier Mellin transform

The Fourier-Mellin transform (FMT) has been widely used to extract features in the area of document processing [82]-[84]. According to recent works, these features represent patterns in a concise way. We find these features particularly appropriate for recognition of unconstrained numeral characters.

- Application of the analytical Fourier-Mellin transform to the images

The major problems encountered in the pattern recognition techniques are often related to the orientations and the changes in size which the object can undergo to be recognized; therefore it would be interesting to find a procedure which would be independent of the *rotation* and the *scaling* of the object or of any other geometrical transformation [82]. For the handwritten numeral recognition, we propose a method which is based on the Fourier-Mellin transform to solve the two constraints previously quoted and gives powerful solutions. We will give briefly the definition as well as the property of this transform, then its application to the images.

The discrete Fourier-Mellin transform [82] is calculated with the object centroid (k_0, l_0) and can be approximated as follows:

$$|I_f(p, q)| = \frac{|M_f(p, q)|}{|M_f(0, 0)|} \quad (2.6)$$

where:

$$M_f(p, q) \approx \sum_k \sum_{\substack{l \\ 1 \leq (k^2 + l^2) \leq \rho_{\max}^2}} h_{p,q}(k, l) \cdot f(k - k_0, l - l_0) \quad (2.7)$$

and $h_{p,q}(k, l)$ is the filter bank given by:

$$h_{p,q}(k, l) = \frac{\exp(-i[\frac{P}{2} \ln(k^2 + l^2) + q \tan^{-1}(\frac{l}{k})])}{(k^2 + l^2)^{-\frac{\sigma_0}{2}}} \quad (2.8)$$

All the filter bank $h_{p,q}(k, l)$ are complex except $h_{0,0}(k, l)$ which is real valued and all the filter bank $h_{p,q}(k, l)$ is orthonormal. It can be noticed that $I_f(p, q)$ are complex valued,

except $I_f(0,0)$ which is equal to one and $I_f(0,1)$ is real valued. Therefore we have the hermitian property of this invariance set which is:

$$I_{f_1}^*(p,q) = I_{f_1}(-p,-q) \quad , \quad \{(p,q) | (p \in N, q=0) \cup (p \in Z, q \in N^*)\} \quad (2.9)$$

where * is the complex conjugate. Figures 2.4 and 2.5 illustrate the invariance of feature extraction for different rotation and change in size (scale factors; S_c) respectively.

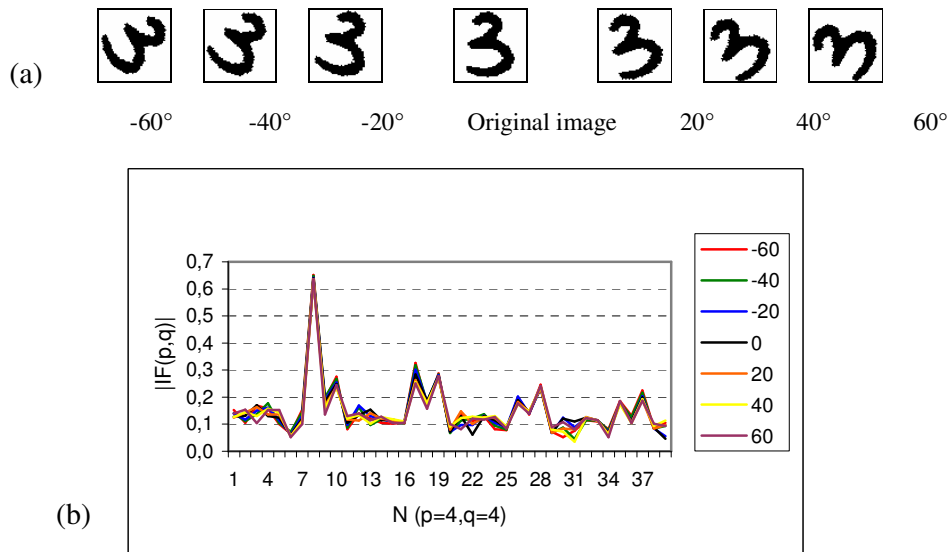


Fig. 2.4 (a) Different rotation of the handwritten character. (b) Feature vector plots with rotation invariance for $p=4$ and $q=4$.

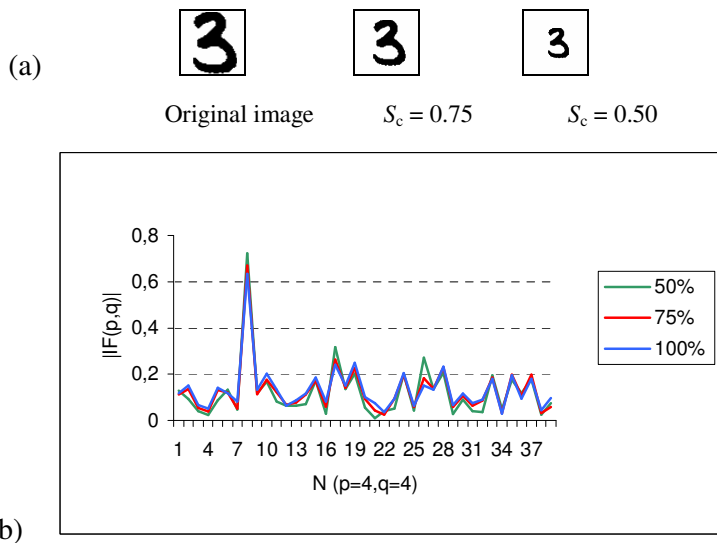


Fig. 2.5 (a) Different scales of the handwritten character. (b) Feature vector plots with scaling invariance for $p=4$ and $q=4$.

2.5 Complementary similarity measure

The complementary similarity measure (CSM) has been applied successfully in the area of character recognition [108]. The CSM is used as a discriminating function for the recognition phase applied to binary images. It is based primarily on the similarity measure between two binary images; a model stored in the training set and a sample image. The attribution of a sample image to a single class among others (where each class is represented by one or more model images) is performed using the highest score of similarity between this sample and the model images of the classes. Let's consider the normalized images x and y (sample and model) of the same size $N = \sqrt{N} \times \sqrt{N}$ pixels. The normalized characters are expressed as N -dimensional binary feature vector as follows:

$$x = [x_1, x_2, \dots, x_i, \dots, x_N] \quad ; \quad \text{where } (x_i = 0 \text{ or } 1)$$

$$y = [y_1, y_2, \dots, y_i, \dots, y_N] \quad ; \quad \text{where } (y_i = 0 \text{ or } 1)$$

The complementary similarity measure S_c of x and y is defined as:

$$S_c(x, y) = \frac{a \cdot e - b \cdot c}{Y(N \cdot Y - Y)} \quad (2.10)$$

$$\text{where } a = \sum_{i=1}^N x_i \cdot y_i, \quad b = \sum_{i=1}^N (1-x_i) \cdot y_i, \quad c = \sum_{i=1}^N x_i \cdot (1-y_i) \quad e = \sum_{i=1}^N (1-x_i) \cdot (1-y_i),$$

$$\text{and } Y = \|Y\| = \sum_{i=1}^n Y_i$$

After having calculated the similarity with the number of existing models or prototypes, only the first two maximas are kept, namely, $S_c(1)$ and $S_c(2)$. These two maximas represent the CSM of the character to be recognized such as: $S_c(1) > S_c(2)$: corresponding to two class candidates (C_{cand1} and C_{cand2}) [132]. There are two possible cases of class candidate membership.

– Membership to the same class:

If C_{cand1} and C_{cand2} belong to the same class, in this case the $S_c(1)$ is compared to a threshold R_C fixed by the user ($R_C \in [0,1]$): $S_c(1) \geq R_C$, if this inequality is verified,

then the character is accepted, otherwise it is rejected and considered in the case of the first rejection (reject(1)).

- Membership to two different classes:

If C_{cand1} and C_{cand2} belong to two different classes, the actual presented pattern is automatically rejected and considered in the case of the second rejection (reject(2)).

Figure 2.6 show an illustration example of the application of the CSM method to character similarity measurement. According to Fig. 2.6 (b), the coefficients a, b, c and e take the following values: a = 486, b = 8, c = 9, e = 430, n = 933 and T = 494.

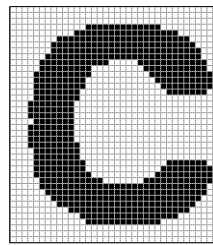
Then the complementary similarity measure between these two images is:

$$S_c(x, y) = \frac{a \cdot e - b \cdot c}{\sqrt{T(n-T)}} = 448.60$$

The model y is represented by: $\sqrt{T(n-T)} = 465.68$

Finally the similarity is: $S_c(\%) = 100 \frac{448.60}{465.68} = 96.33$

Image x is similar to y with a rate of 96.33%.



model y

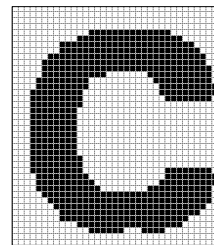


image x

(a)

		model y		total
		1	0	
model x	1	486	9	495
	0	8	430	438
total		494	439	933

(b)

Fig. 2.6: Complementary similarity measure illustration (a) Two character images y and x representing the image model and another image respectively. (b) Results of the application of the CSM to these images.

2.6 Multi-layer perceptron (MLP) neural network

The multi layer perceptron (MLP) has been widely used in the area of document recognition [109][110]. The multi-layer perceptron (MLP) is a feedforward neural network of fixed number of neurons in the input (N) and output (P) as shown in Fig. 2.7. It is trained with the standard back-propagation algorithm to minimize the total error E_T given by:

$$E_T = \sum_{i=1}^m E_i \quad (2.11)$$

$$\text{where, } E_i = \frac{1}{2} \sum_{j=1}^P (y_j - o_j^i)^2 \quad (2.12)$$

and m is the number of training patterns, P number of output neurons or classes, o_j^i are the desired outputs and y_j are the actual outputs of the MLP classifier.

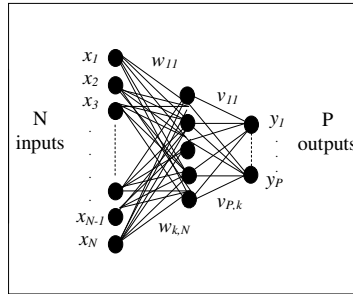


Fig. 2.7 MLP neural network architecture.

The minimization is carried out by propagating the error made from the output of the network towards the internal layers, which makes each neuron be able to calculate its own error signal, then to make the correction of the weights of connections until it reaches a total error already set. The connections weights w_{ij} are adjusted at the time of the iteration $t+1$ according to the formula [111]:

$$w_{ij}^{(l)}(t+1) = w_{ij}^{(l)}(t) + \alpha \cdot \delta_j^{(l)} \cdot y_i^{(l-1)} + \nu \cdot [w_{ij}^{(l)}(t) - w_{ij}^{(l)}(t-1)] \quad (2.13)$$

where α is the training coefficient (between 0 and 1) that characterizes the training speed and ν is the viscosity coefficient which reduces the oscillations in the training phase. The errors $\delta_j^{(l)}$ are calculated from the output and hidden layers. During the

recognition phase, the network is fed with the input pattern X which is propagated through forward steps to the outputs (P outputs). The expected class is simply given by the output unit with the highest value. The classifier can reject patterns whose membership cannot be clearly established. A typical classification criterion which is used consists of rejecting a pattern if $\bar{y} = \max \{y_i\} < R_M$, $i=1,2,\dots,P$, where P is the number of classes, $y_i \in (0,1)$ is the i th output of the network, and R_M is a proper threshold. An unknown pattern is accepted if only at least one output is greater or equal than R_M .

2.7 Hopfield neural network

2.7.1 Autoassociative memories

It is one of the first applications resulting from the adaptive neural network. It has for prime objective to realize a device that is able to memorize information, which one can then retrieve or recover, not only by their complete addresses as in a traditional memory, but by providing even incomplete or disturbed data relating to the stored information. These memories thus are mainly used for the rebuilding of data [111].

The Hopfield model has found applications in the area of optical character recognition and image matching [112][113]. A Hopfield network is basically an addressable memory by its contents. A memorized form $S^{(m)}$, $m=0,1,2,\dots,M$, where M is the number of memorized patterns, is found by a stabilization of the network (see Fig. 2.8), if it is stimulated by an adequate part X of this form using the following equation:

$$S^{(m)} = S_i = F(W.X) = F\left(\sum_{j=1}^N w_{ij}.x_j\right) \quad i = 1,2,3,\dots,N \quad (2.14)$$

Where W is the interconnection weight matrix. The Hopfield neurons are discrete and answer according to a function threshold F . The training of the Hopfield neural network is dynamic, the rule of modification of the weights thus becomes:

$$w_{ij} = \frac{1}{N} \sum_{m \in M} S_i^{(m)} \cdot S_j^{(m)} \quad \text{with} \quad \begin{cases} w_{ii} = 0 \\ \text{and} \\ w_{ij} = w_{ji} \end{cases} \quad (2.15)$$

In equation (2.14) and (2.15), N represents the number of neurons in the network and $S^{(m)}$ represents a stored prototype.

It is for this reason that this type of network is known as associative [111]. Figure 2.9 illustrates some examples of addressing a memory by its content at different iteration number T .

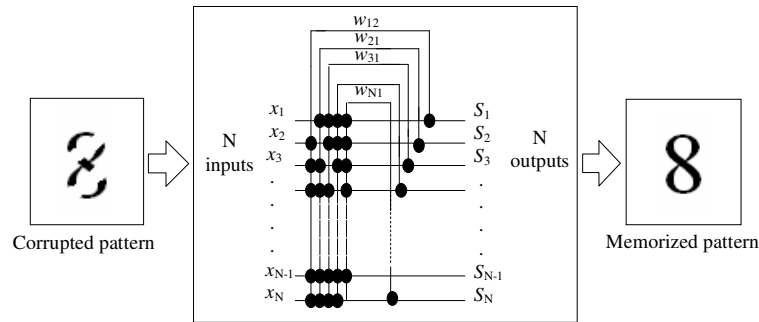


Fig. 2.8 Hopfield model neural network architecture.

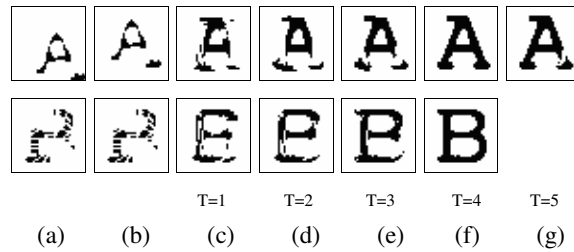


Fig. 2.9 Pattern recovering example (a) Corrupted input pattern. (b) Centered pattern. (c)-(g) Memorized pattern restitution ((c)-(f) for the character "B").

To improve the error correction, noise tolerance and the storage capacity of the Hopfield model, the Gram-Schmidt orthogonal projection procedure is introduced [114]. The orthogonalized vectors $S^{*(m)}$ (orthogonalized memorized pattern) can be described by the Gram-Schmidt orthogonalization procedure as follows:

$$S^{*(m)} = S^{(m)} - \sum_{l=1}^{m-1} \frac{[S^{(m)} \cdot S^{*(l)}]}{\|S^{*(l)}\|} S^{*(l)} \quad m = 1, 2, \dots, M \quad (2.16)$$

Where $[S^{(m)} \cdot S^{*(l)}]$ denotes the inner product, $\|S^{*(l)}\|$ is the norm of $S^{*(l)}$. The associative corresponding matrix $W^{(0)}$ can be expressed as:

$$W_{ij}^{(0)} = \sum_{m=1}^M \frac{S_j^{*(m)} \cdot S_i^{*(m)}}{\|S^{*(m)}\|} \quad (2.17)$$

During the recognition phase, the Hopfield network is fed with the input pattern, and then the output is determined after a fixed iteration number T . Since the output pattern is binary, then the expected class (C) is determined from a distance δ_m of the output Y (y_1, y_2, \dots, y_N) and a memorized pattern $S^{(m)}$ as follows [56]:

$$\delta_m = \frac{1}{2} \sum_{j=1}^N (y_j - S_j^{(m)})^2, \quad m = 1, 2, \dots, M \quad (2.18)$$

where N is the image character size. The class membership is simply established by:

$$C = \underset{m = 1, 2, \dots, M}{\operatorname{argmin}} \{ \delta_m \} \quad (2.19)$$

A typical classification criterion which is used consists of rejecting a pattern if the relative distance [56]:

$$\xi_{\alpha\beta} = \frac{(\delta_\beta - \delta_\alpha)}{\delta_\beta} < R_H \quad (2.20)$$

$$\text{with } \delta_\alpha = \min_{m = 1, 2, \dots, M} \{ \delta_m \} \quad \text{and} \quad \delta_\beta = \min_{m \neq \alpha, m = 1, 2, \dots, M} \{ \delta_m \}$$

This rejection is based on the comparison of the two lowest reproduction errors δ_α and δ_β for an incoming pattern X . R_H is an appropriate threshold which can be chosen depending on the user requirements.

2.7.2 Synchronous and asynchronous modes

In the Hopfield network, the update of the neurons (or outputs) can be either *synchronous* or *asynchronous*. For the synchronous mode, at each time step, all the cells are updated simultaneously. The preceding simplified example (Fig. 2.9) was treated in a synchronous way by considering the update equivalent to a multiplication

of two matrices. For the asynchronous mode, at each time step, the update of only one cell is carried out according to a random order. In the next update, one uses the preceding result (with the updated of preceding cell) to update the following cell in the random order. In figure 2.10 (a), the original image is corrupted with a Gaussian noise of standard deviation $\sigma = 1.0$.

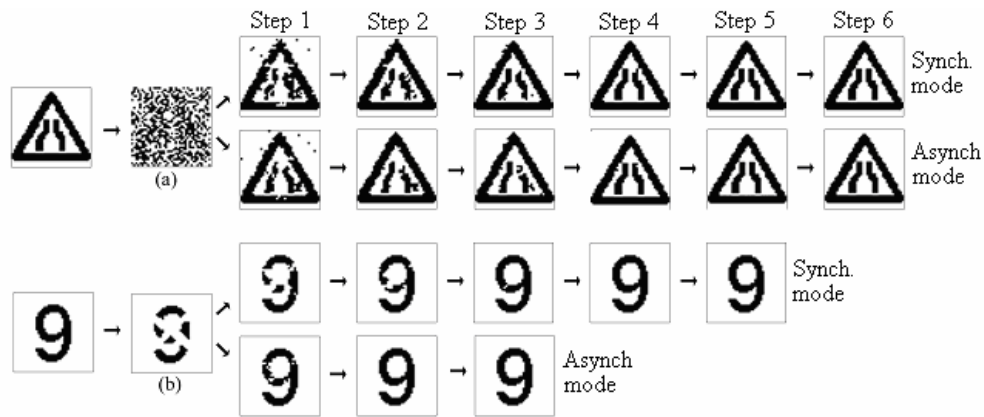


Fig. 2.10. Synchronous and asynchronous illustration of step by step recognition.

It was shown that if an asynchronous mode of Hopfield was considered, the system reached a stable state, but on the other hand, if a synchronous update is chosen, the system could lead to either a stable state, or to oscillate between two states.

2.8 Self organization map (SOM)

The SOM unsupervised training is performed in two phases, namely, the ordering phase and the tuning phase [111]. These two phases are a little bit different one from the other, and this difference appears only on the level of the choice of the neighbourhood A , the learning β and the reduction frequency N . The training procedure steps are:

- 1-Initialize vector weights by low random values such as: $W_j \neq W_k$, for $j \neq k$.
- 2-Presents the input vector $E = (e_1, e_2, e_3, \dots, e_m)$ randomly to the network.
- 3-After having defined the neighbourhood, it is necessary to locate the winning neuron defined as the minimum Euclidian distance:

$$d_j = \|E - W_j\| \quad (2.21)$$

4-Once the winning neuron is located, its synaptic weights will be thus adjusted with those of its neighbours according to the following equations:

$$w_{ij}(t+1) = \begin{cases} w_{ij}(t) + \beta(t) \|E - w_{ij}(t)\| & \text{if } j \in A \\ w_{ij}(t) & \text{if } j \notin A \end{cases} \quad (2.22)$$

5-If the total iteration number is not reached, go to step2.

Where $\beta(t)$ represents the learning rate.

2.9 Hidden Markov model (HMM)

A hidden Markov model (HMM) is a process of Markov doubly stochastic [115]. It consists of a subjacent stochastic process which is not observable directly (thus hidden), and which can be observed only by the intermediate of another whole of stochastic process. For each model, the sequence of the states visited during a private individual production of a word constitutes well a chain of Markov of order one, but it is about a hidden chain. HMM has been applied in several areas, including speech processing [116][117], handwritten word recognition [13][118] and handwritten numeral character [59][65]. The HMMs are characterized by the following parameters:

N: the number of the states of the model, we designate the individual states by:

$$S = \{s_1, s_2, s_3, \dots, s_N\}, \text{ and the state at time } t \text{ by } s_t, s_t \in S.$$

M: the number of the distinct symbols of observations if the observation O_t at the physical emission of the system is represented in its discrete form. These symbols correspond to the physical emission of the system. Thus, the observation symbols are given by:

$$O_t = v_i, v_k \in V = (v_1, v_2, \dots, v_M) \quad (2.23)$$

A: distribution of the transition probabilities of the s from the states:

$$A = \{a_{ij}\} \quad (2.24)$$

where $a_{ij} = p(q_{t+1} = s_i / q_t = s_j), 1 \leq i, j \leq N$.

$$\sum_{i=1}^N a_{ij} = 1, 1 \leq j \leq N \quad (2.25)$$

B: distribution of the observation probabilities at each state j :

$$B = \{b_j(o_t)\}, j=1,2,\dots,N \quad (2.26)$$

where $b_j(o_t = v_k) = p(o_t = v_k / q_t = s_j), 1 \leq j \leq N, 1 \leq k \leq M$

$$\sum_{k=1}^M b_j(o_t = v_k) = 1, 1 \leq j \leq N \quad (2.27)$$

Π : distribution of initial probabilities of states:

$$\Pi = \{\pi_i\} \quad (2.28)$$

where $\pi_i = p(q_1 = s_i), 1 \leq i \leq N$

and

$$\sum_{i=1}^N \pi_i = 1, 1 \leq i \leq N \quad (2.29)$$

We can conclude that complete specification of HMM requires: (1) two parameters (N and M for a discrete HMM), (2) the observation sequence vectors, (3) the probability distributions of A, B and Π .

In this work a model with serial constraints of double transition is used, the initial model; $\lambda = (A, B, \Pi)$ can be for example initialized as follows:

- The matrix A : for N=6.

$$A = \begin{vmatrix} 1/3 & 1/3 & 1/3 & 0 & 0 & 0 \\ 0 & 1/3 & 1/3 & 1/3 & 0 & 0 \\ 0 & 0 & 1/3 & 1/3 & 1/3 & 0 \\ 0 & 0 & 0 & 1/3 & 1/3 & 1/3 \\ 0 & 0 & 0 & 0 & 1/2 & 1/2 \\ 0 & 0 & 0 & 0 & 0 & 1 \end{vmatrix}$$

- The matrix B is initialized with the value 1/M, for $1 \leq j \leq N$ and $1 \leq k \leq M$ (equiobable matrix).

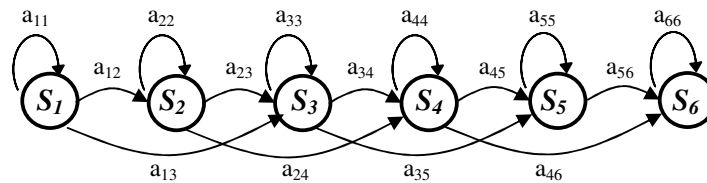


Fig. 2.11 : HMM with serial constraints of double transition.

- Parameter reestimation

How can one adjust the parameters of the model $\lambda = (\Pi, A, B)$ to maximize $P(O_t/\lambda)$? The fact that the length of the observation sequence (training data) is finite, there do not exist a direct analytical solutions (global optimization) to build the model. Nevertheless we can choose $\lambda = (\Pi, A, B)$ such as $P(O_t/\lambda)$ is a local maximum using an iterative procedure such as that of Baum and Welch. In case of multiple sequences each class is represented by a set of sub classes or a finite number of characters, then the observation sequences is $O = \{O^1, O^2, \dots, O^k\}$, and the estimators spread simply in the following way [119][120]:

$$\bar{\pi} = \gamma_1(i) \quad (2.30)$$

$$a_{ij}^{k, actual} = \sum_{t=1}^{T-1} \alpha_t^k(i) a_{ij} b_j(O_{t+1}^k) \beta_{t+1}^k(j) \quad (2.31)$$

$$a_{ij}^{actual} = \frac{\sum_{k=1}^K a_{ij}^{k, prev}}{\sum_{k=1}^K \sum_{j=1}^N a_{ij}^{k, prev}} \quad (2.32)$$

$$\gamma_t^k(i) = \frac{\alpha_t^k(i) \beta_t^k(i)}{\sum_{i=1}^N \alpha_t^k(i) \beta_t^k(i)} \quad (2.33)$$

$$b_j^{actual}(k) = \frac{\sum_{k=1}^K \sum_{t=1}^T \gamma_t^k(j)}{\sum_{k=1}^K \sum_{t=1}^T \gamma_t^k(j)} \quad (2.34)$$

where the abbreviations *actual* and *prev* designate the actual and previous of the estimated parameters A and B. For the training, we apply the Baum-Welch algorithm for the reestimation of the model $\lambda = (A, B, \Pi)$, then one uses the algorithm of Viterbi which gives the optimal way of the transitions between the states. For the recognition we will be able to choose among the calculation algorithm of Forward variable, Backward and the algorithm of Viterbi. In fact generally the first two algorithms are more used in considering their simplicity and the set of probabilities to classify an observation sequence O is:

$$P(O/\lambda) = \sum_{i=1}^N \sum_{i=1}^N \alpha_t(i) a_{ij} b_j(O_{t+1}) \beta_{t+1}(j) \quad (2.35)$$

2.10 Conclusion

In this chapter we have presented a state of the art of document recognition techniques, namely, the degraded printed character, the handwritten numeral character and the handwritten word. It has been shown that the performance of recognition methods depends primarily on the parameter extraction and the classification methods. The performance of recognition method can be also improved by combining two or several parameter extractors and classifiers. The use of several recognizers (recognition system) can lead to performances largely exceeding those obtained by the basic recognizers. This is true, if the basic methods were well combined, making profit of the drawback and the advantage of each method. The methods of parameter extraction and classification making part of this work were also presented briefly in order to simplify the comprehension of the methods developed in this work.

CHAPTER 3 EXPERIMENTAL RESULTS

3.1 Introduction

In this chapter the results are presented in two distinct parts. The first one is related to the results of the preprocessing application, in particular, handwritten numeral slant correction and skew correction, and central zone localization (SC-CZL), which are two new methods developed within the framework of this work. The second one is related to the recognition results, in particular those of the degraded printed characters, the handwritten numerals and the handwritten words. First, recognition results of the handwritten numeral character are presented with the use of two following combinations: the Fourier-Mellin transform (FMT), the self organization map (SOM) and the multi layered perceptron (MLP), then the hidden Markov models (HMM) with a new set of feature extractors. Secondly, we will see the application of the global approach by mean of a new method developed within the framework of this work. It is mainly based on the use of the Hopfield model and the MLP. In third place and finally, we present the recognition of degraded printed characters using two classifier combinations, namely, the sequential and serial combinations.

3.2 Handwritten writing processing

3.2.1 Handwritten numeral slant correction

Due to a large variation in handwriting image data, preprocessing is used to reduce variations and produce a more consistent set of data, this is essential for accurate numeral character recognition. In our system, preprocessing includes filtering, binarization, slant correction, size normalization and centering. A new way of slant correction is developed in the frame of this work, it is applied after a noise reduction stage of the sized 64x64 input image by Gaussian low pass filtering and a binarization stage which consists of thresholding the filtered image. Branches due to the former stage are removed by applying opening morphology which yields a character with smooth contour.

In handwritten numeral characters, one of the major variations in writing style is caused by slant, which is defined as the slope of the general writing trend with respect to the vertical line. The slant correction operation consists in correcting the tilted character in order to return it right. We have developed a new simple and efficient character slant correction based on lower and higher character centroids [55]. The proposed slant correction method (see Fig. 3.1) is performed according to the following steps:

a) Detect the left (x_0), right (x_1), low (y_0) and high limit (y_3).

b) Divide the character height into three equal regions such as; $y_3 - y_2 = y_2 - y_1 = y_1 - y_0$.

c) Calculate the lower centroid N of coordinate (x_{gl}, y_{gl}) of the numeral character; $x \in [x_0, x_1]$ and $y \in [y_0, y_1]$ using the following equations:

$$x_{gl} = \frac{m_{10}}{m_{00}} \quad \text{and} \quad y_{gl} = \frac{m_{01}}{m_{00}} \quad (3.1)$$

$$\text{where } m_{pq} = \sum_{x=x_0}^{x_1} \sum_{y=y_0}^{y_1} x^p \cdot y^q \cdot f(x, y) \quad (3.2)$$

d) Calculate the upper centroid M of coordinate (x_{gh}, y_{gh}) of the numeral character; $x \in [x_0, x_1]$ and $y \in [y_2, y_3]$ using the following equations:

$$x_{gh} = \frac{m_{10}}{m_{00}} \quad \text{and} \quad y_{gh} = \frac{m_{01}}{m_{00}} \quad (3.3)$$

$$\text{where } m_{pq} = \sum_{x=x_0}^{x_1} \sum_{y=y_2}^{y_3} x^p \cdot y^q \cdot f(x, y) \quad (3.4)$$

e) Calculate the slope and the angle θ of the line joining the two centroids N and M as shown in Fig. 3.1 using the following equations:

$$\text{slope} = \frac{y_{gh} - y_{gl}}{x_{gh} - x_{gl}} \quad (3.5)$$

$$\theta = \text{atan}(\text{slope}) \quad (3.6)$$

f) Shear all character pixels (x, y) along the horizontal direction to (x', y) using the following equation:

$$x' = x + (y_g - y) \cdot \sin(\theta) \quad (3.7)$$

where y_g is the centroid abscissa given by:

$$y_g = \frac{m_{01}}{m_{00}} \quad (3.8)$$

$$\text{and } m_{pq} = \sum_{x=x_0}^{x_1} \sum_{y=y_0}^{y_3} x^p \cdot y^q \cdot f(x, y) \quad (3.9)$$

Results of the application of the proposed method are compared to two other methods. The first method is based on the average slant calculated from the outer contour [121] and the second method used a linear regression to all row's centroid to calculate the slant [65]. Figure 3.2 shows results of applying these two methods compared to the proposed method.

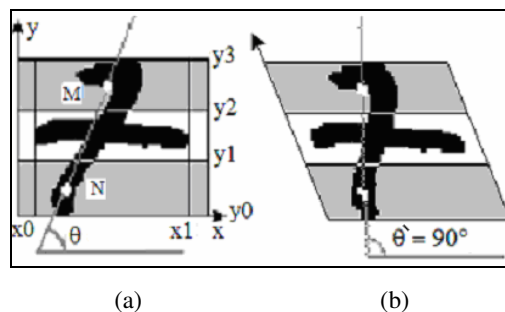


Fig. 3.1 Slant correction method. (a) Slant angle calculation. (b) Character slant correction.

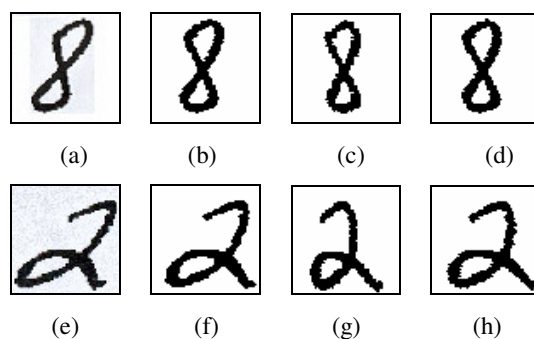


Fig. 3.2 Slant correction example. (a) and (e) Original handwritten numerals. (b) and (f) Results based on contour slant correction. (c) and (g) Results based on rows centroid slant correction. (d) and (h) Results of the proposed method.

The first method doesn't yield a good slant correction as shown in Fig. 3.2 (b) and (f), whereas the second method yields good results but with a small more shearing of the character to the left as can be shown in Fig. 3.2 (c) and (g). We can notice also that the slant correction is in detriment of the character width which decreases. The proposed slant correction method yields very good results in term of slant correction and speed (see Fig. 3.2 (d) and (h)).

3.2.2 New skew correction and central zone localization (SC-CZL)

Most of the popular algorithms for holistic handwritten word [98][100][122] are sensitive to the distortion of word images, particularly when the skew and the central zone of

the word are not correctly detected. The skew may cause serious problems in a recognition system. Therefore, it is necessary to detect and correct the skew of the handwritten word accurately at the preprocessing stage in order to avoid the disturbance of skew to further processing. Several attempts have been made for skew detection [11][123][124]. S. Madhvanath and V. Govindaraju [125] used local minima from lower contours of words as indication of the implicit baseline. Thus by rejecting minima corresponding to descenders, the baseline skew was estimated by linear regression of the remaining minima. A. El Yacoubi et al. [126] estimated the character skew as the average slant of elementary segments obtained by sampling the word image contour, without taking into account horizontal and pseudo-horizontal segments. The upper and lower baselines were estimated using maxima and minima of upper and lower contours respectively. W. Andrew and A. J. Robinson [127] used the minimum above the peak in vertical density histogram for lower baseline estimation, and retain only the points around the minimum of each chain of pixels. The slope of the line of best fit through these points is used for skew correction. The upper line was also estimated using similar procedure.

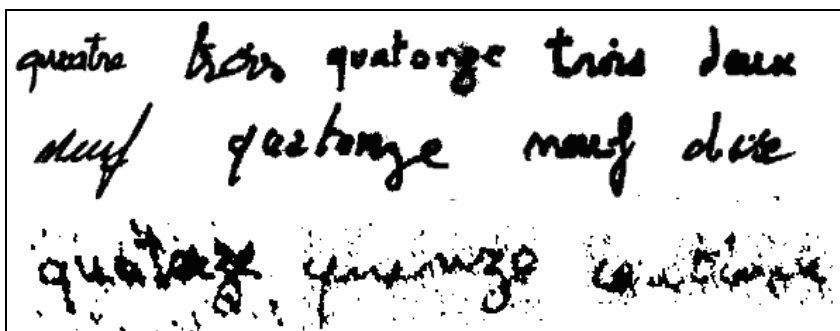


Fig. 3.3 Poor quality handwritten legal amounts.

The proposed work [128] is addressed particularly to poor quality handwritten word recognition where generally the analytical approach for skew correction and central zone localization fail through the contour detection (see Fig. 3.3). The main objective of the present work is to correct the handwritten word in order to enhance the three zones, namely, upper, lower and central zone of the degraded handwritten words accurately. The handwritten words representing the 27 French amount classes are used. Due to some degradation in the handwritten word we have avoided the use of handwritten contour as it was usually used.

The new proposed method performs skew correction, baseline estimation and lower case zone detection simultaneously using the morphologically opened handwritten word and its

corresponding horizontal histogram. The new SC-CZL yields automatically the three zones of interest, namely, ascender, lower case and descender zone (see Fig. 3.4).

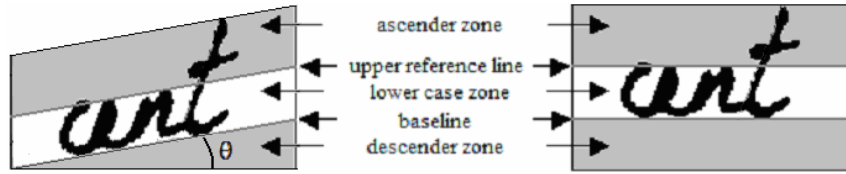


Fig. 3.4 Handwritten zones and skew correction.

The application of morphology in our case is to fill all contours and blanks between two consecutive row pixels belonging to handwritten word. The structuring element was chosen to be horizontal of 1 row by 15 columns using the given equation:

$$g = f \circ h \quad (3.10)$$

Where f is the word image and h is the structuring element. The horizontal histogram of the opened image ($hist(g)$) is thresholded according to the following equation:

$$Thresh = \mu[hist(g)] + k * \sigma [hist(g)] \quad (3.11)$$

$$hist(g) = \begin{cases} 1, & \text{if } hist(g) \geq thresh \\ 0, & \text{if } hist(g) < thresh \end{cases} \quad (3.12)$$

Where μ and σ are the mean and the standard deviation of $hist(g)$, and k is an appropriate constant which can be chosen experimentally. For the present application, k was chosen to be equal to 0.8. Figures 3.5 (b)-(d) show the application of this procedure. The thresholded histogram yields two transitions; the first one is from 0 to 1 that locates the baseline (y_l) and the second one is from 1 to 0 that locates the upper reference line (y_h) and consequently the lower case zone. To perform skew correction, baseline estimation and lower case zone detection simultaneously, the handwritten undergoes several vertical shears with angle $\theta_k \in [-10.0, 10.0]$ expressed in degree varying with an angle step of $\Delta\theta=0.5$ degree which yields 41 shears. For every shear the horizontal histogram of the opened word image is determined and its corresponding lower case zone is calculated as explained earlier. We define the word density ρ as the ratio of the word part lying in the estimated lower case zone delimited on the left by x_l and on the right by x_r (see Fig. 3.5) to the lower case box given by:

$$\rho(\theta_k) = \sum_{x=xl(\theta_k)}^{xr(\theta_k)} \sum_{y=yh(\theta_k)}^{yl(\theta_k)} \frac{f(x,y, \theta_k)}{(yh(\theta_k) - yl(\theta_k)) \cdot (xr(\theta_k) - xl(\theta_k))} \quad (3.13)$$

where $f(x,y, \theta_k)$ is the sheared word image and $yh(\theta_k)$, $yl(\theta_k)$, $xl(\theta_k)$ and $xr(\theta_k)$ are upper reference line, baseline, left and right word zone limit respectively. The skew angle θ is calculated as:

$$\theta = \arg \max \rho(\theta_k) \quad , \quad k = 0,1,2,\dots,40 \quad (3.14)$$

$$x' = x + (y_g - y) \cdot \sin(\theta) \quad (3.15)$$

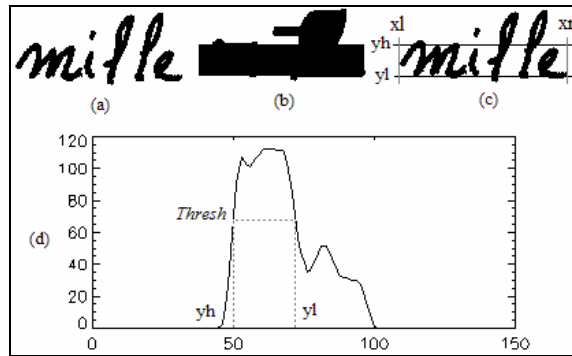


Fig. 3.5 Lower case determination (a) Original word image (b) The opened version of (a). (c) Lower case determination. (d) Horizontal histogram and its thresholded version (represented in shaded lines).

Finally, the handwritten word skew is corrected by a simple shear using the angle determined by equation (3.15) and consequently the baseline and lower case are those corresponding to the same angle θ , namely, $yh(\theta)$, $yl(\theta)$. Figure 3.6 illustrates the proposed method for word deskewing, baseline and lower case determination. Figure 3.7 shows the skew correction and lower case localization on high, medium and poor quality handwritten word. The last three rows show the robustness of the proposed method to extremely degraded and broken handwritten words.

In this work a new simple and efficient method for skew correction and lower case detection was proposed; it is based on the horizontal projection of the opened handwritten word. The present method performs the SC-ZCL simultaneously and accurately of even extremely degraded handwritten. The experiments results conducted on medium and poor quality legal amounts collected from bank checks, show promising results.

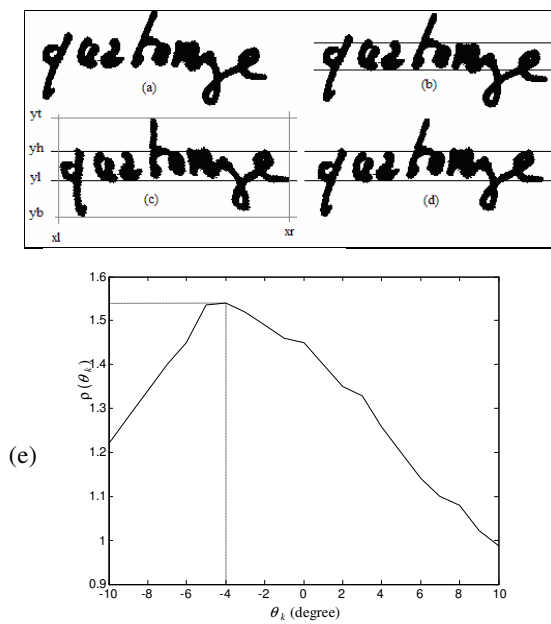


Fig. 3.6 Skew correction and lower case zone detection. (a) Original image. (b) Lower case zone detection before skew correction. (c) and (d) Lower case zone detection after skew correction. (e) The corresponding $\rho(\theta_k)$ with the estimated skew detected at the maximum of ρ ($\max(\rho) = 1.545442$) giving an angle $\theta = -4.0$ degrees.

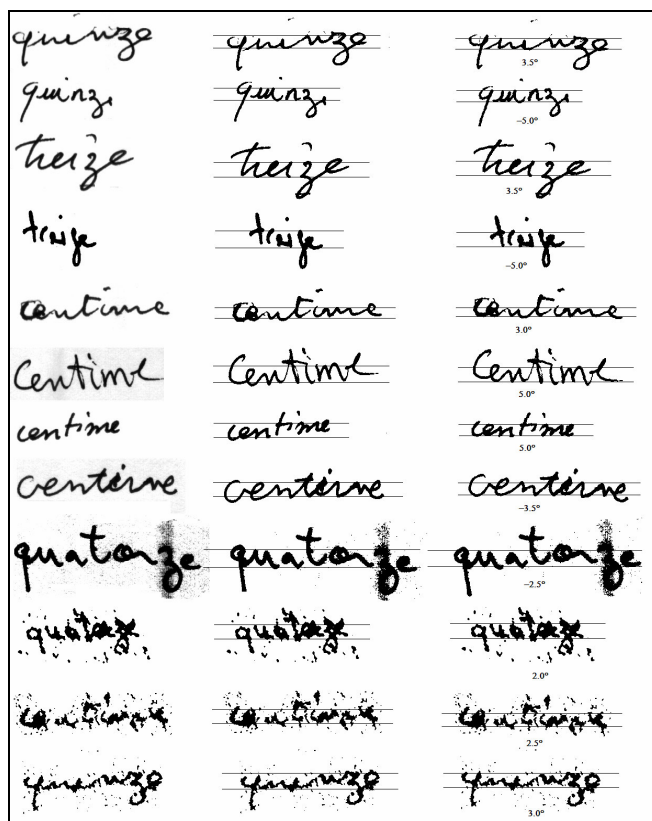


Fig. 3.7 Skew correction and lower case localization; the first column represents the original words, the second column represents lower case localization before skew correction and the last columns represents results of lower case zone localization after skew correction carried out simultaneously.

3.3 Handwritten numeral recognition

In this section we present recognition results related to the handwritten numeral character using the two following combinations:

- 1- Fourier-Mellin transform (FMT), self organization map (SOM) and the multi layered perceptron (MLP).
- 2- Multiple hidden Markov models (HMM) with a new set of feature extractors.

3.3.1 FMT-SOM for handwritten numeral recognition

The proposed method for handwritten numeral recognition [129] is based primarily on the use of Fourier-Mellin transform (FMT) and Self organization map as shown in Fig 3.8. The Fourier-Mellin transform is used to extract the distinctive features of handwritten numeral characters (as mentioned in chapter 2). Whereas the unsupervised neural network (SOM) is used to cluster in prototypes the Fourier-Mellin vectors of each handwritten numeral class. To further enhance recognizing capability and noise tolerance of the proposed system, a MLP-based classifier is introduced. Experimental results are presented first by using various orders and dimension of the Fourier-Mellin transform and self organization map respectively in order to set the FMT order and the SOM card dimension and secondly by using the MLP-based classifier designed and trained by the clusters produced by the SOM.

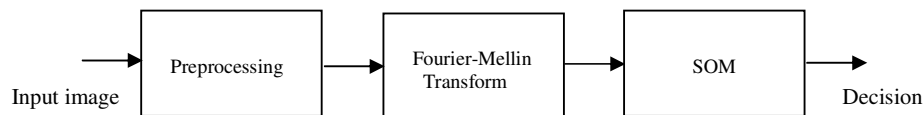


Fig. 3.8 Recognition synoptic block diagram.

a) Handwritten numeral preprocessing

The preprocessing of image character includes, filtering, binarization, horizontal slant correction and size normalization. Size normalization is used to reduce the variation in size and to standardize the input pattern to the subsequent stage. Directly scaling all handwritten numerals to an identical size will result in a standard size. Usually, the height (H) is taken to be greater than the width (W) of the handwritten numeral. Therefore we set the ratio $W/H=0.8$, and by setting H and W to 50 and $W=40$ pixels. We found the scaling method described in [32] adequate for the normalisation procedure, with the scaling factor a_x and a_y

calculated as follows: $a_x = H_{ch} / H$ and $a_y = W_{ch} / W$ where H_{ch} and W_{ch} are the character height and width before normalisation. Figure 3.9 illustrates the preprocessing step of the proposed recognition system.

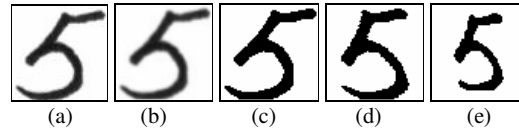


Fig. 3.9 Preprocessing. (a) Original image character of size 64x64 pixels. (b) Filtered character. (c) Binarized character. (d) Application of the proposed slant correction method. (e) Normalised version of the character in (d).

b) Experimental results

A set of 20000 collected handwritten numerals was used in our experiments. We used 10000 numerals for training and the remaining 10000 numerals for test with various feature map dimensions: 15x15, 20x20, 25x25 and 30x30 and different filter bank orders: $p=3, q=3$ and $p=4, q=4$. The handwritten numerals were preprocessed according to section 3.3.1 (a). Figure 3.10 (a) shows recognition results for various FMT order (p, q) and different SOM card dimensions. As it can be noticed, the recognition rate is monotonically increasing with filter bank order. For order $p=4$ and $q=4$, involving 39 coefficients, a recognition rate of 96.6% was achieved on the test set, whereas only 94.0% was reached with 23 coefficients when using order $p=3$ and $q=3$ for the same set (see table 3.1). According to the results presented in table 3.1, one notices that: i) The filter bank order $p=4$ and $q=4$, gives better results comparing with order $p=3$ and $q=3$. ii) The recognition rate remains almost constant beyond the SOM map dimension of 20x20 neurons.

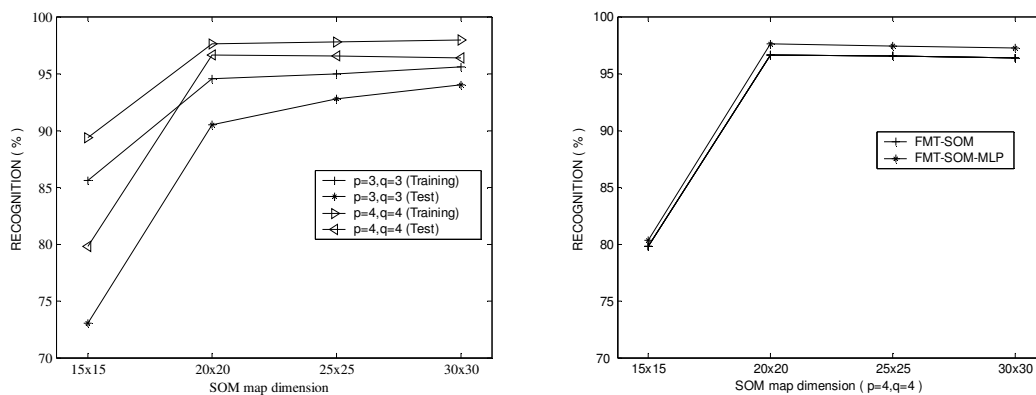


Fig. 3.10 Recognition results comparison (a) for various FMT order and SOM dimension (b) for FMT-SOM and FMT-SOM-MLP ($p=4$ and $q=4$).

To improve the recognizing capability and noise tolerance of the proposed system, a multi-layered perceptron neural network is introduced. The clusters produced by SOM learning contain patterns that have similar characteristics. Thus, the MLP is trained with the back propagation algorithm on such clusters. The prototypes produced by the SOM are used as feature vectors of 39 features ($p=4, q=4$). These feature vectors are used as input prototype class for the MLP based classifier. The training speed α and the viscosity coefficient ξ were set to 0.9 and 0.001 respectively. The number of hidden layers was set to 30 and the total error to 0.001. The connection weights corresponding to the two fully connected MLP are obtained after convergence in the training phase and stored for recognition process. Figure 3.10 (b) and table 3.2 show the noticeable improvement of the recognition rate using TFM-SOM and the MLP (TFM-SOM-MLP) on all the SOM card dimensions. The recognition rate was improved with the use of TFM-SOM-MLP except for the class “0” which remains constant as shown in the confusion matrix given in table 3.3 and 3.4. Finally, the best result was achieved by using the SOM with 20x20 dimension, the FMT order ($p=4, q=4$) and the MLP which yields a recognition rate of 97.6%. Figure 3.11 and 3.12 show the SOM card of 20x20 dimension and the handwritten numerals that were correctly recognized by the proposed recognition system respectively.

Table 3.1 Recognition rate (%) performance as a function of the SOM dimension and filter bank order (p, q).

Card dim.	$p=3, q=3$		$p=4, q=4$	
	Training set	Test set	Training set	Test set
15x15	85.6	73.0	89.3	79.8
20x20	94.5	90.5	97.6	96.6
25x25	95.0	92.8	97.8	96.5
30x30	95.6	94.0	97.9	96.4

Table 3.2 Recognition rate performance as a function of the SOM dimension for FMT-SOM and FMT-SOM-MLP for $p=4$ and $q=4$.

Card dimension	FMT-SOM	FMT-SOM-MLP
15x15	79.80	80.30
20x20	96.60	97.60
25x25	96.50	97.40
30x30	96.40	97.25

Table 3.3 Confusion matrix result of TFM-SOM

	0	1	2	3	4	5	6	7	8	9	Rec.
0	990	0	0	0	5	0	0	2	1	2	99,0
1	0	930	13	5	12	3	3	17	15	2	93,0
2	0	11	945	7	5	5	0	13	9	5	94,5
3	0	3	3	955	7	5	3	8	11	5	95,5
4	2	8	6	5	960	0	0	11	8	0	96,0
5	0	3	4	3	2	970	8	0	3	7	97,0
6	0	0	0	1	1	2	972	2	0	22	97,2
7	0	4	5	1	0	1	2	985	2	0	98,5
8	0	2	4	2	2	3	6	5	968	8	96,8
9	0	0	0	0	0	8	3	1	3	985	98,5
											96.6

Table 3.4. Confusion matrix result of TFM-SOM-MLP

	0	1	2	3	4	5	6	7	8	9	Rec.
0	990	0	0	0	5	0	0	2	1	2	99,0
1	0	950	10	1	10	1	2	10	15	1	95,0
2	0	10	955	2	4	5	0	10	9	5	95,5
3	0	3	3	970	2	1	3	4	9	5	97,0
4	0	4	6	5	975	0	0	5	5	0	97,5
5	0	3	2	3	2	980	2	0	3	5	98,0
6	0	0	0	1	1	0	981	0	0	17	98,1
7	0	2	4	1	0	1	2	988	2	0	98,8
8	0	0	1	2	1	2	4	2	983	5	98,3
9	0	0	0	0	0	6	3	1	2	988	98,8
											97.6



Fig. 3.11 SOM card of 20x20 dimension.

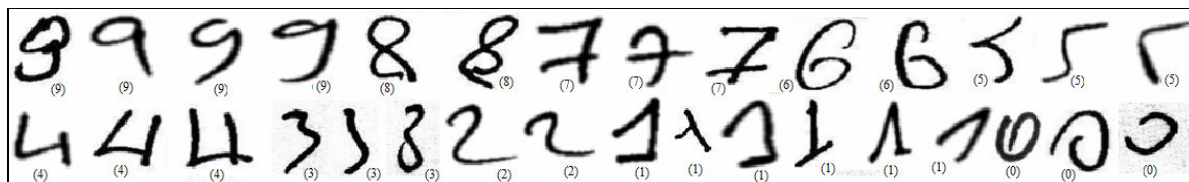


Fig. 3.12 Handwritten numerals correctly recognized.

In this section we have presented a recognition system based on the Fourier-Mellin transform designed for feature extraction to offline unconstrained numeral characters and an unsupervised neural network (SOM) in order to cluster in prototypes or models each handwritten numeral class. In order to improve the performance of the present system, a MLP-based classifier was trained with these clusters. The final developed recognition system exhibits better performance and accuracy when compared to the FMT-SOM based classifier.

3.3.2 Multiple Hidden Markov models for handwritten numeral recognition

The proposed method is a multiple classifier for offline unconstrained numeral characters recognition based on parallel combination using several hidden Markov models (HMM) [55]. A new feature extraction method based on contour background transition is presented [55]. The classification is made using individual classifiers (IC) based on HMM models as well as combining the four IC based on HMM models for each class using two decision strategies: equal combination weight (ECW) and unequal combination weight (UCW).

a) New set of feature extraction

Feature extraction is an essential and important part of a recognition system, it is used in order to reduce redundancy and present the pattern in a set of relevant features including the maximum of information. The extracted parameters must be invariant under geometric transformation. Figure 3.13 shows an illustration example of the new feature extraction method using contour background transition (CBT) performed as follows:

Step 1: We present the image of handwritten character in a contour form.

Step 2: From a $D(i,j)$ point we carry a semi circular sweeping on the whole of the dial of the image with an angle resolution α .

Step 3: For each angle α we note all the values of the pixels covered by the line of sweeping and store them in a matrix $\text{Mat}[\alpha][k]$.

Step 4: On the matrix $\text{Mat}[\alpha][k]$, we count for each $k \cdot \alpha$ the number of transition from contour to background and vice versa, as shown in Fig. 3.13(c).

Four feature extractors were generated in order to capture the whole character from four sides as shown in Fig. 3.13 (a). As it could be noticed the CBT-1 is the clockwise rotated version of CBT-2 by $\pi/2$ and CBT-3 is also the clockwise rotated version of CBT-4 by $\pi/2$.

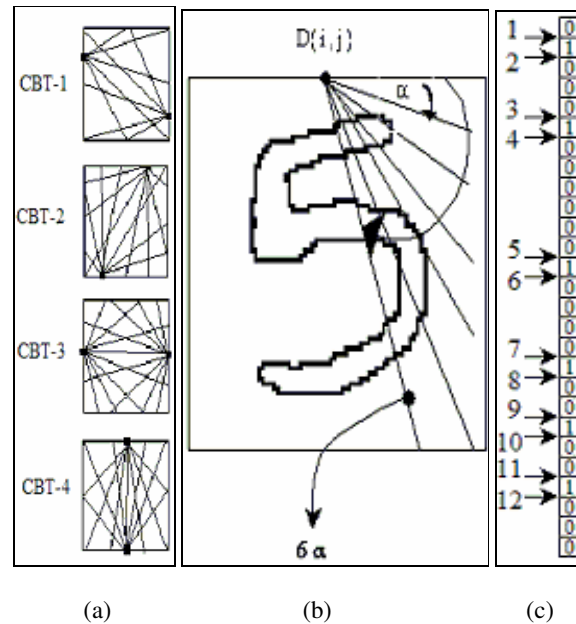


Fig 3.13 Feature extraction. (a) The four CBTs used for feature extraction. (b) CBT-4 showing the transition for 6α (c) Result of feature extraction procedure for 6α .

b) Recognition system presentation

The recognition system consists of two phases (see Fig. 3.14). For each class, in the training phase, multiple HMMs corresponding to different feature types of CBT are built. In the classification phase, the results of individual classifiers to produce the final recognition result for an input character are combined. The final decision is made upon the highest probability.

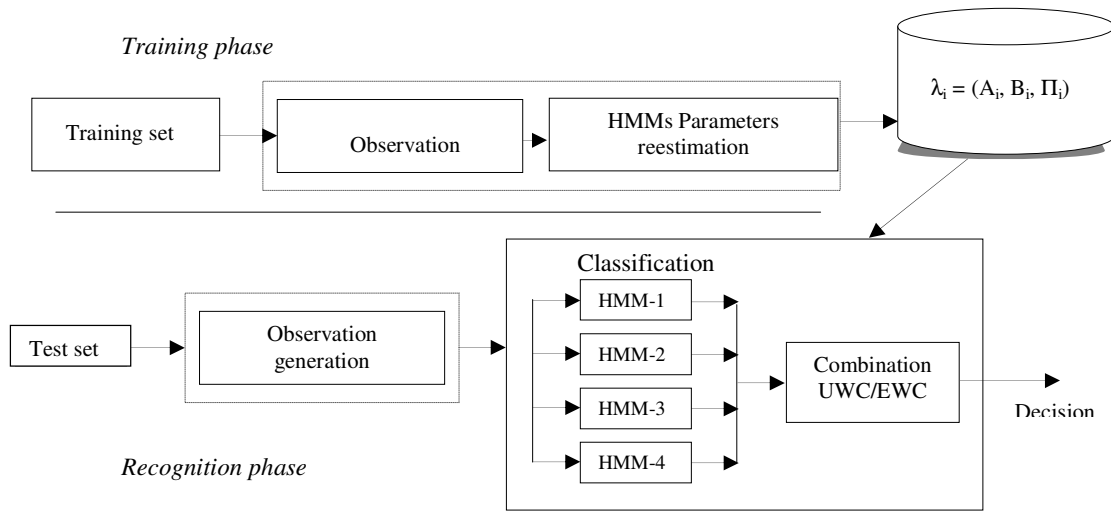


Fig. 3.14 Recognition system block diagram.

- Training phase

The feature extraction described in section 3.3.2 (a), describes the image contour in four feature vectors, namely, CBT-1, CBT-2, CBT-3 and CBT-4. These features were used to build the HMMs, given in the following observation sequences:

$$O = \{ O^{(1)}, O^{(2)}, O^{(3)}, O^{(4)} \}, \quad (3.16)$$

$$\lambda = \{ \lambda^{(1)}, \lambda^{(2)}, \lambda^{(3)}, \lambda^{(4)} \}, \quad (3.17)$$

$$\lambda^{(i)} = (A^{(i)}, B^{(i)}, \Pi^{(i)}) \quad (3.18)$$

where O is the observation sequences generated by the four CBTs, A is the transition probability distribution from the states, B is the the observation probability distribution in each state and Π is the initial probability distribution. Thus each class is composed of HMM-1, HMM-2, HMM-3 and HMM-4. The corresponding parameters of each are estimated on the training data using the Baum-Welch algorithm [115].

- Recognition phase

The performance of the proposed work is tested separately using individual classifier (IC) and combined classifiers (CC).

- Individual classifiers

The classification decision is made using only one and the same model $\lambda^{(i)} = (A^{(i)}, B^{(i)}, \Pi^{(i)})$, $i=1,2,3$ or 4 for all the training set. For each classifier c_i , we use a set of probabilities to classify an observation sequence O :

$$P_i(O^i/\lambda_k^i), \quad 0 \leq k \leq N, \quad i=1,2,3 \text{ or } 4 \quad (3.19)$$

and for any classifier c_i , a definitive decision is made according to :

$$c_i(O^i) = \underset{k \in \Lambda}{\operatorname{argmax}} P_i(O^i/\lambda_k^i) \quad (3.20)$$

ii) Equal weight combination method

This method takes in consideration that all the classifiers c_i have the same recognition performance. Hence, their probabilities can be combined depending on the number of classifiers as follows:

$$P_c(O/\lambda_k) = \frac{1}{4} \sum_{i=1}^4 P_i(O^i/\lambda_k^i), \quad 0 \leq k \leq N, \quad (3.21)$$

A definitive decision is made as:

$$c(O) = \underset{k \in \Lambda}{\operatorname{argmax}} P_c(O/\lambda_k) \quad (3.22)$$

iii) Unequal weight combination method

In this case we suppose that each classifier c_i acts differently from the others with a certain weight w_i and $\sum_{i=1}^4 w_i = 1$. The value of w_i was estimated from the individual classifiers and the probabilities can be combined as follows:

$$P_c(O/\lambda_k) = \sum_{i=1}^4 w_i P_i(O^i/\lambda_k^i), \quad 0 \leq k \leq N, \quad (3.23)$$

and a definitive decision is made using equation (3.23).

c) Experimental results

The proposed scheme was performed according to Fig. 3.14. A set 10000 collected handwritten numerals (see Fig. 3.15) was used in our experiments. We used 100, 500 and 1000 numerals for training and the other 9900, 9500 and 9000 numerals for test with various iteration numbers (L) and state numbers (N). The numeral data was preprocessed according to section 3.3.1 (a). The four CBTs, namely, CBT-1, CBT-2, CBT-3 and CBT-4 were determined according to section 3.3.2 (a) for $\alpha = 4 * \pi / 180^\circ$ which yield T=90 for each CBT.

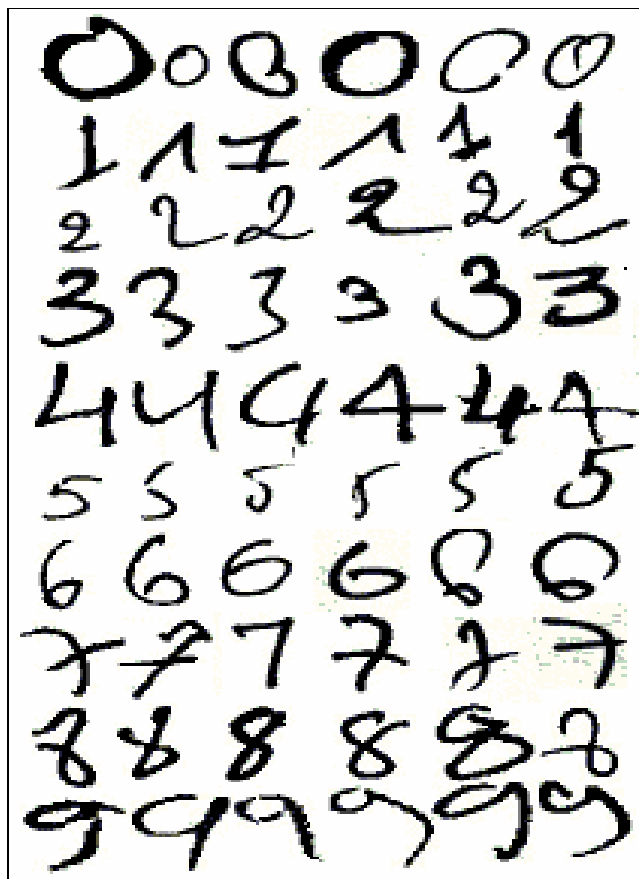


Fig. 3.15 Example of digitized data.

The corresponding HMMs were built using section 2.9 with: the observation symbol number $M=24$, the duration length $T=90$, the number of samples per class in the training set $P=\{10, 50, 100\}$, the iteration number $L=\{10, 30, 50\}$ and the state number $N=\{6, 10, 18\}$. First the experiment was conducted with individual and combined classifiers for various P .

Results are shown in Fig. 3.16, and as it can be noticed, the recognition rate is proportional to P and beyond $P=50$ it remains almost constant for the individual and combined classifiers. This due to the recognition system saturation which means that the system can't learn more using the presented features. Figure 3.16, shows that both the combination methods, namely, EWC and UWC improve impressively the recognition rate in comparing with IC, and the highest performance was achieved by the UWC. In the second experiment we studied the behavior of the proposed scheme with various L and N for $p=100$, $M=24$ and $T=90$. Table 3.5 summarises the performance comparison of the IC and CC and shows that the highest recognition rate is achieved by the combined classifiers: EWC and UWC.

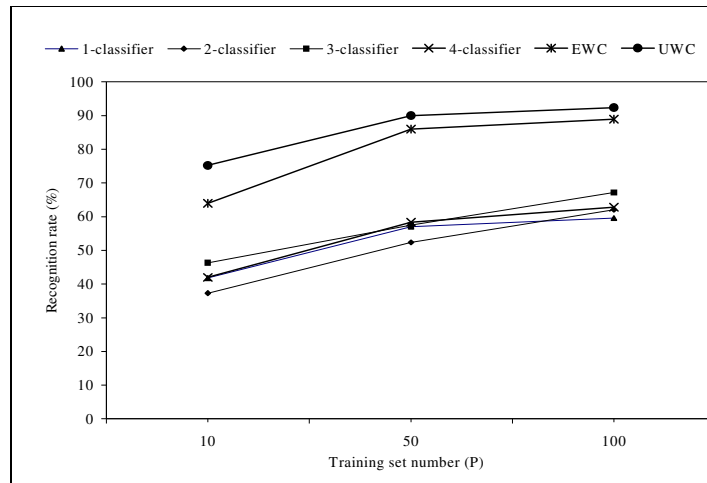


Fig. 3.16 Results of recognition with training set number (P).

Table 3.5 Recognition rate (%) comparison for L=50.

Classifiers	State number (N)		
	6	10	18
HMM-1	51.94	59.24	64.74
HMM-2	58.16	62.25	76.34
HMM-3	59.53	66.44	70.19
HMM-4	58.34	62.83	66.46
ECW	83.45	89.04	93.78
UCW	90.08	93.23	98.08

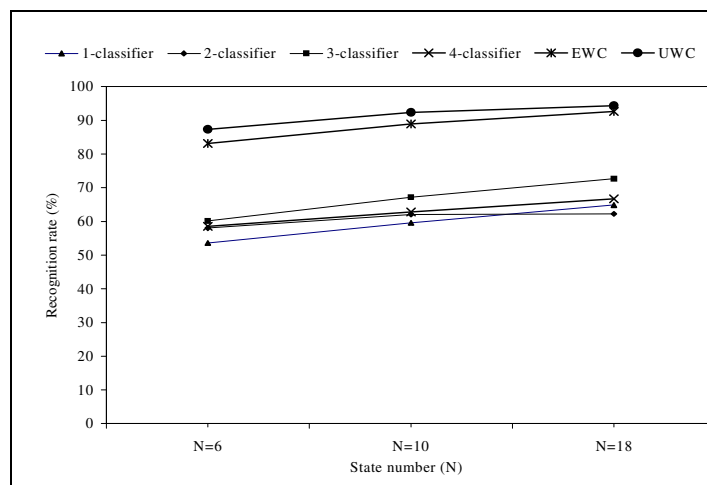


Fig. 3.17 Results of recognition with iteration number L=10.

We can also observe from Figure 3.17, 3.18 and 3.19 that the recognition rate is proportional to the iteration and state number. The combined classifiers improve the recognition rate of the

proposed system and UWC achieve the highest results for $L=50$ and $N=18$ as shown in table 3.6. Figure 3.20 summarises the results of recognition rate using UWC for various L and N with a zero rejection. The recognition rate is proportional to N for a fixed L .

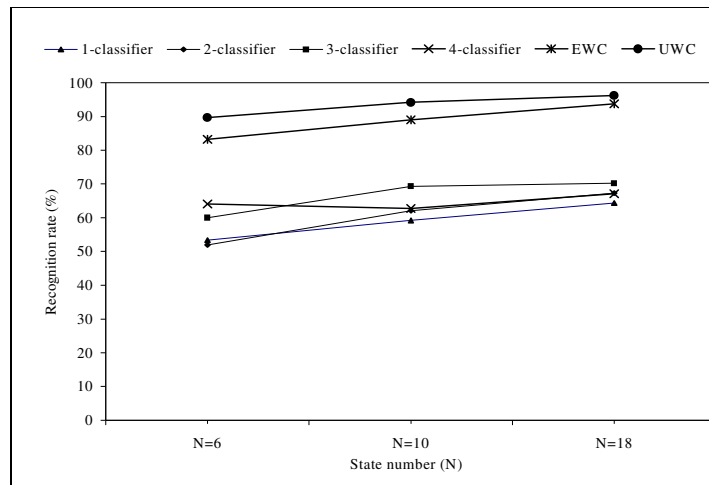


Fig. 3.18 Results of recognition with a number of iteration $L=30$

Table 3.6 Recognition rate (%) with UWC for L and N

State number (N)	Iteration number (L)		
	10	30	50
6	87.29	89.69	90.08
10	92.32	94.19	96.23
18	94.39	96.18	98.08

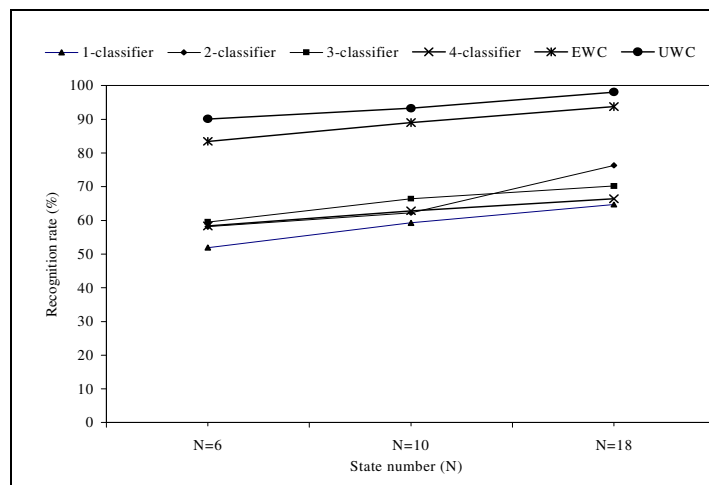


Fig. 3.19 Results of recognition with iteration number $L=50$.

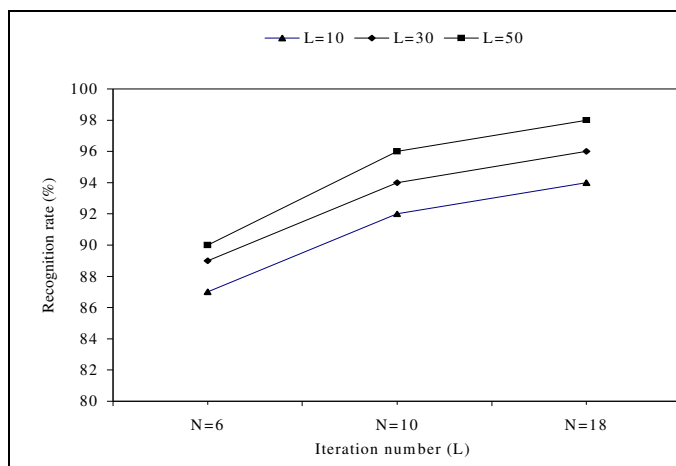


Fig. 3.20 Recognition rate versus state number (N) for fixed iteration number (L).

In this section we have presented a recognition system for offline unconstrained numeral character recognition based on a multiple hidden Markov model (HMM). A new features extraction method based on contour background transition which yield four representations were introduced. First a classification is made using individual HMM classifiers. Second a decision is made with combining four HMM models for each class using two decision strategies: equal weight combination (EWC) and unequal weight combination (UWC). The proposed system achieved a substantial improvement over any one of the individual classifiers (IC), as demonstrated by experimental results on collected handwritten numerals real life data. The proposed system shows promising results for handwritten numeral recognition by achieving a recognition rate of 98.08 %.

3.4 New holistic handwritten word recognition

This section presents a new holistic recognition of handwritten word based on prototype recognition [130]. Its main objective is to arrive at a reduced number of candidates corresponding to a given prototype class and to determine from them the handwritten class to be recognized. The proposed work involves only an accurate extraction and representation of three zones, namely, lower, upper and central zones from the off-line cursive word to obtain a descriptor which provides a coarse characterization of word shape. The recognition system is based primarily on the sequential combination of Hopfield model and MLP based classifier for prototype recognition yielding the handwritten recognition. The handwritten words representing the 27 amount classes are clustered in 16 prototypes or models. These prototypes

are used as fundamental memories by the Hopfield network that is subsequently fed to MLP for classification.

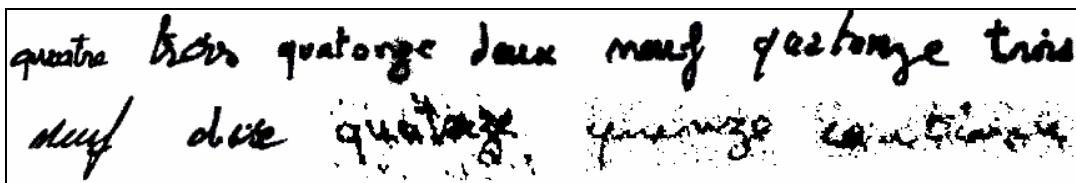


Fig. 3.21 Poor quality handwritten French legal amounts

3.4.1 Proposed method

The new holistic recognition of handwritten words is applied to French legal amount of bank checks containing wholly lower case characters. The proposed system is addressed to poor and medium quality handwritten word recognition where generally the analytical approach fails through the segmental errors (see Fig. 3.21). The proposed system is based primarily on two main phases: preprocessing phase yielding a prototype pattern and a recognition phase which classifies the incoming prototype pattern (preprocessing output) as illustrated by Fig. 3.22. The preprocessing applied consists in filtering, binarizing and correcting the handwritten word in order to enhance the three zones, namely, upper, lower and middle zone (see Fig. 3.22 (a)). Starting from these zones we end up in a global shape of the word that will be used to recover the memorized prototype by the means of neural network (see Fig. 3.22 (b)). The handwritten words representing the 27 amount classes are clustered in 16 prototypes or models created by superposing only four words from each class. The resulting model is processed to yield a final prototype which consists of one memory of Hopfield model of the sequential method [56] as described by Fig. 3.22. Due to some degradation in the handwritten word we have avoided the use of handwritten contours and the structural components as it was usually used. The main objective of the present recognition system is to arrive at a reduced number of candidates (β_i) and to determine from them the handwritten class to be recognized. Each prototype or model corresponds to a finite number of candidates.

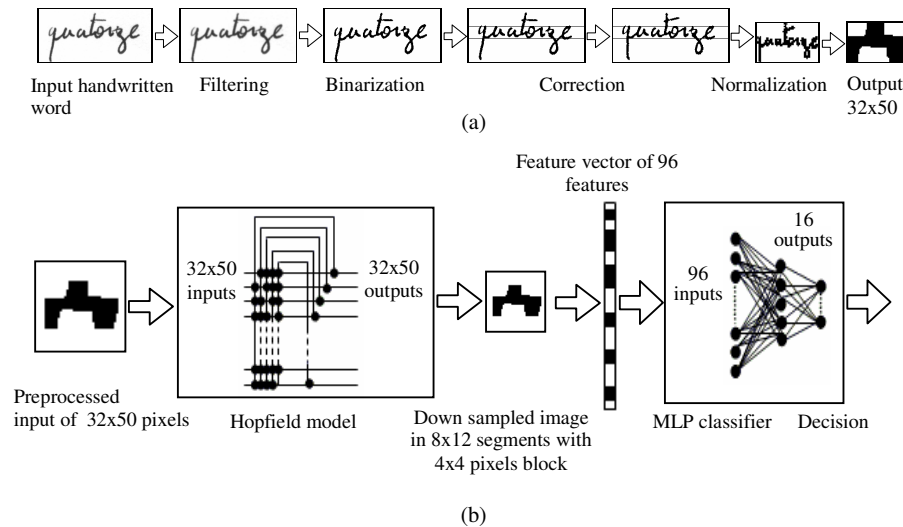


Fig. 3.22 Proposed method illustration example (a) Handwritten word preprocessing (b) sequential combination method for prototype recognition

As an example, the second prototype corresponds to the handwritten words ($\beta_2=3$) “deux”, “trois” and “dix” that have the same global shape. Once the prototype is classified using the prototype recognition system, the candidate choice is based on the presence of dots in the upper zone and the transition number of character-background of the first word character.

3.4.2 Handwritten word preprocessing

a) Word horizontal slant

In handwritten word, one of the major variations in writing style is caused by slant, which is defined as the slope of the general writing trend with respect to the vertical line. This operation is performed after skew correction and central zone localization (SC-CZL) [128]. The horizontal slant correction operation consists in correcting the tilted character in order to return it upright. The slant correction method [55], which is based primarily on the lower and upper centroid (SC-LUC), is used. The application of the slant correction on the vertical segment separately of the image shown in Fig. 3.23 (d) yields a slant estimation angle of 50.0 degrees. In our case the horizontal slant correction consists in rotating rather shearing horizontally this segment using as origin the upper reference line. A comparison result of the application of this method and contour method is shown in Fig. 3.23 (e) and (f) respectively.

We note that in Fig. 3.23 (e), the ascender is well pronounced to the image top than in Fig. 3.23 (f).

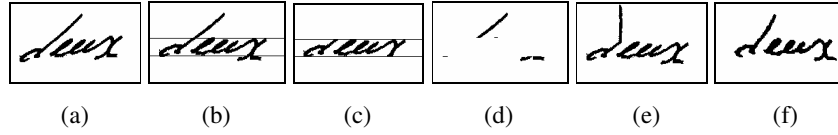


Fig. 3.23 Slant correction (a) Original image (b-d) result of application of SC-CZL (e) Result of application of SC-LUC on (d). (f) Slant correction based on contour slant estimation

b) Word size normalization

Since word sizes differ significantly, this makes it difficult to feed the Hopfield model which requires a standard pattern size for all entries. Thus, images should be normalized to a given standard size of 32x50 pixels. The application of SC-CZL method, yields the three zones of interest that will be used for horizontal slant correction and normalization as shown in Fig. 3.24 (c) and (d). In the normalized image, the baseline or lower reference line is located at $y_{lo}=12$, and the upper reference line is located at $y_{hi}=21$ from top image. However, the scales are determined by the word width and the distances between lower-upper reference lines to the top and the bottom of the word as shown in Fig. 3.24. The scales, S_x and S_y are calculated as follow:

$$S_x = \frac{w_{norm}}{W} \quad (3.24)$$

$$s_y = \begin{cases} \frac{h_{hi}}{y_t - y_h} & \text{if pixels} \in [y_h, y_t] \\ \frac{h_{cent}}{y_h - y_l} & \text{if pixels} \in [y_l, y_h] \\ \frac{h_{lo}}{y_l - y_b} & \text{if pixels} \in [y_b, y_l] \end{cases} \quad (3.25)$$

where $W=xr-xl$, and $w_{norm}=50$ pixels is the normalized width, and $h_{hi}=11$ pixels, $h_{cent}=10$ pixels and $h_{lo}=11$ pixels are, upper, central and lower zones height of the normalized word respectively.

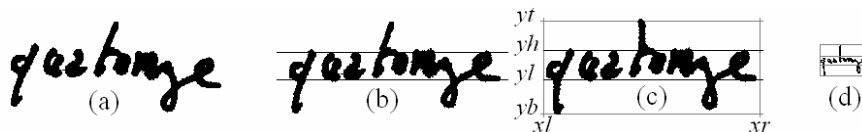


Fig. 3.24 Preprocessing (a) binarized image (b) Application of SC-CZL method (c) Horizontal slant correction (d) Normalized version of (c) in the frame 32-by-50 pixels

c) Prototype creation

The realization of a prototype is carried out by the superposition of four normalized word images within the frame of 32-by-50 pixels of various writings of a word class written in wholly lower case letters; the resulting form is then dilated (see Fig. 3.25). Figure 3.25 (e) shows four samples from each word class in the training set used for prototype creation. The vocabulary of our application is composed of 27 words. During the realization of the 27 prototypes corresponding to these word classes, it can be noticed that certain prototypes have similar shapes. Therefore, it is interesting to group prototypes that have similar global shapes corresponding to different word classes by a unique prototype. This clustering operation yields 16 prototypes (see Fig. 3.26) representing the 27 classes (N_H) of French legal amounts with $\beta_k, k=1, 2, \dots, P$ ($P=16$), the number of handwritten word class per prototype class.

$$N_H = \sum_{k=1}^P \beta_k, \quad k = 1, 2, \dots, P \quad (3.26)$$

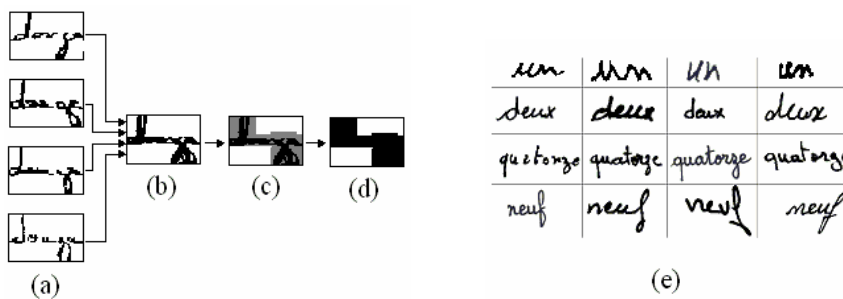


Fig. 3.25 Prototype creation (a) Four different normalized words from handwritten word class “douze” (b) Superposition operation (c) Dilation and prototype processing (d) Prototype result. (e) Samples of handwritten words used for prototype creation.

1	2	3	4	5	6	7	8
un six euro	deux trois dix	quatre	cinq	sept vingt	huit trente	neuf	onze seize
$\beta_1=3$	$\beta_2=3$	$\beta_3=1$	$\beta_4=1$	$\beta_5=2$	$\beta_6=2$	$\beta_7=1$	$\beta_8=2$
9	10	11	12	13	14	15	16
treize douze	quatorze	quinze	quarante	cinquante	cent soixante	mille et	million centime
$\beta_9=2$	$\beta_{10}=1$	$\beta_{11}=1$	$\beta_{12}=1$	$\beta_{13}=1$	$\beta_{14}=2$	$\beta_{15}=2$	$\beta_{16}=2$

Fig. 3.26 Prototypes used for holistic recognition and their corresponding handwritten classes and β_K (below each prototype image)

3.4.3 Experimental results

a) Training phase

The prototypes shown in Fig. 3.26 are fed to Hopfield model and memorized for $P=16$ (number of memorized patterns), and $N=1600$ neurons (32x50 pixels), then the output from Hopfield model is down sampled in a 4x4 pixel block. The MLP was trained only with 810 handwritten words, which corresponds to 30 (810/27) words for each handwritten class. This training set was not chosen to be large due to the strong similarity of global shapes existing among the handwritten words belonging to the same prototype class. However, the global shape of words of the same prototype does not change significantly, particularly when the word image is down sampled to 8x12 yielding feature vectors of 96 features (see Fig. 3.22 (b)). The down sampling operation is acting as a second noise filter which makes the patterns of the same prototype class to be very similar in the input of the MLP-based classifier. Thus, we found experimentally that when increasing the number of words per prototype beyond 30=810/27 (for a prototype having one handwritten class), the error-reject plot of the proposed method does not change. Finally, the resulting feature vectors (8x12=96 features) of 810 handwritten words are used to train a two layers of fully connected MLP neural network module with $\alpha=0.9$ (The training speed), $\xi=0.001$ (viscosity coefficient), the number of hidden layer was fixed to 40, the number of outputs of the MLP corresponds to the number of prototype classes which is in our case sixteen and the total error to 0.001. The expected prototype class is simply given by the output unit with the highest value. The MLP classifier

can reject patterns whose membership cannot be clearly established. A typical classification criterion which is used consists of rejecting a pattern if:

$$\bar{y} = \max_{i=1,2,\dots,P} \{y_i\} < R_M \quad (3.27)$$

where P is the number of prototype classes, $y_i \in (0,1)$ is the i th output of the network, and R_M is a proper threshold. An unknown pattern is accepted if only at least one output is greater or equal than R_M .

The associative matrix $W^{(o)}$ is directly calculated and stored, whereas the connection weights v_{ij} and w_{ij} corresponding to the two fully connected MLP are obtained after convergence and also stored for recognition process. We precise, that the Hopfield model memorises the 16 created prototypes as classes. Two word characteristics were used to distinguish word classes belonging to the same prototype class, namely, the dot and the starting loop in case of words starting with “d” (see Fig. 3.27 (c)) as follows:

- 1- The existing dot is detected using an empty mask of dimension 20-by-20 pixels, fixed experimentally in which the detected dot lies inside.
- 2- The starting “d” is detected using the intersection of a vertical line with the left part of the word in the lower case zone.

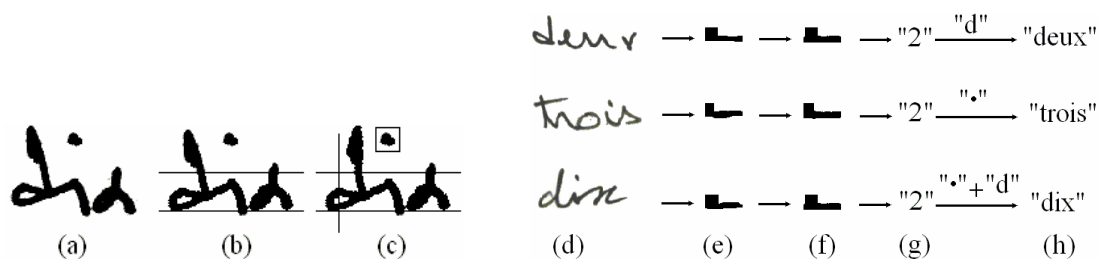


Fig. 3.27 Starting “d” and dot detection (a) Original image word (b) Application of SC-CZL method (c) Starting “d” and dot detection (d) Original images (e) Dilated version of the normalized image (32-by-50). (f) Hopfield model output (g) Result of prototype recognition by Hopf-MLP classifier. (h) Results of holistic word recognition by combining result of (g) and word characteristics (“d” and dot).

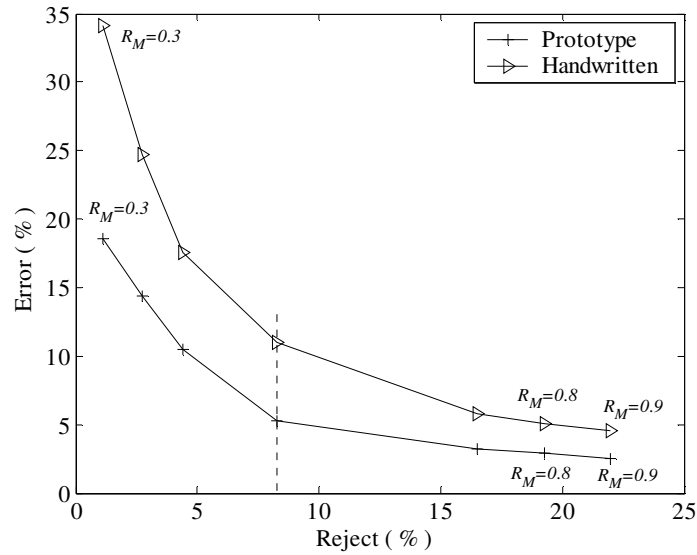
These two characteristics are combined with the prototype recognition results to make a final decision of the unknown handwritten word. Figure 3.27 (d-h) illustrates the combination of these two characteristics and the results of the combined neural networks for prototype recognition. All the 27 legal amounts are distinguished using prototype recognition results

associated with the “d” and dot characteristics. Another characteristic was introduced to discriminate classes belonging to the prototype “1”, namely, “un”, “six” and “euro”. It consists of intersecting a horizontal line at the half lower case zone with word parts.

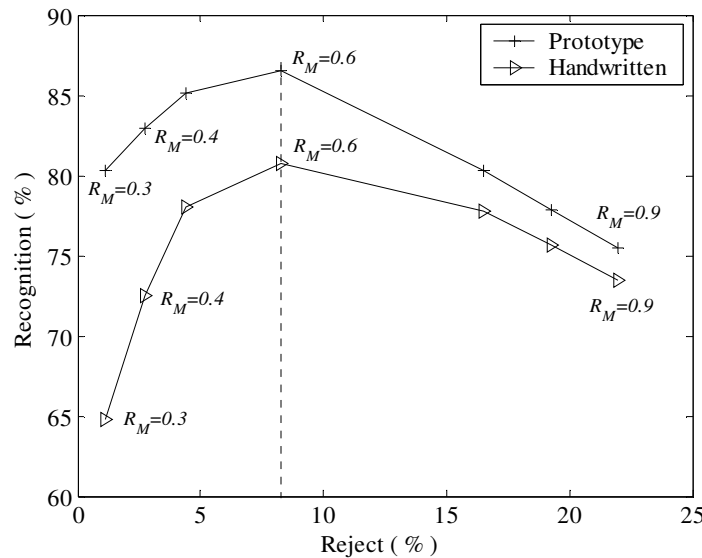
b) Recognition phase

The system has been tested using our proper database of 27 basic words written by 200 writers. The test database consists of 5400 (27x200) legal amounts collected and extracted manually from 20 A4 format papers that were scanned at 300 dpi. The experiments are conducted in two parts, the first part consists in testing the performance of the prototype recognition and the second part presents results of the handwritten word recognition. Figure 3.28 (a) summarizes the results obtained on the same database of handwritten words of medium and low quality by the sequential combination method. The handwritten words in the test set are uniformly distributed (200 words/class). The plots for the prototype and handwritten methods are obtained for different values of the rejection threshold R_M ($0.3 \leq R_M \leq 0.9$). When using the sequential combination method, the preprocessed handwritten word character (global shape) is processed with the Hopfield model for $T=1$ (Hopfield iteration number), and then the resultant output is down sampled before it is fed to the MLP. According to the results obtained, it can be noticed that for the same rejection rate, the handwritten error rate is always greater than those obtained by prototype recognition. Thus the handwritten recognition is strongly dependant on the results of the prototype recognition used as global shape classifier. When the rejection rate of the prototype recognition system is very low (lower R_M), this ensures higher errors for handwritten classification when comparing to prototype errors. Whereas for higher rejection rate (higher R_M), the proposed system ensures lower errors for handwritten classification which are similar to those obtained with the prototype recognition. This could be explained by the fact that the proposed system rejects (for higher R_M) not only the poor quality words but also a great part of those of low-medium quality and accepts high-medium quality words, and gives less errors in prototypes and consequently in handwritten words (dots and starting “d” clearly detected).

The error-reject plots of Fig. 3.28 (a) shows that the recognition system gives best results for prototype recognition when comparing to handwritten recognition. This difference in recognition rate is due to starting “d” and dot detection to determine the handwritten class from the recognized prototype.



(a)



(b)

Fig. 3.28 Recognition results. (a) Error-reject plots (b) Recognition-reject plots

The handwritten recognition rate converges to the prototype recognition rate when the above mentioned characteristics are correctly detected. Hence the handwritten word recognition can only be as good a solution as the prototype recognition, or it can be worse.

Figure 3.28 (b) presents recognition-reject plots showing best results for both prototype and handwritten recognition for a threshold reject $R_M=0.6$ (in dashed line) corresponding to the same global reject of 8.25%, and global errors of 5.25 % and 11.00 % for both prototype and handwritten recognition respectively. A recognition rate of 86.50 and 80.75 % for prototype

and handwritten recognition respectively is achieved. Figure 3.29 shows results of correctly recognized handwritten words.

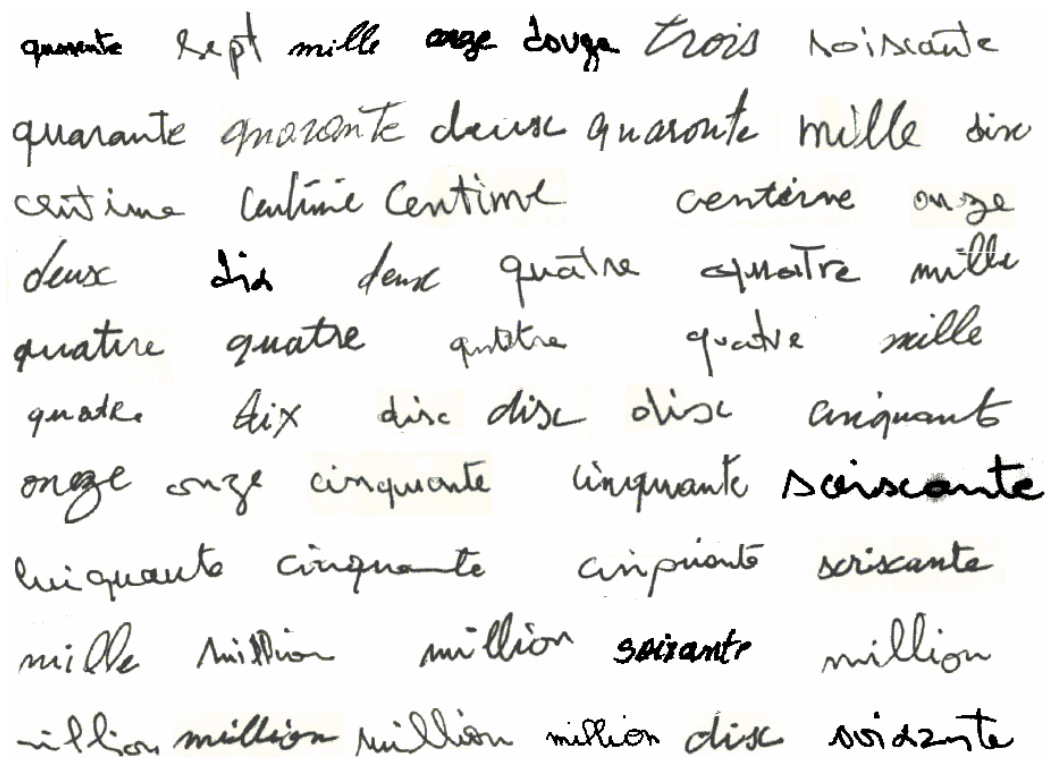


Fig. 3.29 Handwritten word samples correctly recognized

In this section, holistic handwritten word recognition based primarily on accurate zones detection, namely, upper, lower and central zones was presented. Experimental results conducted on prototypes and handwritten word show the robustness of the proposed system. It has been shown that the holistic handwritten word recognition with combined neural network involves only few training words. Experiments were conducted on data set of handwritten words of medium and low qualities and have shown interesting results.

3.5 Degraded printed character recognition

The recognition of degraded printed documents remains an ongoing challenge in the field of optical character recognition. This is due to the degradation which could be originated from: low quality originals, quantization errors in the digitization process and non optimal

light and contrast settings. This could come from the copying or scanning process, non-sharp or low-contrast printing on the document, transmission errors, or paper defects and/or dirty optical or sensor systems. The targeted application of our method is third world bank check processing and especially the Algerian post check selected as an example, for the following two reasons:

- Printing and paper are of poor quality.
- The important daily use of account numbers for customer balances.

The ACN is used to retrieve from the customer reference database: the personal information about the customer account and customer's signature for check validation by signature verification. Bank customers are often asking about their account balance at bank counter, before doing withdrawal operation. Thus, only the account number is used in account balance operation. Hundreds of thousands of the latter operation are daily operated in such banks.

In spite of significant improvements in the area of optical character recognition, the recognition of degraded printed characters, in particular, is still lacking satisfactory solutions. Studies on designing recognition systems with high performance for degraded documents are in progress along three different aspects. One is to use a robust classifier, a second is to enhance the degraded documents images for better display quality and accurate recognition, and the third is to use several different classifiers. The idea of combining different classifiers for improving their performance received a lot of attention in the last few years. Obviously performance of the system cannot be improved if the individual classifiers make the same mistakes, thus it is important to use different features and different structures in the individual classifiers. In this section two types of combination of neural network classifiers are presented. The sequential and the parallel combination for degraded printed character recognition.

3.5.1 Sequential combination for degraded character recognition

Degraded printed character recognition is a hard and ever present problem in optical character recognition (OCR). In this section we propose a sequential neural network combination method for degraded printed character recognition [56]. This method combines a Hopfield network with two perceptron layers applied to Algerian postal check due to its strong degradation (see Fig. 3.30). The Hopfield network stores M prototype characters used

as main classes. After the preprocessing, an image of a character is given to a Hopfield network which can yield after a fixed iteration number, a pattern that is subsequently fed to an MLP network for classification. The main idea is to enhance or restore such degraded character images with Hopfield model at different iteration number for recognition accuracy applied to poor quality bank check (see Fig. 3.31).

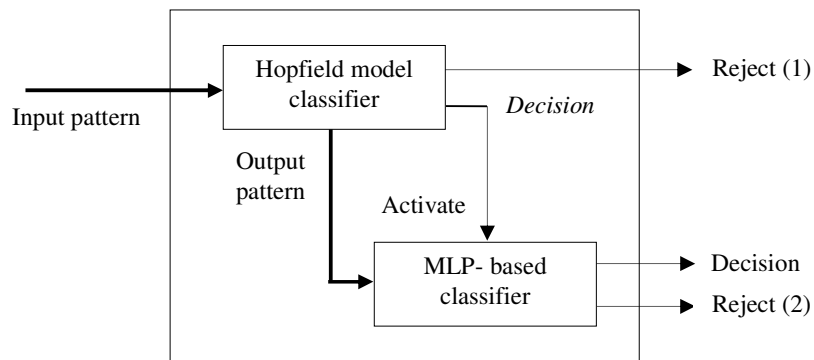


Fig. 3.30 Recognition synoptic block diagram of sequential combination method.

The main motivation is to use the Hopfield model as a first stage acting not only as a noise filter but also as a character enhancing and restoring, especially for broken, missed part and scratched characters (see Fig. 3.31). The Hopfield network is then followed by a down sampling module used mainly as an additional noise-filtering step. Thus, the down sampled image is classified during a second stage by the MLP based classifier known by its discrimination capabilities in presence of noise when comparing to classical classifiers. Classification accuracy for ten digits and twenty six alphabetic characters from a single font is also studied in the presence of additive Gaussian noise.

a) Recognition system

The proposed recognition method is based on two cascaded artificial neural networks modules connected to a down-sampling block [85] as shown in Fig. 3.32. The Hopfield neural network is tailored to recover the memorized pattern class after a fixed iteration number T and the subsequent one (MLP) is tailored for the classification.

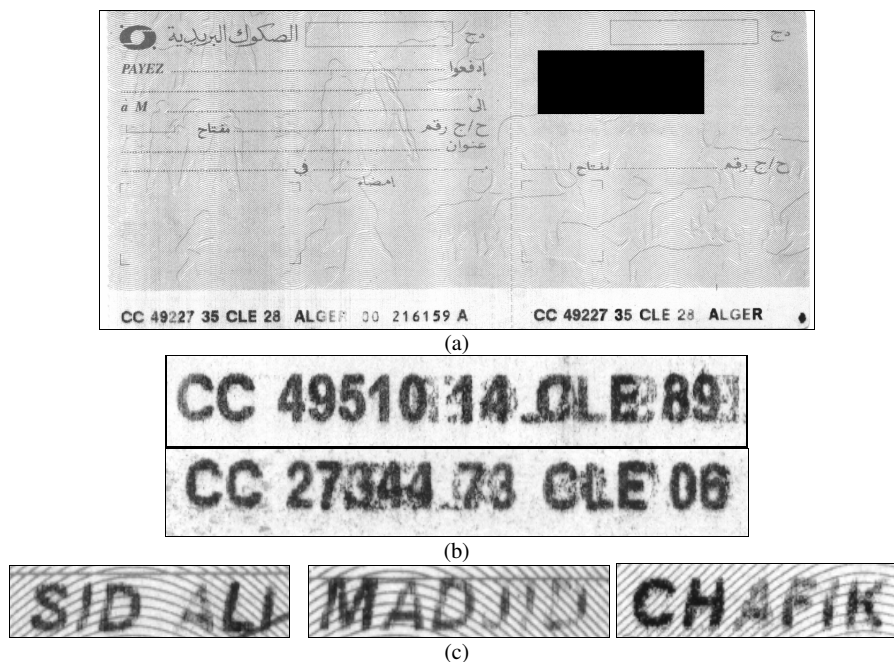


Fig. 3.31 Poor quality documents a) Algerian post check b) Account check number c) Customer first and last name.

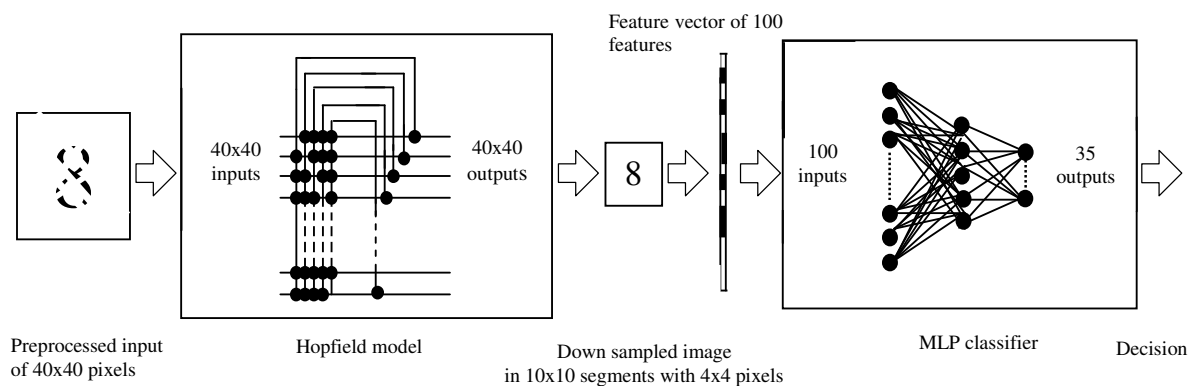


Fig. 3.32 Proposed method illustration example for printed character recognition.

In the down sampling step, the character images were divided into 10×10 segments as in Figure 3.33, where each segment consists of 4×4 pixels. The mean of the grey level for each segment were then used as input data to train MLP network. Therefore, the MLP network would have 100 input nodes (one for each segment) and 36 output nodes, where each output node represents one class. The down sampling module is also used to speed up the

classification stage rather than feeding the MLP with a feature vector of 1600 features (40x40 image size).

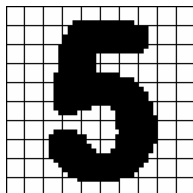


Fig. 3.33 Character image divided into 10×10 segments.

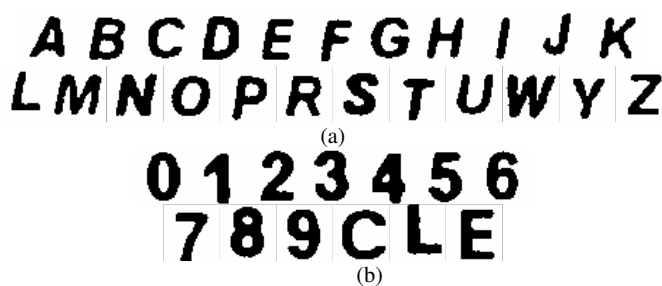


Fig. 3.34 40-by-40 pixels character class a) Customer first and last name character classes b) Account check number character classes.

The Hopfield network stores 36 prototype characters shown in Fig. 3.34. The letters QVX are omitted because this project works exclusively with Latin transcriptions of Arabic names which do not use these letters. After the preprocessing, an image of a character is given to Hopfield network which can yield after a finite iteration number, a pattern that is subsequently down sampled and fed to MLP for classification. The retrieved pattern from the Hopfield model represents an enhanced or restored version of the degraded character. The main idea of the proposed method is to test the MLP-based classifier with the Hopfield model outputs for different iteration number. Figure 3.32 presents an illustration example of the proposed sequential combined method.

b) Experimental results

The experiments are conducted in two parts; the first part presents a comparative study of the proposed method with the individual classifiers, namely, the Hopfield model and the MLP network for isolated printed character check recognition. The second part is devoted

firstly to study the robustness of the combined method in presence of additive Gaussian noise and secondly to degraded real printed characters.

i) Prototype extraction and training phase

The character data set represents a single font gray level character that was collected from 490 post checks belonging to the same post. The post checks were scanned at 300 dpi, which avoids the scaling procedure. Hence a frame of 40x40 pixels is sufficient to include each of the 36 pattern classes. The classes considered consist of ten numeral characters and twenty five alphabetic characters of 40-by-40 pixel size. The characters used for learning the MLP were extracted from 70 post checks, and gave rise to 2800 characters. Before they are fed to the MLP classifier for training phase, the characters are firstly preprocessed using median filtering and binarised with Otsu's method, and secondly processed with down sampling procedure. The remaining 420 post checks were used for testing, which consist of 16800 characters. The Hopfield model was trained only with thirty five clean characters and tested with 16800 characters. The MLP used in the proposed work is a two layer of fully connected neural network module with $\alpha=0.9$ (training speed), $\xi=0.001$ (viscosity coefficient), the number of neurons in the input layer was fixed to 100, the hidden layer was fixed to 40 neurons, the number of outputs of the MLP corresponds to the number of classes which is in our case thirty five and the total error to 0.0001. The connection weights v_{ij} and w_{ij} corresponding to the two layers fully connected MLP are obtained after convergence and stored for the recognition process. The Hopfield parameters were fixed to: $M=36$, $N=1600$ (40x40 pixels), where M is the number of memorized patterns. The associative matrix $W^{(o)}$ is directly calculated and also stored for the recognition process.

ii) Recognition phase

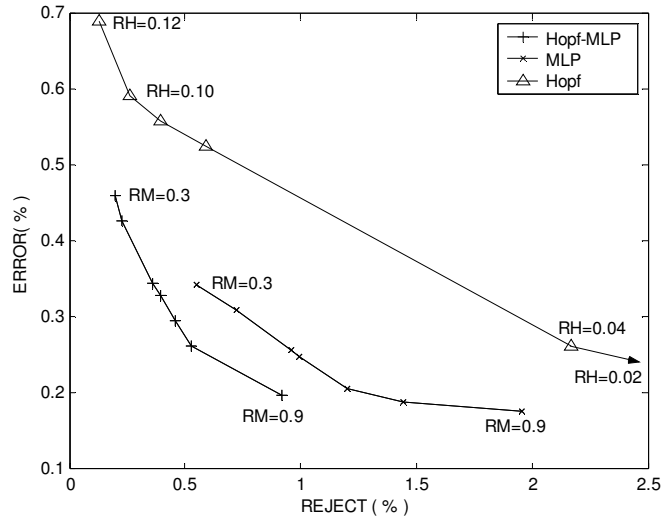
1-Real printed character recognition

Figure 3.35 (a) summarizes the results obtained on this dataset by the classification methods described in chapter 2. The plot for the Hopfield model is obtained for different values of the rejection threshold R_H ($0.02 \leq R_H \leq 0.12$). The other plots are obtained for the MLP based classifier with R_M ranging from 0.3 to 0.9 and for the combined approach with R_M ranging

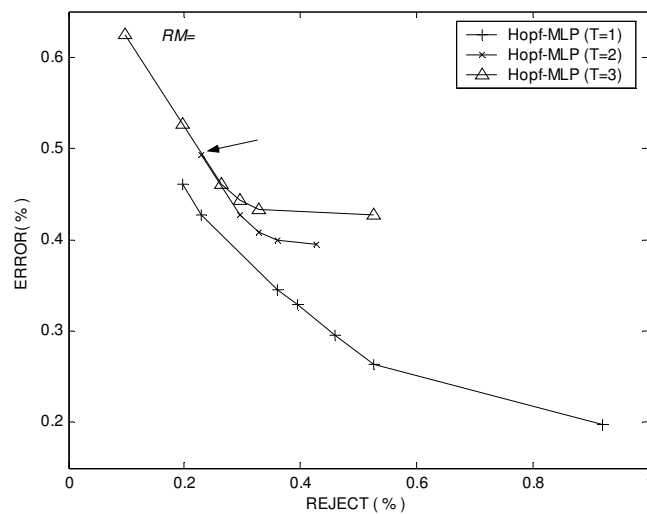
from 0.3 to 0.9. When using the combined method the preprocessed character is processed with the Hopfield model at different iteration number T , and then the resultant output will be down sampled before it is fed to the MLP. The curve describing the combination of Hopfield model and MLP is obtained by choosing $R_H=0.12$, the number of iterations $T=1$ and various R_M ($0.3 \leq R_M \leq 0.9$). Figure 3.35 (b) presents the error-reject plot of the proposed method for different iteration numbers of the Hopfield model and shows that the best performance is achieved for $T=1$. As it can be noticed in Fig. 3.35 (a), the MLP based classifier outperforms clearly the Hopfield model based classifier. The error-reject plots of Fig. 3.35 (a) shows that the proposed modular approach outperforms both the Hopfield model and the MLP-based classifiers. The plot corresponding to the combined approach reaches the plot of the Hopfield based classifier for very low rejection rates. Equally, for high rejection rates, the combined approach outperforms both the Hopfield and MLP based classifiers. Table 3.7 summarizes the best performance achieved by the three classifiers, namely, the MLP, the Hopfield and the proposed classifier. According to these results, it is clear that the proposed approach outperforms both the individual classifiers. The high performance of the proposed approach when comparing to the Hopfield network as an individual classifier is due to the use of the down sampling and the MLP based classifier known by its robustness in presence of noise. The hamming distance used in the individual classifier to classify the output of the Hopfield network is noise sensitive. The MLP based classifier when acting as an individual classifier uses as input data the down sampled version of the preprocessed character which could be a noisy pattern that was not processed as in the case of the combined method with the Hopfield network acting as a noise filter. Thus the Hopfield model when combined to the MLP, acts as a noise filter and enhance the MLP degraded character input.

Figure 3.36 and 3.37 show degraded characters that were correctly recognized and misclassified respectively. The character images shown in Fig. 3.38 (c) represent the Hopfield model outputs.

The corresponding gray level characters (shown in top) were correctly recognized by the proposed method. Whereas these images were misclassified by the Hopfield model (for $R_H > 0.6$) and totally misclassified by the MLP based classifier (for $R_M < 0.5$). The main objective of the Hopfield model is to make the degraded character input identical as possible to the memorized pattern.



(a)



(b)

Fig. 3.35 Error versus reject plots a) Error versus reject plot for three classifiers using various threshold values for R_H and R_M b) Error versus reject plot for the combined method showing the effect of using different Hopfield iteration number; $R_H=0.12$ and $T=\{1, 2, 3\}$.

However the Hopfield model acts as an enhancement procedure as shown in Fig. 3.38 (b) and (c), which improves the recognition rate especially when using an insensitive noise classifier like the MLP to classify the images in Fig. 3.38 (c). This high improvement could be clearly noticed from the plots of the recognition rate versus the proper threshold R_M (see Fig. 3.39) for the proposed method and the MLP.

Table 3.7. Best performance comparison of the three classifiers using the test set of 16800 characters. For the combined method we chose $R_H=0.12$, $R_M=0.3$ and $T=1$.

Classifier	Errors (%)	Rejected (%)	Recognized (%)
Hopfield ($R_H=0.12$)	116 (0.69)	22 (0.13)	16662 (99.18)
MLP ($R_M=0.3$)	59 (0.35)	92 (0.55)	16649 (99.10)
Hopfield-MLP	77 (0.46)	32 (0.19)	16691 (99.35)

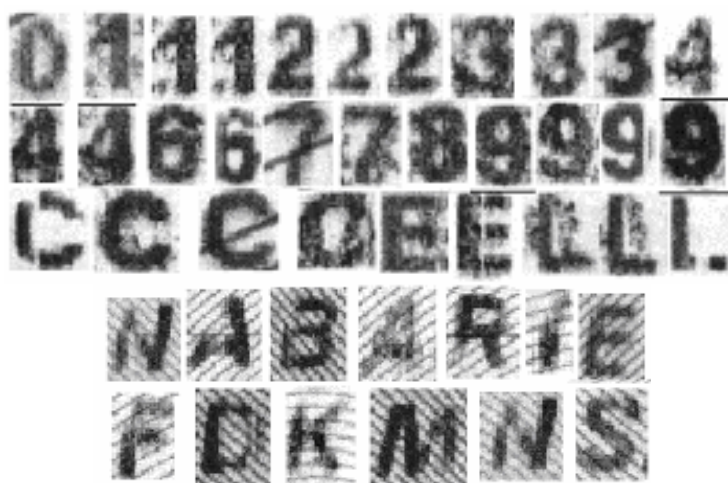


Fig. 3.36 Gray level real printed characters recognized correctly



Fig. 3.37 Misclassified gray level real printed characters

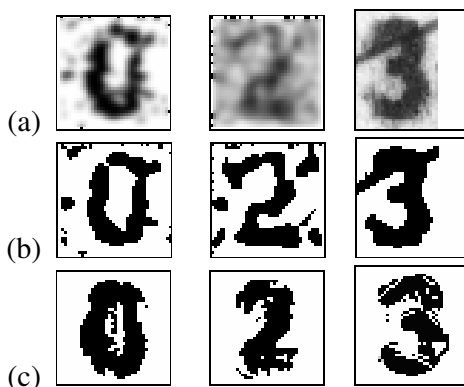


Fig. 3.38 Degraded character processing a) Original images b) Binarization of (a) c) Corresponding Hopfield model outputs of images in (b) for $T=1$.

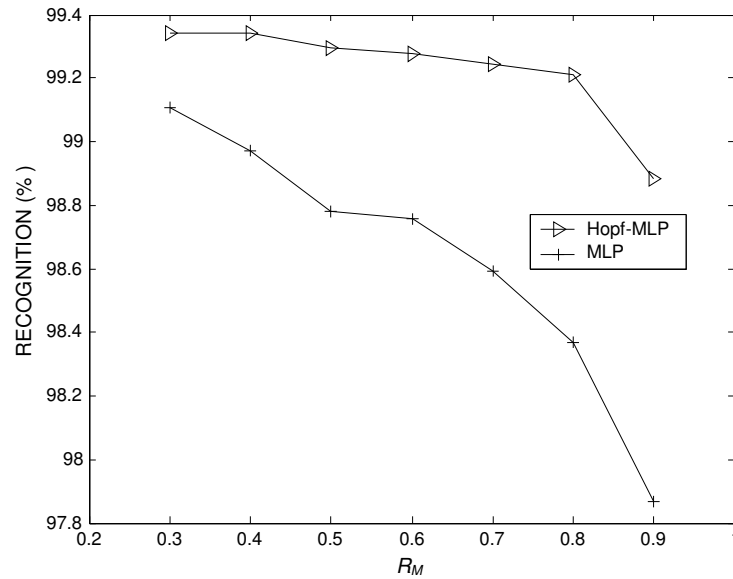


Fig. 3.39 Recognition versus reject thresholds (R_M) plots; the MLP based classifier plot and the combined method plot for $R_H=0.12$ and $T=1$.

2-Degraded printed character recognition

To test the robustness of the proposed method on effective poor quality character checks, first, it was applied to the Hopfield training set (see Fig. 3.34) corrupted with added Gaussian noise (AGN) and secondly to real broken and incomplete characters. The training set was corrupted with an added gaussian noise, and a recognition rate of 100 % was achieved for a SNR up to -2.10 dB ($\sigma=1.27$) as shown in Fig. 3.40. It can be concluded from these results, that for a SNR up to 3.0 dB ($\sigma=0.7$), the 36 noisy classes are successfully recognized. Figure 3.41 shows, noisy gray level account number characters for various added gaussian noise levels, that were correctly recognized up to $\sigma=0.6$. Experiments were also conducted on real broken and incomplete character images. Figure 3.42 shows many of these characters, in spite of the important degradation, the proposed method was able to recognize the degraded printed characters.

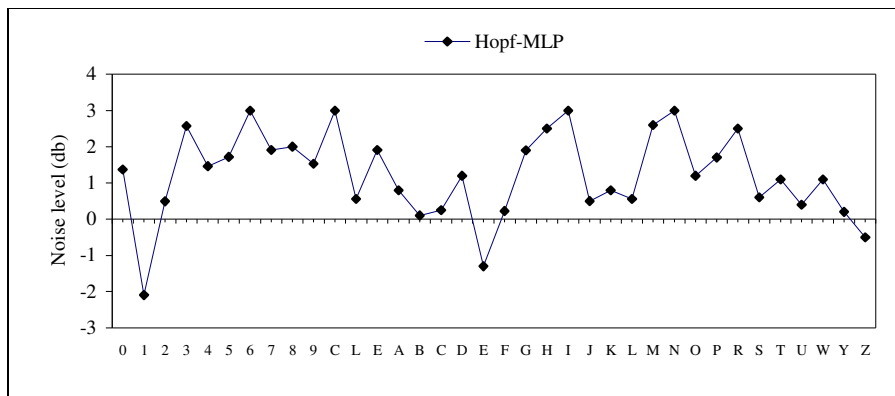


Fig. 3.40 Reached SNR for 100% recognition rate for account number and customer first and last name

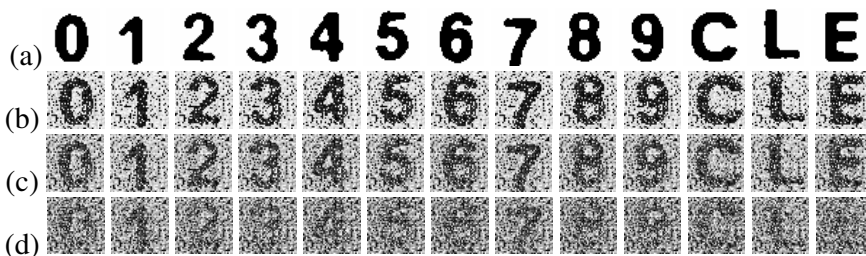


Fig. 3.41 Recognized degraded account number characters by various Added Gaussian Noise (AGN) a) Original image characters b) Noisy grey level images with $\sigma = 0.2$ c) Noisy grey level images with $\sigma = 0.4$ d) Noisy grey level images with $\sigma = 0.6$.

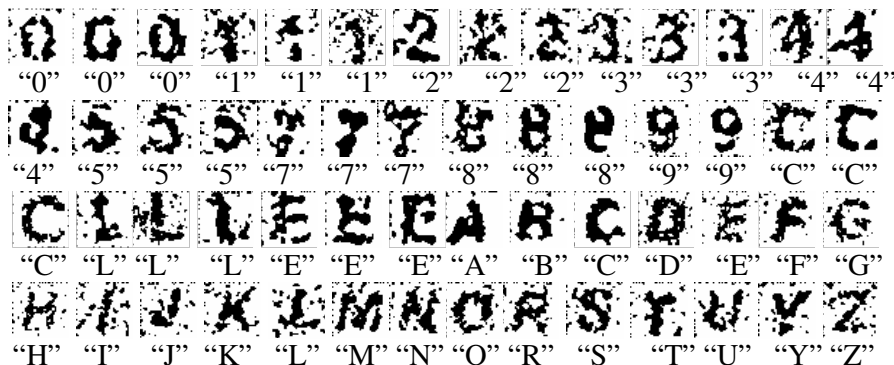


Fig. 3.42 Broken and incomplete real characters correctly recognized.

In this section we presented a sequential neural network architecture combining two noise insensitive neural networks, namely, the Hopfield model and the MLP network. This combination gives strong noise robustness for the tasks supported. Experiments were conducted on collected printed characters check of medium and low quality. We reported

experimental results for a comparison of three neural architectures: the Hopfield network, the MLP-based classifier and the proposed combined method. They show that the combined classifier outperforms both the individual classifiers, namely, the Hopfield and MLP classifiers. We achieved successful results concerning the recognition of extremely degraded printed character recognition. The proposed method could be addressed to solve the problem of multi font by increasing the number of the prototypes and the pattern size.

3.5.2 Serial combination for degraded character recognition

In this section we propose a serial combination of the Hopfield and MLP networks, to achieve accurate recognition of degraded printed characters [131]. We introduce a relative distance, used as a quality measurement of the degraded character which makes the Hopfield based classifier very powerful and very well suited for rejection. This relative distance is compared to a rejection threshold in order to accept or reject the incoming degraded character by the Hopfield model used as a first classifier. Due to its discrimination capability, the MLP network is used as a second classifier to avoid rejection error and to diminish computational complexity.

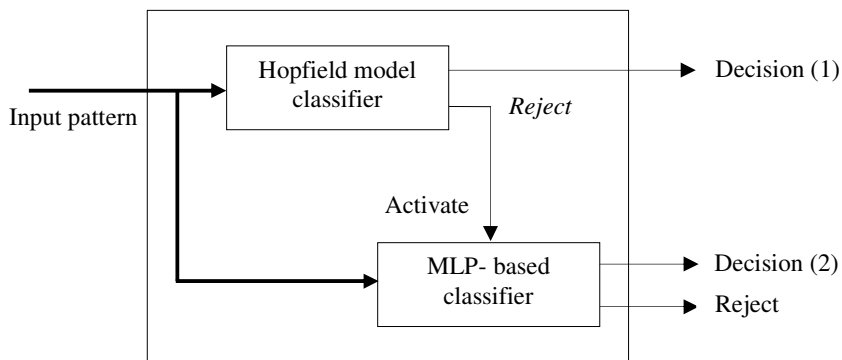


Fig. 3.43 Recognition synoptic block diagram (a) Sequential combination method (b) Serial combination method

The proposed method is devoted to solving the problem of recognition of single font characters collected from poor quality bank checks. The proposed method is compared to five other recognition systems. They show that the proposed architecture exhibits the best performance, with no significant increase in the computational burden. In this we also present

a bank check processing procedure for account check number (ACN) detection, localization and character retrieval. The recognition system is applied to ACN which is doubly printed in two serial numbers on each side of poor quality bank checks and to verify if they are identical. Experimental results related to the proposed method with various added Gaussian noise (AGN) levels, as well as tests with broken and incomplete characters are presented.

a) Serial combination of Hopfield network and MLP-based classifier

The main idea is to combine properly the Hopfield model used as a first classifier with the MLP as a second classifier as shown in Fig 3.43. Thus, a relative distance (ξ) (see equ. 2.20) is introduced as a quality measurement of the degraded character. This relative distance will be compared to a rejection threshold (R_H) in order to accept or reject the incoming character by the Hopfield model used as a first classifier. The proper rejection threshold (R_H) and the iteration number (T) of the Hopfield network should be chosen so as to keep the error very low. Thus, the rejected Hopfield patterns are then classified by the MLP-based classifier known by its discrimination capability using an adequate proper rejection threshold (R_M). The two neural networks are separately trained. The Hopfield network is trained with a fixed number of clean characters representing prototypes or memories, whereas the MLP is trained with a large number of various printed characters collected from post checks. When applying these two NN separately to collected printed characters, we have found out that they exhibit almost a complementary behavior. The Hopfield model is more suitable for rejection and keeps the error low for higher rejection, whereas the MLP is more suitable for low error and keeps the rejection low [61]. In order to take advantage of both classification schemes, the Hopfield model is used as a first classifier to take a decision only on the accepted pattern leading to low errors. On the other hand, the MLP, as a second classifier, is activated only when the first classifier rejects the incoming pattern. Thus, the rejected characters by the Hopfield model are then classified by the MLP-based classifier. The performance of the proposed method depends strongly on T and the proper thresholds, namely, R_H and R_M . The error-reject plots of the Hopfield and MLP networks are used to determine R_H and R_M respectively that gives high performance.

b) Bank check processing application

The main processing of bank checks that we have considered consists of account number detection and localization (ANDL) followed by character retrieval. The account number zone is variable in the case of the present application. This zone (white zone that includes the account number) could be in the extreme bottom or often a little bit higher as shown in Fig. 3.44 (c). A horizontal projection of the check image followed by an appropriate thresholding is used to exactly detect and localize this white zone.

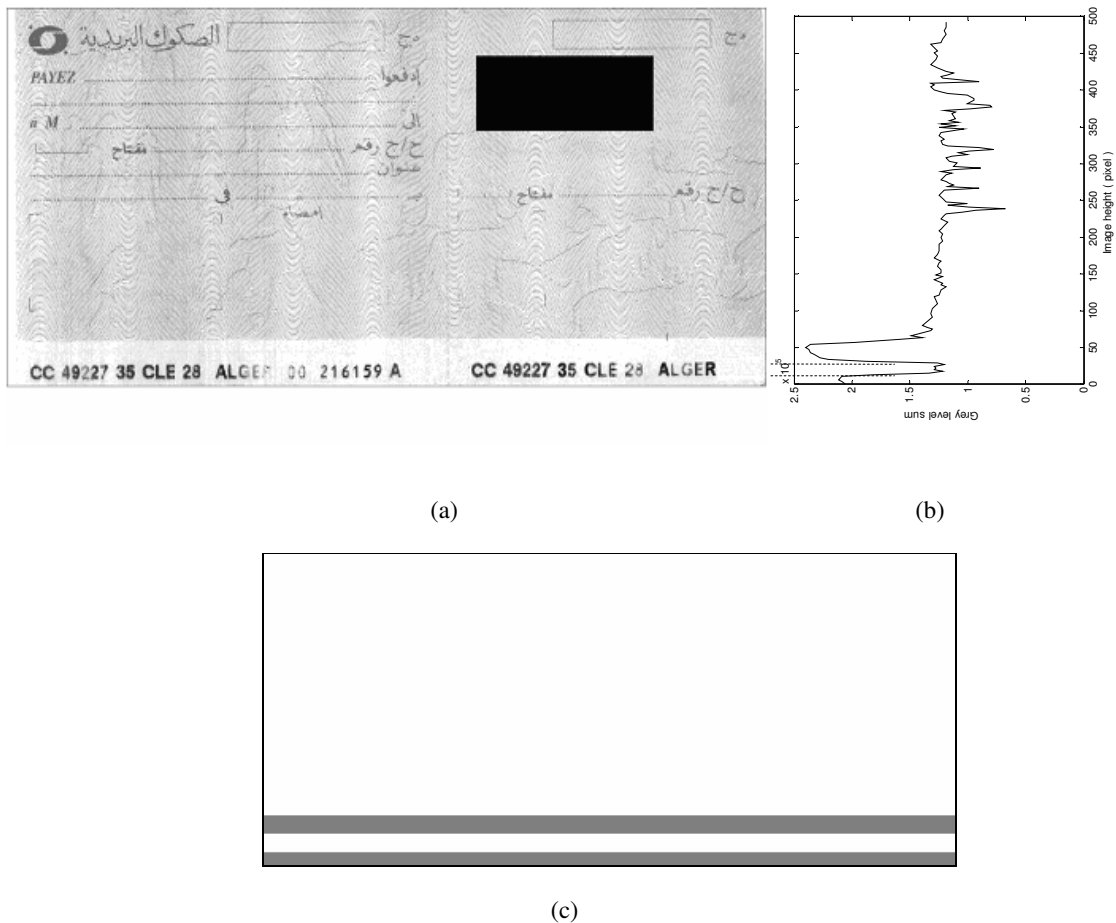


Fig. 3.44 ANDL procedure (a) Post check. (b) Opened image horizontal projection. (c) Post check thresholding.

i) Account check number localization

The application of morphology in our case is to detect, localize and to segment in blocks the ACN. Once the post check is acquired it is automatically opened using the following equation:

$$g = f \circ h \quad (3.28)$$

where f is the input image and h is the structuring element. The latter was chosen to be horizontal with 3 rows by 5 columns. The horizontal projection of the opened image shown in Fig. 3.44 (b) is calculated and thresholded to detect and localize the white horizontal band (see Fig. 3.44 (c)). The threshold value is calculated as follows:

$$\text{thresh} = \mu[\text{Proj}(g)] + k * \sigma[\text{Proj}(g)] \quad (3.29)$$

where $\text{Proj}(g)$ is the horizontal projection of the opened image g , μ and σ are the mean and the standard deviation of $\text{Proj}(g)$, and k is an appropriate constant which can be chosen experimentally. For the present application, k was chosen to be equal to 0.2. Figure 3.44 shows the application of this procedure.

ii) Account number presentation and processing

The ANDL procedure is followed by a morphological closing. Horizontal and vertical structuring elements of size 1x13 and 13x1 were used. The resulting image is then processed using local thresholding and contour detection, which enables to locate all the ten regions of interest as shown in Fig. 3.45. The ACN zone is processed to yield 10 distinct blocks in the left and the right sides. The first block "CC" is the abbreviation of account check which means in French "Compte Chèque", blocks 2 and 3 are two parts of the account number, block 4 is "CLE" written in French which means key, and block 5 indicates the two digits access key number. The ten digits numbers are of a fixed pitch with a width of 23 pixels. The "CC" and "CLE" are also of a fixed pitch but with 30 pixels width. The "CC" and "CLE" are used as main references for the account and the access key numbers detection respectively. Once these ten blocks are detected, their segmentation in characters is a straight forward

operation, since the first and the fourth blocks are of 30 pixels pitch, and the second, the third and the fifth blocks are of 23 pixels pitch.

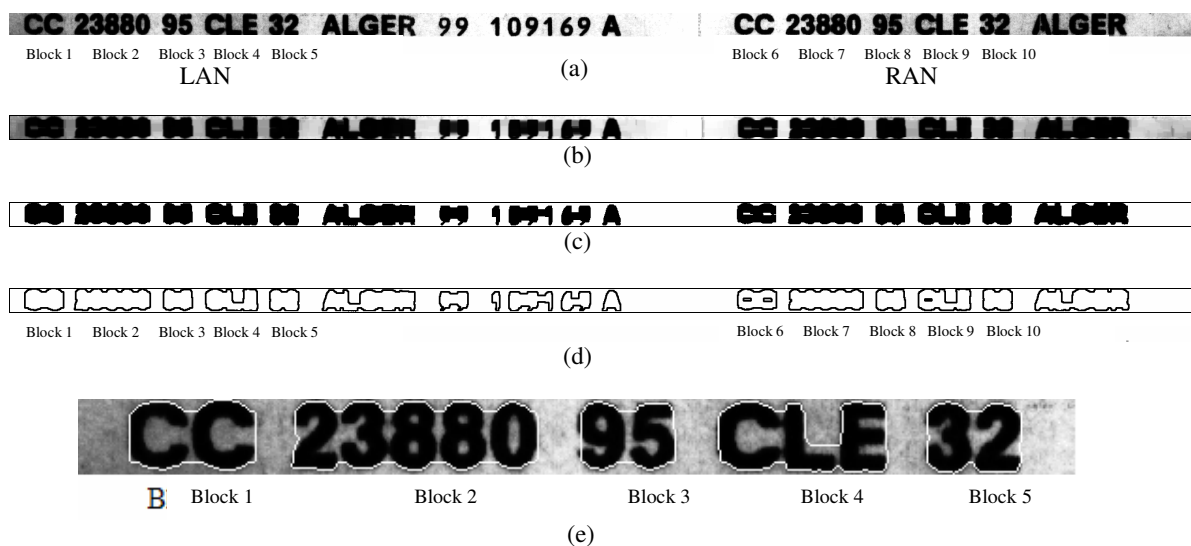


Fig. 3.45 ANS procedure (a) Account number zone showing ten regions of interest. (b) Morphological closing operation of image in (a). (c) Binarisation operation of the closed image in (b). (d) Contour detection. (e) The LAN of (a) zoomed for illustration, showing the detected blocks delimited by five contours of (d).

c) Experimental results

The experiments are conducted in two parts, the first part presents a comparative study of the proposed method with the individual classifiers for isolated printed character check recognition. To show the high performance of the proposed approach (Hopfield-MLP), it is also compared to five other classifiers, namely, the first nearest neighbor (1-NN), the MLP-autoassociator serial combination (MLP-Assoc.) [58], the sequential combination method (SC) [56], the complementary similarity measure method (CSM) [79] and the highly degraded printed character method (HDM) [81]. Since the HDM method is applied in this work to only isolated printed characters, it is implemented without using the blind deconvolution and MRF-based segmentation techniques, usually used for segmentation problem. The second part is devoted firstly to automatic account number reading of post checks, and secondly to test the robustness of the method in the presence of added Gaussian noise (AGN) and on the degraded real printed characters.

i) Prototype extraction and training phase

The character data set represents a single font character that was collected from 700 post checks belonging to the same post. The post checks were scanned at 300 dpi resolution, which avoids the scaling procedure. Hence a frame of 40-by-40 pixels is sufficient to include each of the 13 pattern classes. The sample characters representing the data set were manually cut and labeled to their corresponding classes. The classes considered consist of ten numeral characters and three alphabetic characters, “C,L,E” of 40-by-40 pixels size. The characters used for learning the MLP were extracted from 100 post checks, and gave rise to 2445 characters. The remaining 600 post checks were used for testing, and consist of 15052 characters. The Hopfield model was trained only with thirteen clean characters and tested with 15052 characters. Figure 3.46 shows the thirteen clean centered characters of 40-by-40 pixels size used as fundamental memories for the Hopfield network.

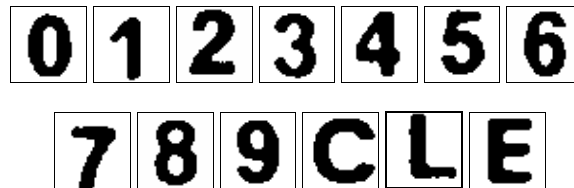


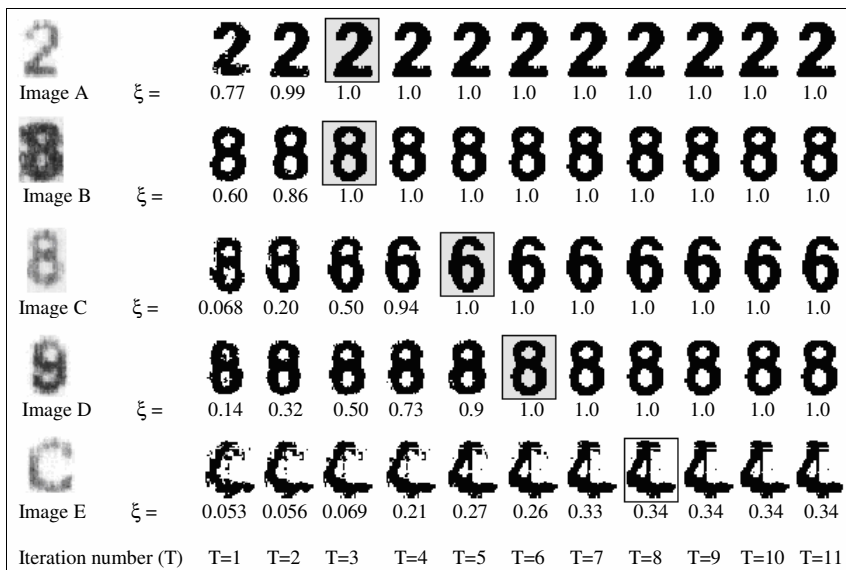
Fig. 3.46 Clean account number character set of 40x40 pixels.

The MLP used in the proposed work is a two layer of fully connected feedforward neural network module with $\alpha=0.9$ (training speed), and $\nu =0.001$ (viscosity coefficient). The number of neurons in the input layer was fixed to 100. Therefore the character image of size 40-by-40 pixels should be down sampled to 10x10 segments. Therefore, the MLP network would have 100 input nodes (one for each segment). The number of neurons in the hidden layer was experimentally fixed to 40 neurons and the number of outputs P was fixed to 13 output nodes, where each output node represents one class, and the total error E_T to 0.0001. The connection weights v_{ij} and w_{ij} corresponding to the two layers fully connected MLP are obtained after convergence and stored for recognition process. The Hopfield parameters were set to: $M=13$ and $N=1600$ (40-by-40 pixels). The associative matrix $W^{(o)}$ is directly calculated and also stored for recognition process.

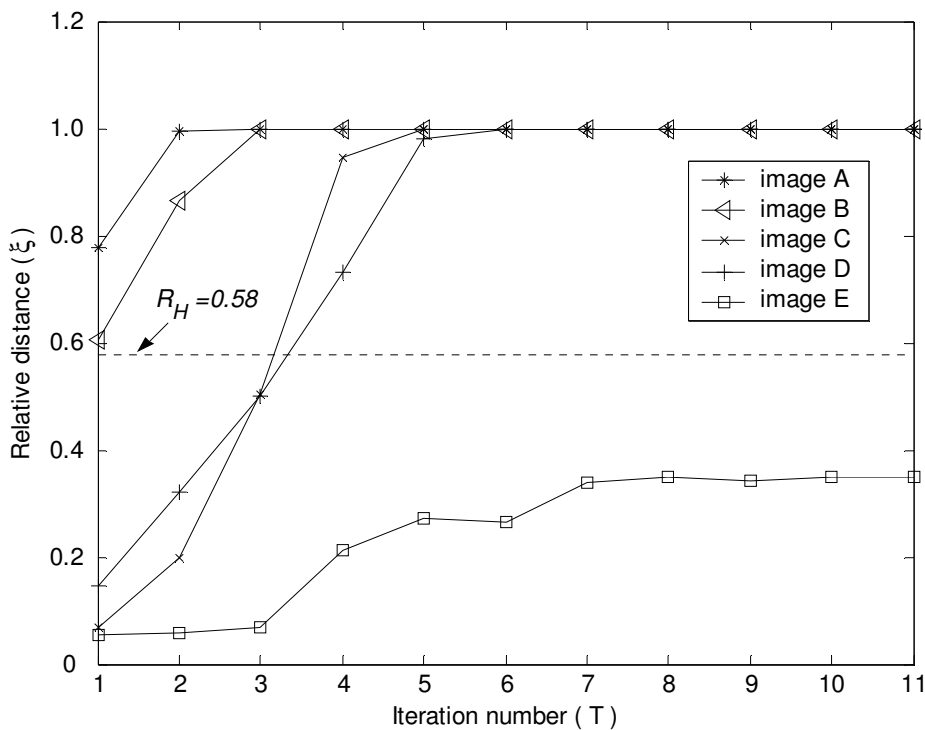
ii) Character recognition phase

Figure 3.47 shows the effect of the Hopfield iteration number T on the relative distance ξ and its relationship with the quality of the printed character. According to this figure, one can notice that for $T=1$, the correctly recognized characters (image A and B) start with higher ξ , whereas the misclassified (image C and D) starts with lower ξ . On the other hand for $T>1$ (higher T) insuring stable cases (convergence) the correctly and the misclassified characters have their $\xi=1$. The corresponding images are represented with shaded rectangles as shown in Fig. 3.47 (a). Hence to reduce errors, in order to reject all the misclassified characters (images of C and D), we try to keep $T=1$. In this case, the rejection threshold R_H should be chosen so as to be greater than ξ of images C and D (for example $\xi < R_H = 0.58$) as shown in Fig. 3.47 (b). The spurious case or unstable state is considered as a rejected case (image E). It starts always with very low ξ and stabilizes at $\xi < 1$ for higher T (see Fig. 3.47 (b)). The first iteration and the relative distance can be used to determine the tendency to correct or misclassified recognition of the Hopfield recovered pattern. The relative distance can be used also as a quality measurement of the printed character for $T=1$ as shown in Fig. 3.48. Medium and high quality printed characters have their $\xi_{\alpha\beta} \rightarrow 1$ ($\delta_\alpha \rightarrow 0$) for $T=1$, whereas low quality characters have their $\xi_{\alpha\beta} \rightarrow 0$ ($\delta_\beta \rightarrow \delta_\alpha$).

Figure 3.49 shows the error-reject plots of the Hopfield-based classifier for different T and R_H ($0.18 \leq R_H \leq 0.98$). As can be noticed, the error falls for lower T and higher R_H , and the best performance in terms of low errors is achieved for $T=1$. Figure 3.50 summarizes the results obtained on the dataset by the classification methods described in chapter 2 and the proposed method. The plot for the Hopfield model is obtained for different values of the rejection threshold R_H and $T=1$ that insures low errors compared to higher T ($T>1$). The other plots are obtained for the MLP-based classifier with R_M ranging from 0.2 to 0.9 and for the combined approach with R_H ranging from 0.18 to 0.98. The curve describing the combination of Hopfield model and MLP is obtained by choosing $R_M=0.5$ and the number of iterations $T=1$. The threshold R_M is chosen according to the high performance achieved by the combined approach for $R_M = \{0.5, 0.6, 0.7, 0.8, 0.9\}$ as shown in Fig. 3.51.



(a)



(b)

Fig. 3.47 Effect of the iteration number on the pattern recovering (a) Image recovering of degraded patterns at different T and their corresponding ξ (below each image). (b) Relative distance variation (ξ) for the images shown in (a) at different T.

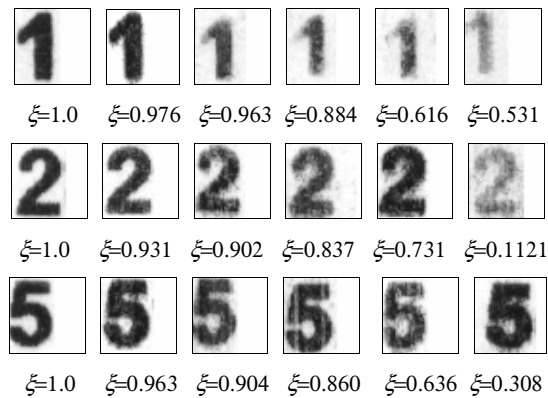


Fig. 3.48 Relative distance (ξ) for quality measurement of the printed character for $T=1$.

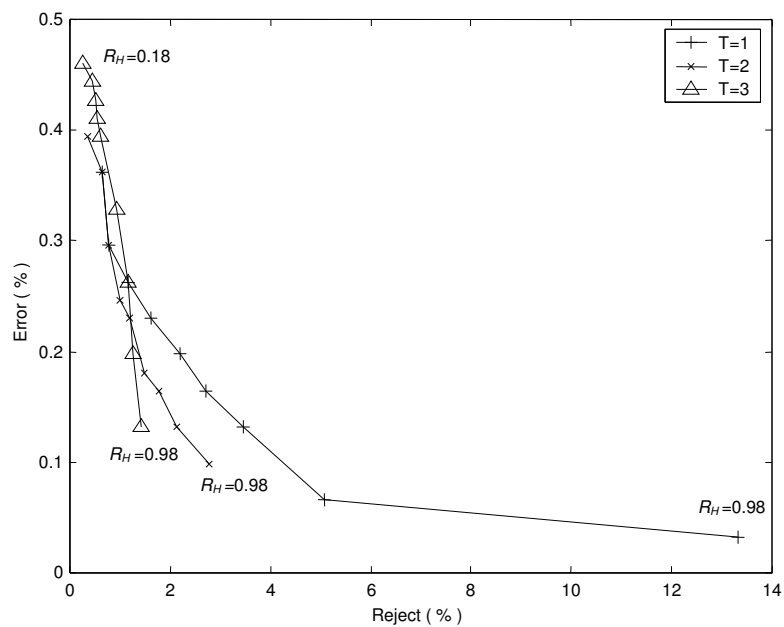


Fig. 3.49 Error vs reject plot for the Hopfield-based classifier showing the effect of using different iteration numbers; $T = \{ 1, 2, 3 \}$.

As can be seen in Fig. 3.50, the MLP-based classifier outperforms clearly the Hopfield model based classifier for very high reject, whereas the two neural networks show almost similar performance for very low reject. The error-reject plot of Fig. 3.50 shows that the proposed modular approach outperforms both the Hopfield model and the MLP-based classifiers. The plot corresponding to the combined approach reaches the plot of the Hopfield and MLP-based classifiers for very low rejection rates. On the other hand, for high rejection rates, the combined approach outperforms both the individual classifiers.

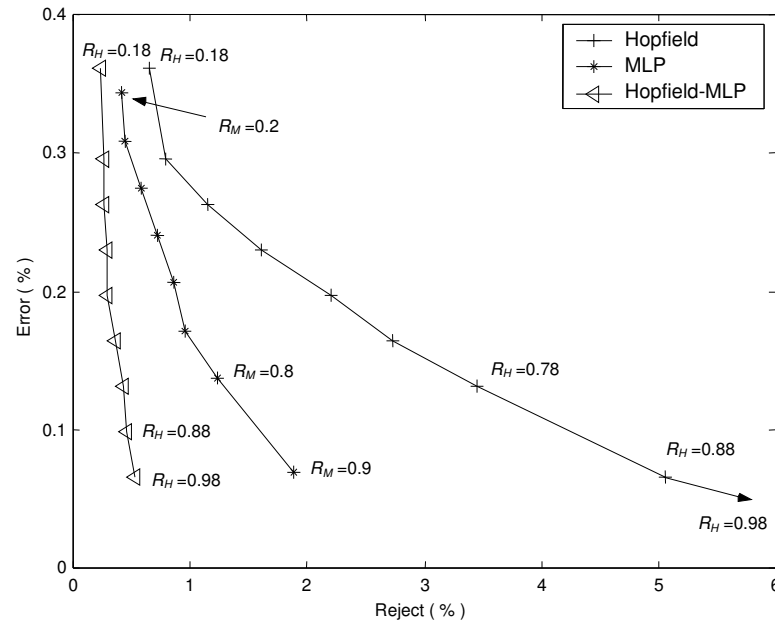


Fig. 3.50 Error vs reject plot for three classifiers using various thresholds values for R_H and R_M .

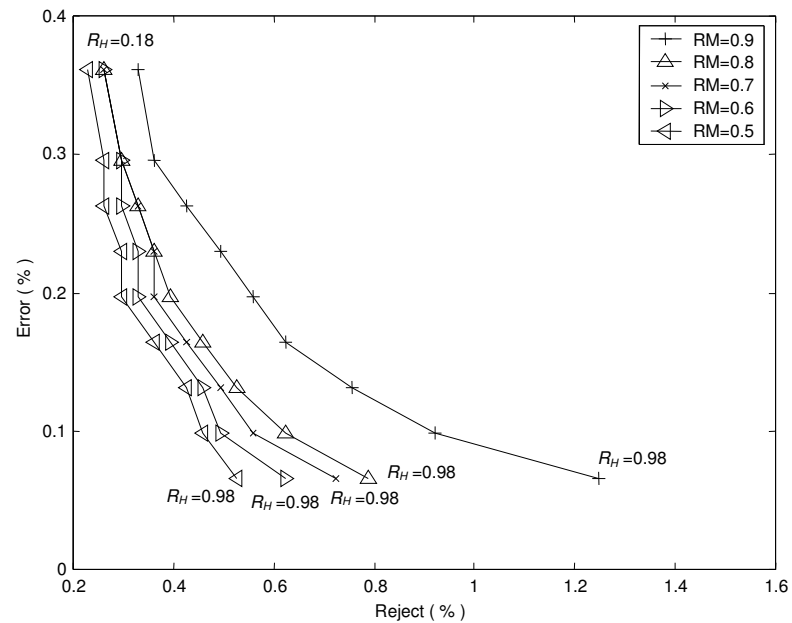


Fig. 3.51 Error vs reject plot for the combined method showing the effect of R_M using various thresholds values; $R_M = \{0.5, 0.6, 0.7, 0.8, 0.9\}$.

The recognition-error plot of Fig. 3.52 shows clearly the high performance achieved by the combined approach compared to the single classifiers. The combined approach outperforms clearly both the single classifiers for very low and medium errors rate, and still shows lightly

better performance for very high error rate. This can be explained by the fact that the combined method rejects less the incoming patterns than the single classifiers for the same error rates, which results in higher recognition rates. This high performance is due to the serial combination using the best choice of the proper thresholds, R_H , R_M and iteration number T .

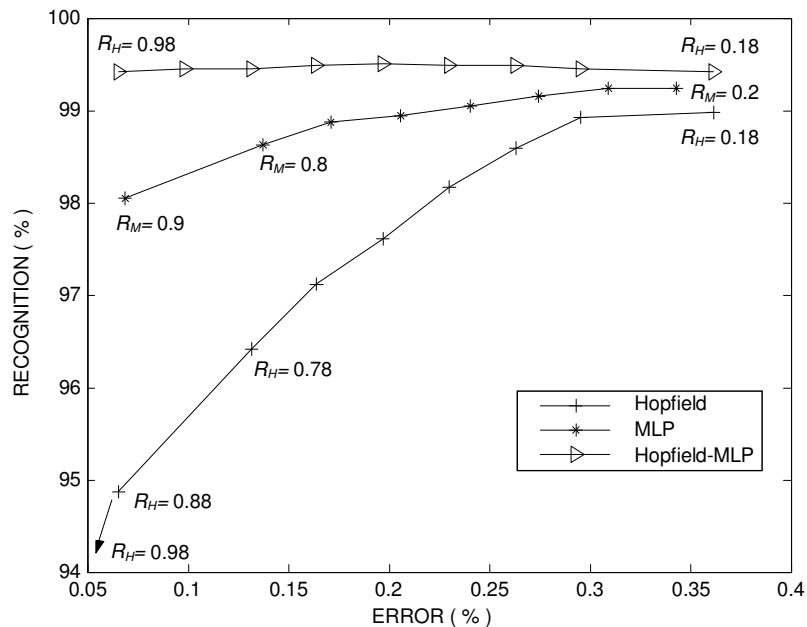


Fig. 3.52 Recognition vs error plot for three classifiers using various thresholds values for R_H and R_M .

Table 3.8 Best performance comparison of the three classifiers; the Hopfield network is trained with 13 printed characters and the MLP network with 2445 printed characters. The three classifiers were tested using the 15052 printed characters test set. For the proposed work we chose $R_H=0.58$, $R_M=0.5$ and $T=1$.

Classifier	Errors (%)	Reject (%)	Reliability (%)	Recognized (%)
Hopfield	54 (0.36)	96 (0.64)	99.64	14902 (99.00)
MLP	45 (0.30)	67 (0.45)	99.70	14940 (99.25)
Hopfield-MLP	28 (0.19)	43 (0.29)	99.81	14981 (99.52)

Table 3.8 summarizes the best performance achieved by the three classifiers, namely, the MLP, Hopfield and the proposed classifier. Figure 3.53 shows the real degraded gray level printed characters that were correctly recognized, rejected and misclassified by the proposed method.

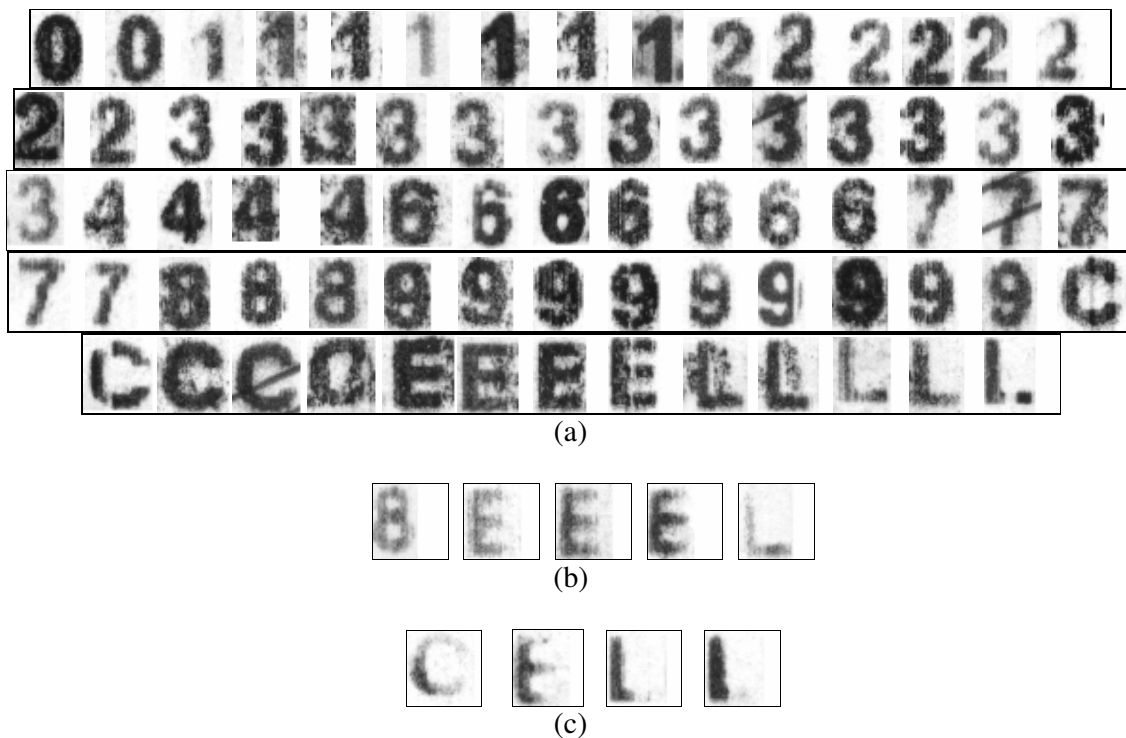


Fig. 3.53 Gray level real printed characters recognition results (a) Recognized characters (b) Rejected characters (c) Misclassified characters.

Figure 3.54 summarizes the results obtained on the dataset using six classifiers for degraded character recognition. The parameters corresponding to these classifiers were chosen so as to give the highest recognition rate. For the proposed method we chose $R_M=0.5$, $0.18 \leq R_H \leq 0.98$ and $T=1$. The sequential combination parameters were set to $R_H=0.12$, $0.3 \leq R_M \leq 0.9$ and $T=1$. The parameters of the MLP-Assoc. method were set to $R_A=0.4$ (auto-associator rejection threshold), and $0.2 \leq R_M \leq 0.9$. As can be seen in Fig. 3.54, the proposed method outperforms clearly the other classifiers. The plots corresponding to the MLP-Assoc., the SC, the CSM and the HDM reach the plot of the proposed method for very low rejection rates. On the other hand, for high rejection rates, the combined approach outperforms all these classifiers and the 1-NN classifier. The recognition-error plot of Fig. 3.55 shows clearly the high performance achieved by the Hopfield-MLP compared to these classifiers. The combined approach outperforms clearly the other classifiers for very low and medium error rates, and still has lightly better performance for very high error rates. This can be explained by the fact that the combined method rejects less the incoming patterns than the mentioned classifiers for the

same error rates, which results in higher recognition rates. Table 3.9 summarizes recognition results achieved by the six classifiers, namely, the 1-NN, CSM, MLP-Assoc., SC, DHM and Hopfield-MLP. According to these results, it is clear that the proposed approach outperforms all the five other classifiers in terms of reliability and recognition rate.

The extremely small difference between the proposed method and the worst network (1-NN) in term of reliability and recognition rates is due to the mixture of quality of the post check characters. These characters are of high, medium and low quality. Figure 3.48 shows samples of these characters with their corresponding relative distances. As a consequent result, if these characters are all of poor quality (lower relative distance, $\xi \rightarrow 0$) there will be a big difference in reliability and sensitivity which creates more variance between our proposed method and the five other methods. On the other hand these methods, including the proposed method, give practically the same performances for high quality check characters ($\xi \rightarrow 1$) and lightly the same performance for characters of medium quality. So this extremely small difference is the result of applying these methods on the existing degraded characters in the dataset. Thus, this difference is inversely proportional to the quality of the dataset. This extremely small difference becomes progressively important when the number of the dataset characters increases. A difference in sensitivity of 0.34% (99.52 (proposed method) -99.18 (worst network)) when applied for example to 600 post checks, which corresponds to about 18000 characters (30 characters/check), results in 61.2 (18000x0.34%) more recognized characters than by the worst classifier. This value could correspond to a gain difference of $61.2/600=10.2\%$ in check recognition if we assume the worst case, i.e. one misclassified character per post check. On the other hand if we assume all these 61.2 not recognized characters (related to the worst classifier) belong entirely to 2.04 (61.2/30) post checks, we get a gain difference of $2.04/600=0.34\%$ in check recognition rate. Hence this difference in character recognition rate could be mapped to a considerable check recognition rate interval as follows:

0.34 % (gain in character recognition rate) \rightarrow [0.34, 10.2] % (gain in check recognition rate)

The values of 0.34 and 10.2% represent the best and the worst gain in check recognition rates respectively. In practice the value of 0.34% is far from being reachable, because the system can not make errors in all the characters of the same check (30 errors per check). The difference of 0.34% related to the character recognition when applied to 600 post checks give 1.50% (98.33-96.83%) of gain in check recognition as shown in Table 3.10.

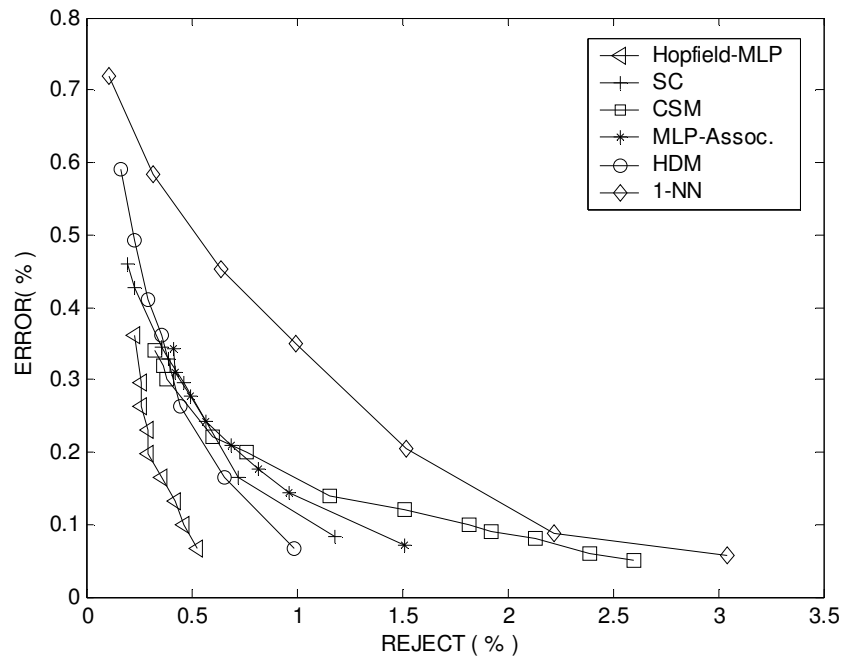


Fig. 3.54 Error vs reject showing comparison results of six classifiers.

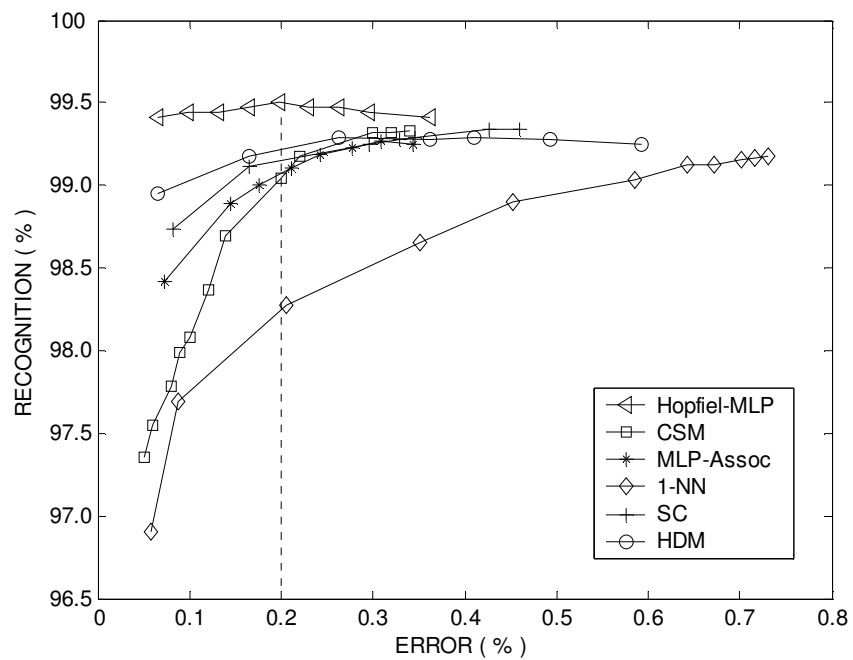


Fig. 3.55 Recognition vs error showing comparison results of six classifiers.

Table 3.9 Best performance comparisons of the six classifiers; the Hopfield network that constitutes the proposed work was trained with 13 characters, whereas the MLP and the five other classifiers were trained with 2445 printed characters. The six classifiers were tested using the 15052 printed characters test set. For the proposed work we chose $R_H=0.58$, $R_M=0.5$ and $T=1$. The parameters of the SC were set to $R_H=0.12$, $R_M=0.8$ and $T=1$, and those of the MLP-Assoc. to $R_M=0.8$ and $R_A=0.4$.

Classifier	Errors (%)	Reject (%)	Reliability (%)	Recognized (%)
Hopfield-MLP	28 (0.19)	43 (0.29)	99.81	14981 (99.52)
SC	69 (0.46)	30 (0.20)	99.54	14953 (99.34)
CSM	51 (0.34)	49 (0.33)	99.66	14952 (99.33)
HDM	39 (0.26)	66 (0.44)	99.74	14947 (99.30)
MLP-Assoc.	46 (0.31)	63 (0.42)	99.69	14943 (99.27)
1-NN	108 (0.72)	15 (0.10)	99.28	14929 (99.18)

Table 3.10 Application results of the proposed method ($R_H=0.58$, $R_M=0.5$ and $T=1$) and the 1-NN-based classifier on 600 post checks.

Classifier	Errors (%)	Rejected (%)	Recognized (%)
Hopfield-MLP	0 (0.0)	10 (1.67)	590 (98.33)
1-NN	0 (0.0)	19 (3.17)	581 (96.83)

iii) Automatic account number reading

Figure 3.56 shows the bank check processing for account number recognition based on the right and left parts of the check. After applying ANDL and account number segmentation (ANS) procedures, the check is partitioned in two parts; right and left account numbers (RAN and LAN), using right and left account number localization (RANL and LANL) modules respectively. These parts are processed separately by right account number recognition (RANR) and left account number recognition (LANR) which consist of the segmentation of

the account number in characters and the recognition with the proposed method. Finally, the RANR and LANR results are compared to accept or reject the check which will then be processed manually. The experiment was based on the procedure illustrated in Fig. 3.56 and applied to 600 post checks. Table 3.10 summarizes the results obtained with the proposed method. It results in the correct recognition of 590 post checks, the rejection of 10 post checks and hence no errors occurred which corresponds to a 98.33 % of recognition rate. Figure 3.57 illustrates the cases of correctly recognized and rejected post checks. The account numbers in Fig. 3.57 (a) and (b) were correctly recognized according to the identical results of the RANR and LANR “CC 27344 73 CLE 06” and “CC 49510 14 CLE 89” respectively. On the other hand the account number of Fig. 3.57 (c) was rejected due to the different RANR and LANR results. The LANR results in “CC 44354 24 CLE 85” but the RANR results in “CC 443?4 24 CLE 85”, where “?” denotes the rejected printed character by the combined approach. Thus the automatic post check reader rejects consequently the post check.

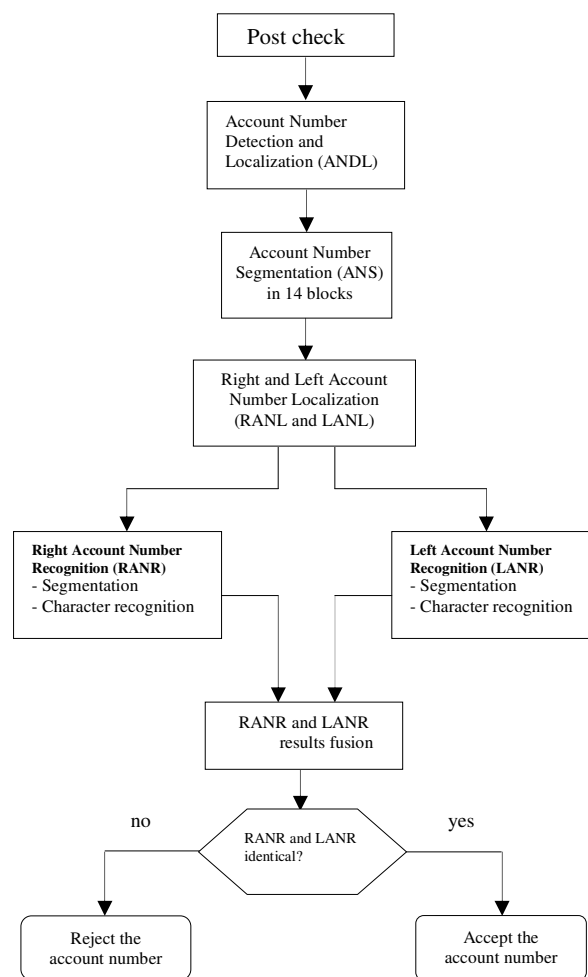
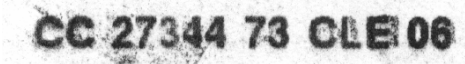
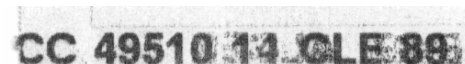



Fig. 3.56 Post checks processing for account number recognition.

LAN 
"CC 27344 73 CLE 06"

RAN 
"CC 27344 73 CLE 06"

(a)

LAN 
"CC 49510 14 CLE 89"

RAN 
"CC 49510 14 CLE 89"

(b)

LAN 
"CC 44354 24 CLE 85"

RAN 
"CC 443?4 24 CLE 85"

(c)

Fig. 3.57 Recognition results illustration (a-b) Recognized account number images and their corresponding output results (below each image). (c) Rejected account number images and their corresponding output results (below each image).

iiii) Degraded real printed characters

To test the robustness of the proposed method on effective poor quality characters, it was first applied to the training set shown in Fig. 3.46 corrupted with added Gaussian noise (AGN), and then to real broken and incomplete characters. The training set was corrupted with an added Gaussian noise, and a recognition rate of 100% was achieved for a signal to noise ratio (SNR) up to -2.10 dB ($\sigma=1.31$) as shown in Fig. 3.58. It can be concluded from these tests, that for a SNR up to 2.37 dB ($\sigma=0.761$), the 13 noisy classes (0, 1, 2, 3, 4, 5, 6, 7,

8, 9, C, L and E) are successfully recognized. Figure 3.59 shows successfully recognized noisy characters for $\sigma=0.6$. These noisy characters are correctly recognized with the Hopfield model for $R_H=0.58$ and $T=1$. On the other hand they are all rejected with the MLP-based classifier for $R_M=0.5$. Figure 3.60 shows, recognized, rejected and misclassified cases for $\sigma=0.8$, $R_H=0.58$, $R_M=0.5$ and $T=1$, using the proposed method.

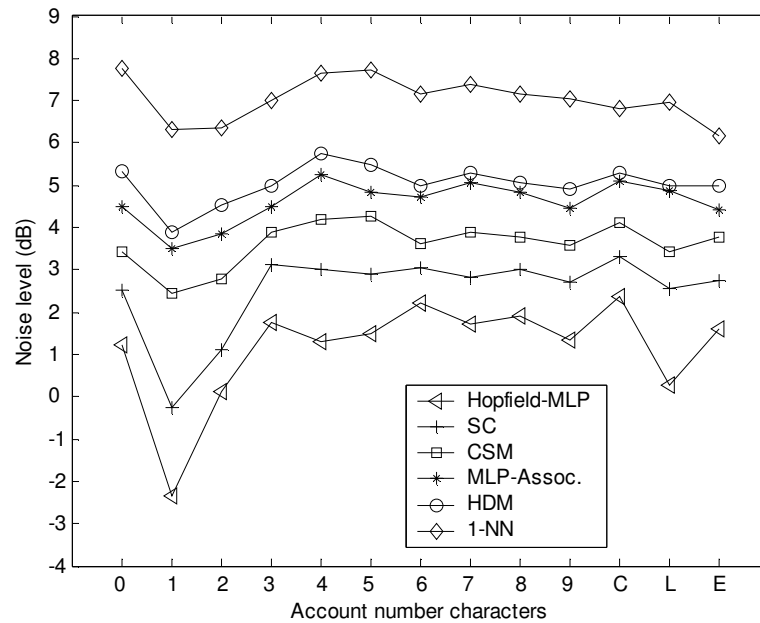


Fig. 3.58 Reached SNR for 100% recognition rate.

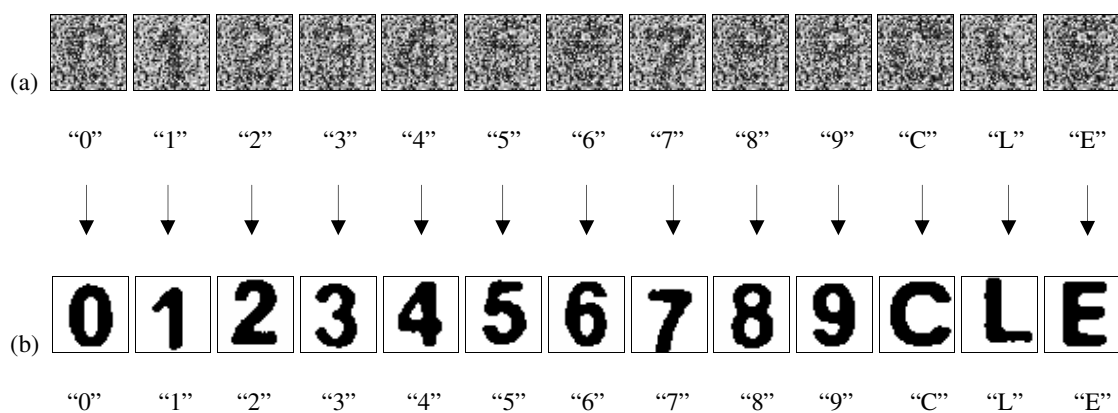


Fig. 3.59 Recognition results for characters corrupted with Added Gaussian Noise (AGN). (a) Noisy grey level images with $\sigma=0.6$ and their corresponding class between “ ”. (b) Successfully recovered and recognized pattern of (a) and their corresponding output results (below each image).

The robustness of the proposed method was also compared to the five previously mentioned methods in presence of added Gaussian noise (AGN) applied to the training set. The AGN is applied progressively to characters in order that the six classifiers would achieve 100% recognition rates (see Fig. 3.58).

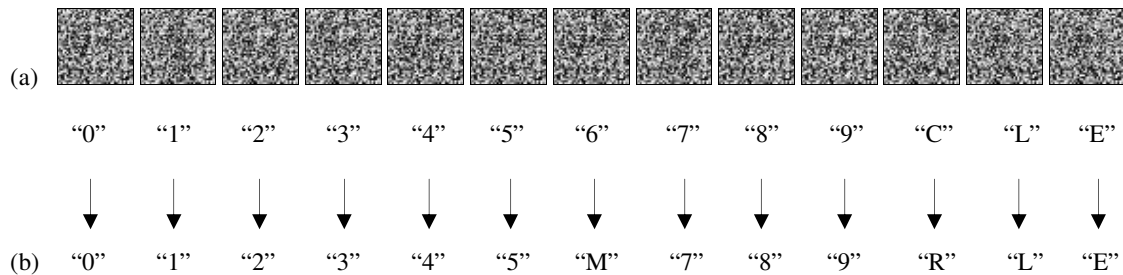


Fig. 3.60 Rejection and misclassification of characters corrupted with Added Gaussian Noise (AGN). (a) Noisy grey level images with $\sigma=0.8$ and their corresponding class between " ". (b) Proposed method output results; misclassified ("M") and rejected ("R") patterns of (a).

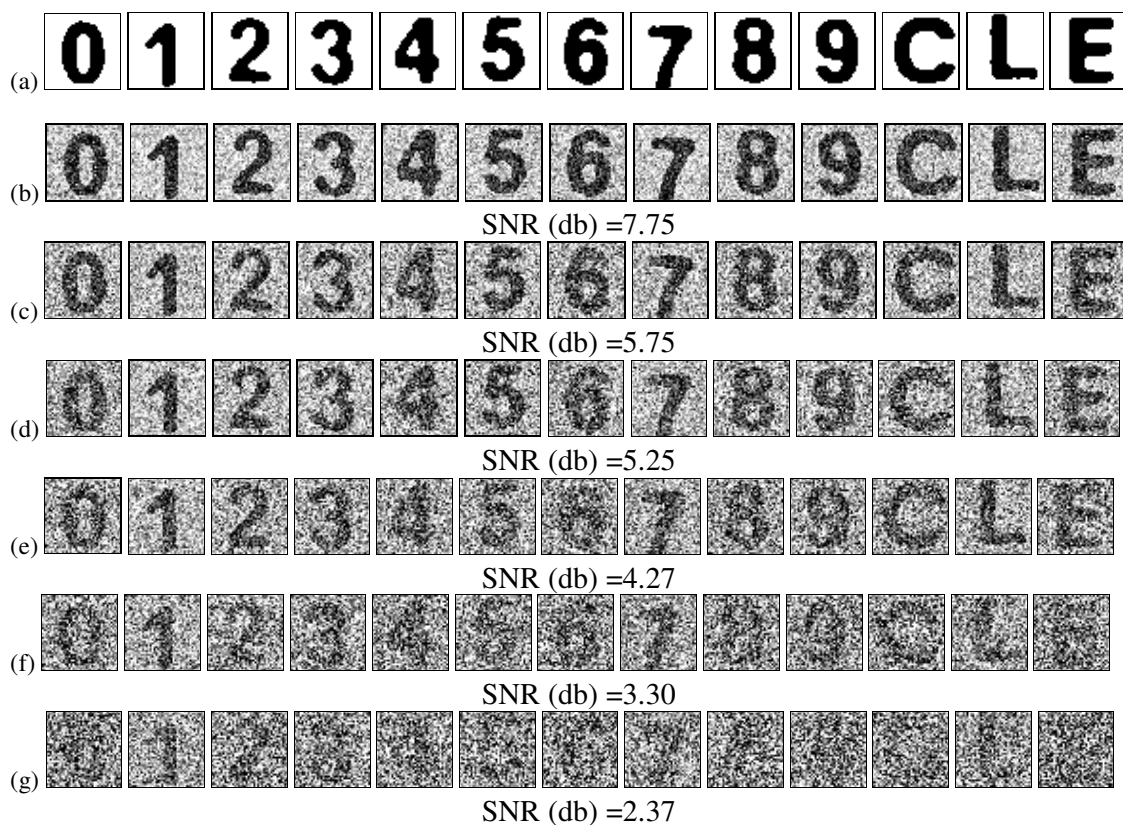


Fig. 3.61 Successfully recognized patterns and their corresponding SNR (below each set) at different noise level (a) Training set (b) 1-NN (c) HDM (d) MLP-Assoc. (e) CSM (f) SC (g) Hopfield-MLP.

The corrupted training characters correctly recognized by the six classifiers and their corresponding reached SNRs are presented in Fig. 3.61. The difference in performance among the methods is quite clear, since the character degradation increases and could be noticed visually when going from one classifier to another. Hence the performance of the proposed method over the five other classifiers is quite clear especially when the characters are noisy and degraded. Experiments were also conducted on real broken and incomplete character images. Figure 3.62 shows many of these characters, and in spite of the important degradation of the characters, the proposed method was able to recognize even highly degraded printed characters.

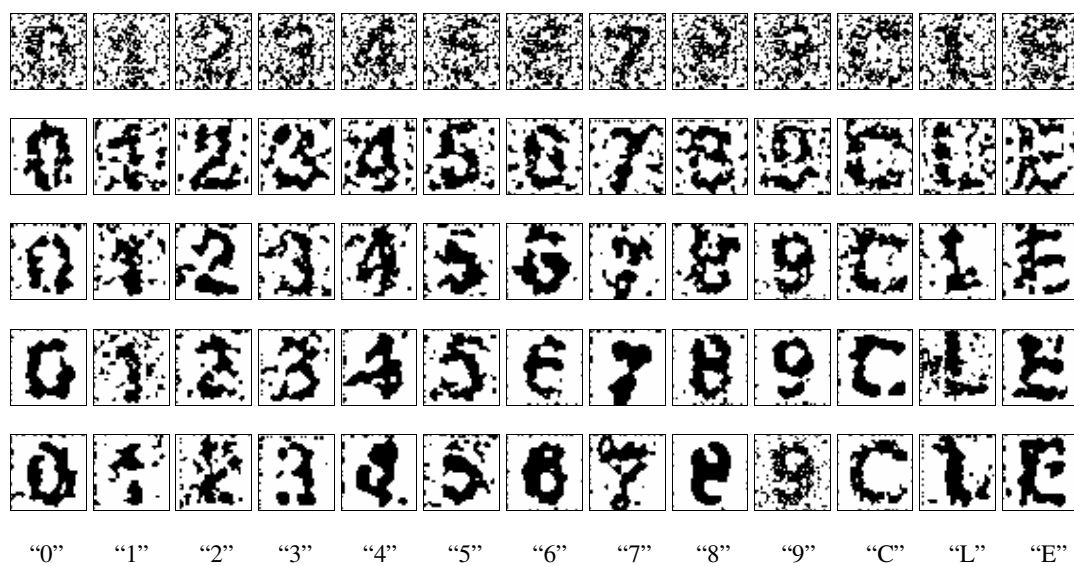


Fig. 3.62 Broken and incomplete real post check characters correctly recognized and their corresponding output results (below each column images of the same class).

In this section we have presented a serial neural architecture combining two noise insensitive networks, namely, the Hopfield model and the MLP-based classifier. Experiments were conducted first on isolated printed characters collected from post checks and a comparative study of our method was achieved with individual classifiers on one hand, and with five other classifiers found in the literature on the other hand. Second, a bank check processing procedure was proposed for ACN detection, localization and character retrieval. The proposed recognition method was applied successfully to the recognition of ACNs which are doubly printed in two serial numbers on each side of poor quality bank checks. The last experiment was conducted on noisy images for various AGN and real degraded characters.

3.6 Conclusion

In this chapter experimental results related to the document processing have been presented. We have first started by showing results of preprocessing applied to the handwritten numerals and words and secondly results of recognition of the handwritten numerals, the handwritten and the degraded machine printed characters. In the preprocessing phase, best results were obtained for the horizontal handwritten correction when compared to two other methods found in the literature. We also obtained promising results for skew correction and central localisation of the handwritten word. In the recognition phase, the results related to the proposed methods present real contributions to the area of document image analysis. We have shown how the performance of a given system can be improved by using: competitive learning, the parallel, the sequential and the serial combinations. We have also introduced a new method for holistic handwritten word recognition. The recognition rates obtained confirm that the proposed approach shows promising performance results and can be successfully used in the processing of poor quality bank checks.

CONCLUSION

In this thesis we have developed methods of preprocessing and character recognition. The first one is related to the preprocessing phase, in particular, handwritten numeral slant correction and skew correction, and central zone localization (SC-CZL) methods. The second one is related to the character recognition, in particular those of the degraded printed characters, the handwritten numerals and the handwritten words. First, recognition methods of the handwritten numeral characters are presented with the use of two following combinations: the Fourier-Mellin transform (FMT), the self organization map (SOM) and the multi layered perceptron (MLP), then the hidden Markov models (HMM) with a new set of feature extractors. Secondly, the application of the global approach by mean of a new method developed within the frame of this work was presented. It is mainly based on the use of the Hopfield model and the MLP. In third place and finally, the recognition of degraded printed characters using two classifier combinations, namely, the sequential and serial combinations were presented. The results related the preprocessing and recognition methods are summarized in the following paragraphs.

A new simple and efficient character slant correction based on lower and higher character centroids was presented. This method yields very good results in term of slant correction and speed when compared to two other methods found in the literature. Another new efficient method for skew correction and lower case detection was proposed. The method performs the SC-ZCL simultaneously and accurately for even extremely degraded handwritten words. The experiments show promising results when conducted on medium and poor quality legal amounts.

A recognition system based on the Fourier-Mellin transform was conceived and designed for feature extraction. An unsupervised neural network (SOM) was introduced to cluster in prototypes or models each handwritten numeral class. A MLP-based classifier was trained with these clusters in order to improve the performance of the recognition system. The final developed recognition system achieved high recognition rate of 97.6% than the FMT-SOM based classifier which achieved only 96.6%.

Another recognition system for offline unconstrained numeral character recognition based on a multiple hidden Markov model (HMM) was presented. New set of feature

extractors was introduced. It is based on contour background transition which yields four representations. Experiments were conducted through three decisions strategies; i) Classification with individual classifiers ii) Classification with ECW combination iii) Classification with UCW combination. We achieved the best performance with the UCW for 98.08% of recognition rate, 93.78% and 76.34 for the ECW and the HMM-4 respectively.

A new holistic handwritten word recognition method based primarily on prototype or model recognition was presented. Experiments were conducted on our proper database for prototype and extended to handwritten word recognition. The obtained results show significant robustness of the method for handwritten word of medium and low qualities.

A sequential neural network architecture combining two noise insensitive neural networks, namely, the Hopfield model and the MLP network was presented for degraded character recognition. We show that the combined classifier when applied to medium and low quality printed characters outperforms both the individual classifiers. Successful results concerning the recognition of extremely degraded printed character recognition were obtained. We achieved a 99.35% of recognition rate with the combined approach, 99.18% and 99.10 with the Hopfield and the MLP based classifiers respectively.

Finally a serial neural architecture was presented for degraded printed character recognition. This method combines the Hopfield model and the MLP-based classifier. A new relative distance was introduced and used as a quality measurement of the degraded character. This relative distance gives strong reject capability to the Hopfield model used as a first classifier. The proposed recognition method was applied successfully to the recognition of ACNs which are doubly printed in two serial numbers on each side of poor quality bank checks and a recognition rate of 98.33% was obtained. The recognition rates achieved for isolated characters are; 99.00, 99.25 and 99.52% for Hopfield, MLP and combined method respectively. The high performance of the combined method has been shown through a comparison results with five methods found in the literature.

Through what have been mentioned previously in the present conclusion, we can say that we have contributed by the development of the described methods to solve problems related particularly to the handwritten and the degraded printed characters which are commonly the most challenging problems for the scientific community and pattern recognition area.

We proposed for future work the introduction of wavelet filters to enhance the image quality, and the use of hybrid architecture, combining serial and parallel classifiers.

REFERENCES

1. W. H. Abdulla, A. O. M. Saleh and A. H. Morad, "A preprocessing algorithm for handwritten character recognition," *Pattern Recognition lett.* 7, 13-18 (1988).
2. N. Papamarkos and B. Gatos, "A new approach for multilevel threshold selection," *Comput. Vision Graphics Image Process., Graphical Models and Image Process.*, 56(5), 357-370, September (1994).
3. E M. Wahl, K. Y. Wong and R. G. Casey, "Block segmentation and text extraction in mixed text image documents," *Comput. Graphics Image Process.*, 20, 375-390 (1982).
4. P. Chauvet, I. Lopez-Krahe, E. Tatlin and H. Maitre, "A system for an intelligent office document analysis recognition and description," *Signal Process.*, 32, 161-190 (1993).
5. F. W. M. Stentiford, "Automatic features design for optical character recognition using an evolutionary search," *IEEE Trans. Pattern Analysis Mach. Intell.*, 7, 349-355 (1985).
6. G. L. Cash and M. Hatamian, "Optical character recognition by the method of moments," *Comput. Vision Graphics Image Process.*, 39, 291-310 (1987).
7. B. Gatos and N. Papamarkos, "A Novel method for character recognition," *Proc. Forth Int. Conference on Advances in Communication and Control, COMCON 93*, 493-503, Rhodos, Greece (1993).
8. B. Jahne, "Digital Image Processing," 2nd edn. Springer, Berlin (1993).
9. G. Wilfong et al, "On-Line Recognition of Handwritten Symbols", dans les comptes rendus de l'IEEE sur *Pattern Analysis and Machine Intelligence*, 18(9), (1996).
10. J. Hu, M.K. Brown and W. Turin, "HMM Based On-Line Handwriting Recognition," *IEEE Trans. Pattern Analysis and Machine Intelligence*, 18(10), 1,039-1,045 Oct. (1996).
11. Jinhai Cai and Zhi-Qiang Liu "Off-line unconstrained handwritten word recognition," *International Journal of Pattern Recognition and Artificial Intelligence*, 14(3), 259-280, (2000).
12. S.W. Lee, "Off-Line Recognition of Totally Unconstrained Handwritten numerals using Multilayer Cluster Neural Network," *IEEE Trans. Pattern Analysis and Machine Intelligence*, 18(6), 648-652, June (1996).
13. H.Bunke, M.Roth and E.C.Schukat Talamazzini, "off-line cursive handwriting recognition using hidden Markov models," *Proceeding of the IEEE*, 28(9), 1399-1413, (1995).

14. Sargur N. Srihari, "Recognition of handwritten and machine- printed text for postal address interpretation," *Pattern Recognition Letters*, 14, 291-302 (1993).
15. R. M. Bozinovic and S. N. Srihari, "Off-line cursive script word recognition," *IEEE Trans. Patt. Anal. Mach. Intell.*, 11, 68-83 (1989).
16. R. Buse, Z. Q. Liu and T. Caelli, "A structural and relational approach to handwritten word recognition," *IEEE Trans. Syst. Man, Cyber.*, Part B, 27, 847-861, (1997).
17. M. Mohamed and P. Gader, "Handwritten word recognition using segmentation-free hidden Markov modeling and segmentation-based dynamic programming techniques," *IEEE Trans. Patt. Anal. Mach. Intell.* 18, 548-554, (1996).
18. S. Madhavanath and V. Govindaraju, "Holistic Lexicon Reduction," *Proc. Third. Int. Workshop Frontiers in Handwriting Recognition*, Buffalo, N.Y., 71-81, May (1993).
19. S. Madhavanath and V. Govindaraju, "Contour-Based Image Processing for Holistic Handwritten Word Recognition," *Proc. Fourth. Int. Conf. Document Analysis and Recognition (ICDAR 97)*, Ulm, Germany, Aug. (1997).
20. G. Kim and V. Govindaraju, "Handwritten Phrase recognition as Applied to State Name Images," *Pattern Recognition*, 31(1), 41-51, (1998).
21. E. Lecolinet and O. Baret, "Cursive word recognition: methods and strategies," *Fundamentals in Handwriting Recognition*, ed. S. Impedovo, NATO ASI Series F, vol. 24, Springer-Verlag, 235-263 (1994).
22. N. Gorski, V. Anisimov, E. Augustin, O. Baret and S. Maximov, "Industrial bank check processing: the A2iA check reader," *International Journal on Document Analysis and Recognition*, 3, 196-209 (2001).
23. K.. M. Hussein, "A knowledge-based segmentation algorithm for enhanced recognition of handwritten courtesy amount," *Pattern Recognition* 32, 305-316 (1999).
24. Kinameri T., Kawada M., Pecharanin N., Mitsui H., Sone M., Akima Y., "The preprocessing for recognition of rotative and different scale character," *Proceedings of the IASTED International Conference. Modelling and Simulation - MS'94*, 394-397, (1994).
25. Nellis, J., Stonham T.J., "Novel preprocessing techniques as an aid to hand-printed character recognition," *IJCNN-91-Seattle; International Joint Conference on Neural Networks (Cat. No.91CH3049-4)*, 2, 943- , (1991).
26. Ming-Wen Chang, Bor-Shenn Jeng, Dung-Ming Shieh, Shih-Fu Shy, Chao-Hao Lee, Chi Jain Wen and Char-Shin Miou, "Feature-based noise reduction in preprocessing for optical Chinese handwritten character recognition," *Proceedings of the SPIE - The International Society for Optical Engineering*, 2298, 624-633, (1994).
27. Ying Liu, Srihari S.N, "Document image binarization based on texture features," *IEEE Transactions on Pattern Analysis and Machine Intelligence*, 19(5), 540-544, (1997).

28. Yibing Yang, Hong Yan, "An adaptive logical method for binarization of degraded document images," *Pattern Recognition*, 33(5), 787-807, (2000).
29. N. Otsu, "A threshold selection for gray-level histograms," *IEEE Trans. Syst. Man Cybern.*, 8, 62-66, (1978).
30. W. Niblack, "An introduction to digital image processing," Englewood Cliffs, N.J.: Prentice Hall, 115-116, (1986).
31. R. He, H. Yan and J. Hu, "Skeletonization algorithm based on cross segment analysis," *Optical Engineering Journal*, 38 (4) 662-671, (1999).
32. A. Namane and M.A. Sid_ahmed, "Digital character scaling by contour method," *IEEE Trans. Pattern Anal. Mach. Intell.*, 12 (6), 600-606, (1990).
33. Bansal, V. and Sinha, R.M.K., "Integrating knowledge sources in Devanagari text recognition system," *IEEE Transactions on Systems, Man & Cybernetics, Part A (Systems & Humans)*, 30(4), 500-505, (2000).
34. slanyan, L.A. and Saakyan, A.A. "System for recognizing printed Armenian texts," *Pattern Recognition and Image Analysis*, 9(1), 17-18, (1999).
35. A.J. Elms, "The Representation and Recognition of Text Using Hidden Markov Models," PhD thesis, Dept. of Electronic and Electrical Eng. Univ. of Surrey, (1996).
36. L. Heutte, T. Paquet, J.V. Moreau, Y. Lecourtier and V. Olivier, "A structural/statistical feature based vector for handwritten character recognition," *Pattern Recognition Letters*, 19, 629-641 (1998).
37. J. C. Simon, "Off line cursive word recognition," *Proc. IEEE* 80, 1150-1161 (1992).
38. T. Caesra et al., "Handwriting Recognition by Statistical Methods", dans « *Fundamentals of Handwriting Recognition* », par Sebastiano Impedovo (éditeur), publié par Springer-Verlag, (1994).
39. Hanel S., Jouvét D., "Detecting the end of spellings using statistics on recognized letter sequences for spelled names recognition," *IEEE International Conference on Acoustics, Speech, and Signal Processing. Proceedings (Cat. No.00CH37100)*, 3, 1755-1758 (2000).
40. Dong Hai-Wei, Jiang Zao and Wang Yong-Jun, "Statistic and structure integrated approach of symbol recognition for engineering drawings," *Journal of Computer Aided Design & Computer Graphics*, 12(5), 375-379 (2000).
41. Jinhai Ca and Zhi-Qiang Liu, "Integration of structural and statistical information for unconstrained handwritten numeral recognition," *IEEE Transactions on Pattern Analysis and Machine Intelligence*, 21(3) 263-270 (1999).
42. Chi-Fang Lin and Cheng-Yi Hsiao, "Structural recognition for table-form documents using relaxation techniques," *International Journal of Pattern Recognition and Artificial Intelligence*, 12(7), 985-1005 (1998).

43. Liu X., Paweska R. and Rowlands, H., "A study of neural network structures and training data formats for an optical character recognition system," *Workshop on European Scientific and Industrial Collaboration. WESIC '99. Promoting: Advanced Technologies in Manufacturing*, 267-274 (1999).
44. Leng Li-Qiu, Li Tao, Wang Xian-Wang and Wang Hai-Bin, "Chinese character recognition based on the theory of intelligent neural network system," *Mini-Micro Systems*, 21(10), 1032-1034, (2000).
45. Kimura, Y., Wakahara T. and Sano M., "The proposal of growing neural networks and its application to handwritten Kanji character recognition," *Journal of the Institute of Image Electronics Engineers of Japan*, 29(5), 600-609 (2000).
46. Pessoa L.F.C. and Maragos, P., "Neural networks with hybrid morphological/rank/linear nodes: a unifying framework with applications to handwritten character recognition," *Pattern Recognition*, 33(6), 945-960 (2000).
47. Hori, K., Sugawara H. and Itoh A. "A unified neural network for handwritten similar characters recognition by using peripheral local outline vector," *Transactions of the Information Processing Society of Japan*, 40(12), 4239-4247 (2000).
48. Xu Zhiming and Wang Xiaolong, "A new linguistic decoding method for online handwritten Chinese character recognition," *Journal of Computer Science and Technology (English Language Edition)*, 15(6), 597-603 (2000).
49. Geunbae Lee, Jong-Hyeok Lee and Jinhee Yoo, "Multi-level post-processing for Korean character recognition using morphological analysis and linguistic evaluation," *Pattern Recognition*, 30(8), 1347-1360 1997.
50. Sural S. and Das P.K., "Fuzzy Hough transform, linguistic sets and soft decision MLP for character recognition," *Proceedings of the 5th International Conference on Soft Computing and Information/Intelligent Systems. Methodologies for the Conception, Design and Application of Soft Computing*, 2, 975-978 (1998)
51. Kang Ryoung Park, Byung Hwan Jun, Chang Soo Kim, Woo Sung Kim and Jaihie Kim, "A study on character segmentation and determination of linguistic type for recognition of on-line cursive characters," *Journal of the Korea Institute of Telematics and Electronics*, 34(7), 61-69 (1997).
52. J. Cao, M. Ahmadi and M. Shridar, "Recognition of handwritten numerals with multiple feature and multistage classifier," *Pattern Recognition*, 28(2), 153-160 (1995).
53. J. K. Hee and W.L. Seong, "Combining classifiers based on minimization of a Bayes error rate," *Proceedings of the Fifth International Conference on Document Analysis and Recognition, ICDAR '99*, 398-401, (1999).
54. J. Grim, J. Kittler, P. Pudil and P. Somol, "Multiple classifier fusion in probabilistic analysis neural networks," *Pattern Analysis and Applications*, 5(2), 221-33, (2002).

55. A. Namane, M. Arezki, A. Guessoum, E.H. Soubari, P. Meyrueis, and M. Bruynooghe, "Off-line unconstrained handwritten numeral character recognition with multiple Hidden Markov models," *Proceeding of the 4th IASTED International Conference on Visualization, Imaging, and Image Processing*, VIIP '04, 269-276, (2004).
56. A. Namane, M. Arezki, A. Guessoum, E.H. Soubari, P. Meyrueis and M. Bruynooghe, "Sequential neural network combination for degraded machine-printed character recognition," *Document Recognition and Retrieval XII, Proc. SPIE 5676(12)*, 101-110, Jan. (2005).
57. L. Xu, A. Krzyzak and C. Suen, "Methods of combining multiple classifiers and their applications to handwriting recognition," *IEEE Trans. Systems, Man Cybern.*, 22(3), 418-435 (1992).
58. E. Francesconi, M. Gori, S. Marinai and G. Soda, "A serial combination of connectionist-based classifiers for OCR," *International Journal on Document Analysis and Recognition*, 3, 160-168, (2001).
59. Z. Chi, M. Sutters and H. Yan, "Handwritten digit recognition using combined ID3-derived fuzzy rules and Markov chains," *Pattern Recognition*, 29(11), 1821-1833 (1996).
60. M. Last, H. Bunke and A. Kandel, "A feature-based serial combination approach to classifier combination," *Pattern Analysis and Applications*, 5, 385-398 (2002).
61. Dong Hai-Wei, Jiang Zao and Wang Yong-Jun, "Statistic and structure integrated approach of symbol recognition for engineering drawings," *Journal of Computer Aided Design & Computer Graphics*, 12(5), 375-379 (2000).
62. P. D. Gader, "Automatic feature generation for handwritten digit recognition," *IEEE Trans. Patt. Anal. Mach. Intell.*, 18, 1256-1261 (1996).
63. T. Caesar, J.M. Gloger, A. Kaltenmeier and E. Mandler, "Handwritten word recognition using statistics," *IEE European Workshop on Handwriting Analysis and Recognition, A European Perspective (Digest No.1994/123)*, 5/1-7 (1994).
64. C. Y. Suen, C. Nadal, R. Legault, T. A. Mai and L. Lam, "Computer recognition of unconstrained handwritten numerals," *Proc. IEEE* 80, 1162-1180 (1992).
65. Jinhai Cai and Zhi-Qiang Liu, "Integration of structural and statistical information for unconstrained handwritten numeral recognition," *IEEE Trans. Patt. Anal. Mach. Intell.*, 21(3), 263-270 (1999).
66. F. Kimura and M. Shridhar, "Handwritten numeral recognition based on multiple algorithms," *Pattern Recognition*, 24(10), 976-983 (1991).
67. G. Dimauro, S. Impedovo, G. Pirlo and A. Salzo, "Automatic bank check processing, A new engineered system," *International Journal of Pattern Recognition and Artificial Intelligence*, 11(4), 467-504 (1997).

68. G. Nagy, "Twenty years of document image analysis in PAMI," *IEEE Trans. Pattern Anal. Mach. Intell.*, 32(1), 38-62 (2000).
69. M. Leroux, E. Lethèlier, M. Gilloux and B. Lemarié, "Automatic reading of handwritten amounts on French checks," *International Journal of Pattern Recognition and Artificial Intelligence*, 11 (4), 619-638 (1997).
70. G. Kim and V. Govindaraju, "Bank check recognition using cross validation between legal and courtesy amounts," *International Journal of Pattern Recognition and Artificial Intelligence*, 11(4), 657-674 (1997).
71. M. H. Thien and H. Bunke, "Modelbased analysis and understanding of check forma," *International Journal of Pattern Recognition and Artificial Intelligence*, 8(5), 1053-80 (1994).
72. F. Chin, F. Wu, "A Microprocessor-Based Optical Character Recognition Check Reader", *Proceedings of the third International Conference on Document Analysis and Recognition*, 2, 982-985 (1995).
73. C. L. Tan, W. Huang, Z. Yu and Y. Xu, "Imaged document text retrieval without OCR," *IEEE Trans. Pattern Anal. Mach. Intell.*, 24(6), 838-844 (2002).
74. B. A. Yanikoglu, "Pitch-based segmentation and recognition of dot matrix text," *International Journal on Document Analysis and Recognition*, 3, 34-39 (2000).
75. H. Penz, I. Bajla, A. Vrabl, W. Krattenthaler and K. Mayer, "Fast real-time recognition and quality inspection of printed characters via point correlation," *Proc. SPIE*, 4303, 127-137 (2001).
76. A. J. Elms and J. Illingworth, "A hidden Markov model approach for degraded and connected character recognition," *Handwriting Analysis and Recognition: A European Perspective, IEE European Workshop on*, 8/1-8/7 (1994).
77. J. D. Hobby and T. K. Ho, "Enhancing Degraded Document Images via Bitmap Clustering and Averaging," *Proceedings of the 4th International Conference on Document Analysis and Recognition*, Ulm, Germany, 394-400 (1997).
78. T. K. Ho, J. Hull and J. Srihari, "Decision Combination in Multiple Classifier Systems," *IEEE Trans. Pattern Anal. Mach. Intell.*, 16(1), 66-75 (1994).
79. M. Sawaki and N. Hagita, "Text-Line Extraction and Character Recognition of Document Headlines With Graphical Designs Using Complementary Similarity Measure," *IEEE Trans. Pattern Anal. Mach. Intell.*, 20(10), 1103-1109 (1998).
80. H. Liu, M. Wu, G.F. Jin, and Y. Yan, "A postprocessing algorithm for the optical recognition of degraded characters," *Proc. SPIE* 3651, 41-48 (1999).
81. A. Tonazzini, S. Vezzosi and L. Bedini, "Analysis and recognition of highly degraded printed characters," *International Journal on Document Analysis and Recognition*, 6(4), 236-247 (2004).

82. C. Cariou, J. M. Ogier, S. Adam, R. Mullot, Y. Lecourtier and J. Gardes, "A multiscale and multiorientation recognition technique applied to document interpretation: application to the French telephone network maps," *International Journal of Pattern Recognition and Artificial Intelligence*, 13(8), 1201-18 Dec. (1999).
83. R. Kh. Sadykhov and M.L. Selinger, "Fast algorithm for calculating the Fourier-Mellin moments for binary images," *Automatic Control and Computer Sciences*, 33(6), 54-60 (1999).
84. S. Adam, J. M. Ogier, C. Cariou, R. Mullot, J. Labiche and J. Gardes, "Symbol and character recognition: application to engineering drawings," *International Journal on Document Analysis and Recognition*, 3(2), 89-101, Dec. (2000).
85. Z. Chi, J. Wu and H. Yan, "Handwritten numeral recognition using self-organizing maps and fuzzy rules chains," *Pattern Recognition*, 28(1), 59-66 (1995).
86. S. B. Cho, "Neural network classifiers for recognizing totally unconstrained handwritten numerals," *IEEE Trans. On Neural Networks*, 8(1), 43-53 (1997).
87. K. T. Lim, Y. S. Nam, H. K. Kim and S. I. Chien , "Classification of handwritten numerals using modular neural networks," *Proc. of the Int'l Conf. on Artificial Intelligence-ICAI'2000*, 2, 875-81 (2000).
88. L. Xu, A. Krzyzak and C. Suen, "Methods of combining multiple classifiers and their applications to handwriting recognition," *IEEE Trans. Systems, Man Cybern.*, 22(3), 418-435 (1992).
89. Z. Chi, M. Sutters and H. Yan, "Handwritten digit recognition using combined ID3-derived fuzzy rules and Markov chains," *Pattern Recognition*, 29(11), 1821-1833 (1996).
90. S. N. Srihari, E. Cohen, J. J. Hull and L. Kuan, "A system to locate and recognize ZIP codes in handwritten addresses," *Internat. J. Research and Engineering Postal Applications*, 1, 37-45 (1989).
91. J. Cao, M. Ahmadi and M. Shridar, "Recognition of handwritten numerals with multiple feature and multistage classifier," *Pattern Recognition*, 28(2), 153-160 (1995).
92. A. Jr. Britto, R. Sabourin, F. Bortolozzi and C.Y. Suen, "A two-stage HMM-based system for recognizing handwritten numeral strings," *Proceedings of Sixth International Conference on Document Analysis and Recognition*, 396-400 (2001).
93. H. J. Kang and S. W. Lee, "Evaluation on selection criteria of multiple numeral recognizers with the fixed number of recognizers," *Proceedings-16th-International Conference on Pattern Recognition*, 3, 403-406 (2002).
94. Ye Xiangyun, M. Cheriet and C.Y. Suen, "StrCombo: combination of string recognizers," *Pattern Recognition Letters*, 23(4), 381-94 (2002).

95. L. Kwanyong, B. Hyeran and L. Yillbyung, "Unconstrained handwritten numeral recognition using multistage combination of multiple recognizers," *Journal-of-KISS(B)-(Software-and-Applications)*, 26(1), 93-105 (1999).
96. J. Grim, J. Kittler, P. Pudil and P. Somol, "Multiple classifier fusion in probabilistic analysis neural networks," *Pattern Analysis and Applications*, 5(2), 221-33 (2002).
97. T. D. Pham and Y. Hong, "Combination of handwritten-numeral classifiers with fuzzy integral," *Fuzzy theory systems: techniques and applications*, Ed. C. T. Leondes, Academic Press, New York, 3, 1111-1127 (1999).
98. J. K. Hee and W.L. Seong, "Combining classifiers based on minimization of a Bayes error rate," *Proceedings of the Fifth International Conference on Document Analysis and Recognition, ICDAR '99*, 398-401 (1999).
99. D. Guillevic and C. Y. Suen, "Recognition of legal amounts on bank checks," *Pattern-Analysis-and-Applications*, 1(1), 28-41 (1998).
100. T. Paquet, M. Avila and C. Olivier, "Word modeling for handwritten word recognition," *Proceedings Vision Interface '99. Canadian Image Process. & Pattern Recogniton Soc*, Toronto, Ont., Canada, 49-56 (1999).
101. Co. de-Almendra-Freitas, A. El-Yacoubi, F. Bortolozzi and R. Sabourin, "Brazilian bank check handwritten legal amount recognition," *Proceedings 13th Brazilian Symposium on Computer Graphics and Image Processing*, 97-104 (2000).
102. L. Granado, M. Mengucci, F. Muge, H. Emptoz, and N. Vincent, "Extraction de texte et de figures dans les livres anciens a l'aide de la morphologie mathématique," *CIFED '2000 : colloque international francophone sur l'écrit et le document*: Lyon, 81-90 (2000).
103. E.N. Zois and V. Anastassopoulos, "Contour features using morphological transforms," *IEE Electronics Letters*, 34(1), 56-58 (1998).
104. L. SU, M. Ahmadi and M. Shridar, "A Morphological Approach to Text String Extraction from Regular Periodic Overlapping Text Background Images," *GMIP(56)*, 5, 402-413 (1994).
105. E.N. Zois and V. Anastassopoulos, "Fusion of correlated decisions for writer verification," *Pattern Recognition*, 32(10), 1821-1823 (1999).
106. E. R. Dougherty, "An introduction to morphological image processing," *SPIE, Opt. Eng. Press*, (1992).
107. R.C. Gonzalez and R.E. Woods, "Digital image processing," Addison-Wesley, (1992).
108. M. Sawaki and N. Hagita, "Text-Line Extraction and Character Recognition of Document Headlines With Graphical Designs Using Complementary Similarity Measure," *IEEE Trans. Pattern Anal. Mach. Intell.*, 20(10), 1103-1109 (1998).

109. H. I. Avi-Itzhak, Thanh A. Diep, and Harry Garland, "High accuracy optical character recognition using neural network with centroid dithering," *IEEE Trans. Pattern Anal. Mach. Intell.*, 17(2), 218-223 (1995).
110. H. Kim and K. Nam, "Object recognition of one-dof tools by a back propagation neural net," *IEEE Trans. On Neural Network*, 6(2), 484-487 (1995).
111. S. Haykin, "Neural networks, A comprehensive foundation," *Macmillan Publishing College, 1 ed., New York*, (1994).
112. P. Patrick van der Smagt, "A comparative study of neural network algorithms applied to optical character recognition," *International Conference on Industrial and Engineering Applications of Artificial Intelligence and Expert Systems, Proceeding of the 3rd ICIEAAIES*, 2, 1037-1044 (1990).
113. N. Sang and T. Zhang, "Rotation and scale change invariant point pattern relaxation matching by the Hopfield neural network," *Opt. Eng.*, 36(12), 3378-3385 (1997).
114. Taiwei Lu, Shudong Wu, Xin Xu, and Francis T.S. Yu, "Two-dimensional programmable optical neural network," *Appl. Opt.*, 28(22), 4908-4913 (1989).
115. L.R. Rabiner, A tutorial on hidden Markov models and selected applications in a speech recognition, *Proc. of the IEEE*, 77(2), 257-285 (1989).
116. S. E. Levinson, L. R. Rabiner, M. M. Sondhi, "An introduction to the application of the theory of probabilistic functions of a Markov process to automatic speech recognition," *Bell Syst. Tech. J.*, 62(4), 1035-1074 (1983).
117. F. Sadaoki and I. Daisuke, "Neural network based HMM adaptation for noisy speech," *Proc. ICASSP 2001*, Salt Lake City, U.S.A., 1, 365-368 (2001).
118. S. Knerr, E. Augustin, O. Baret, and D. Price, "Hidden Markov model based word recognition and its application to legal amount reading on French checks," *Computer Vision and Image Understanding*, 70(3), 404-419 (1998).
119. L. Yang, B.K. Widjaja and R. Parasad, "Application of hidden Markov models for signature verification," *Proc. of the IEEE*, 28(2), 161-170 (1995).
120. H. J. Kim, S. K. Kim, K. H. Kim and J. K. Lee, "An HMM based character recognition network using level building," *Proc. of the IEEE*, 30(3), 491-502 (1997).
121. F. Kimura, M. Shridar and Z. Chen, "Improvements of a lexicon directed algorithm for recognition of unconstrained handwritten word," *Proc. of third ICDAR*, Tsukuba Science city, Japan, 18-22 (1993).
122. S. Madhvanth, E. Kleinberg and V. Govindaraju, "Holistic verification of handwritten phrases," *IEEE Trans. Patt. Anal. Mach. Intell.*, 21(12), 1344-1356 (1999).
123. S. Madhvanath, V. Krpasundar and V. Govindaraju, "Local reference lines for handwritten phrase recognition," *Pattern-Recognition*, 32, 2021-2028 (1999).

124. Y. Cao, S. Wang and H. Li, "Skew detection and correction in document images based on straight-line fitting," *Pattern Recognition Letters*, 24, 1871-1879 (2003).
125. S. Madhvanth, G. Kim and V. Govindaraju, "Chaincode contour processing for handwritten word recognition," *IEEE Trans. Patt. Anal. Mach. Intell.*, 21(9), 928-932 (1999).
126. A. El Yacoubi, M. Gilloux, R. Sabourin and C. Y. Suen, « An HMM-based approach for off-line unconstrained handwritten word modeling and recognition," *IEEE Trans. Patt. Anal. Mach. Intell.*, 21(8), 752-760 (1999).
127. W. Andrew and Anthony J. Robinson, "An off-line cursive handwriting recognition system," *IEEE Trans. Patt. Anal. Mach. Intell.*, 20(3), 309-318 (1998).
128. A. Namane, A. Guessoum and P. Meyrueis, "New skew correction and central zone localization for handwritten word and its application to French legal amounts," *Proc. of International Conference on Multimedia, Image Processing and Computer Vision*, 305-309, Madrid, Spain, April (2005).
129. A. Namane, A. Guessoum and P. Meyrueis, "FMT-SOM for handwritten numeral recognition," *Proc. of International Conference on Multimedia, Image Processing and Computer Vision*, 191-195, Madrid, Spain, April (2005).
130. A. Namane, A. Guessoum and P. Meyrueis, "New holistic handwritten word recognition and its application to French legal amount," *Proc. of Third International Conference on Advances in Pattern Recognition, ICAPR 2005*, 654-663, Bath, UK, August (2005).
131. A. Namane, E. H. Soubari, A. Guessoum, M. Djebari, P. Meyrueis and M. Bruynooghe, "Hopfield-multilayer-perceptron serial combination for accurate degraded printed character recognition," *Optical Engineering Journal*, 45(8), 7201-15, August (2006).
132. A. Namane, N. Khorissi, Z.A. Benselama, A. Guessoum, A. Mellit and P. Meyrueis, "CSM-Autoassociators combination for degraded character recognition," *International Symposium on Signal Processing and its Applications, ISSPA'07, IEEE Proc.*, UAE, Sharjah, February (2007).